TG 451

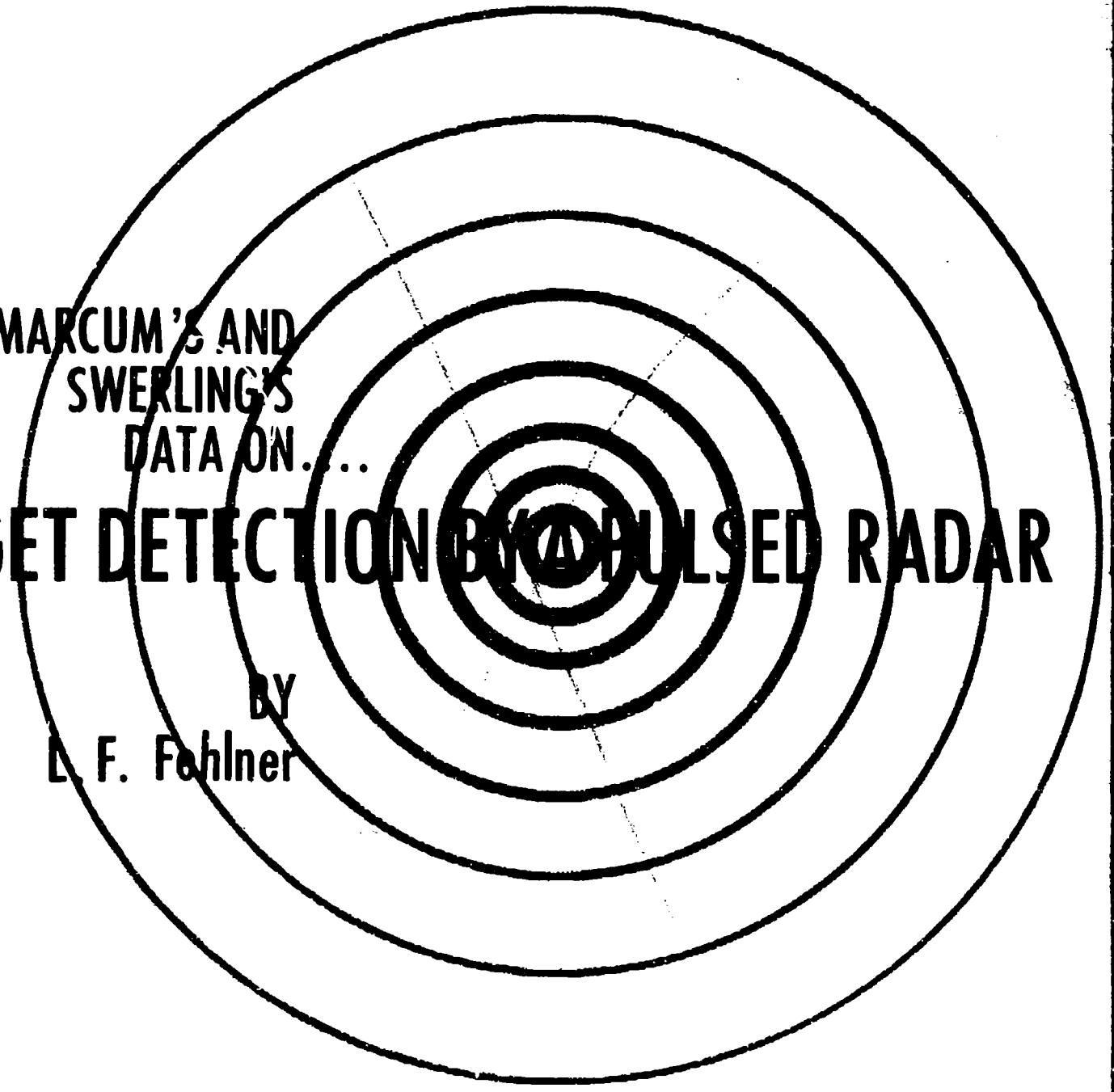

MARCUM'S AND SWERLING'S DATA ON... TARGET DETECTION BY A PULSED RADAR

BY

L. F. Fehlner

HE JOHNS HOPKINS UNIVERSITY • APPLIED PHYSICS LABORATORY • SILVER SPRING, MARYLAND
ERATING UNDER CONTRACT NOw 62-0604-c, BUREAU OF NAVAL WEAPONS, DEPARTMENT OF THE NAVY

CONTENTS

THE JOHNS HOPKINS UNIVERSITY
APPLIED PHYSICS LABORATORY
SILVER SPRING MARYLAND

2 July 1962

MARCUM'S AND SWERLING'S DATA ON TARGET DETECTION BY A PULSED RADAR

Introduction

Marcum has produced (Reference (a))* a definitive treatment of the statistical problem of target detection by a pulse radar. His papers have withstood the test of time since their original publication (1947-48). They have been republished twice -- most recently by the Institute of Radio Engineers as a part of a special monograph issue. They are widely referenced.

However, the text and graphs of Marcum's papers are presented in terms so highly mathematical that his results may not appear as useful as they really are. The purpose of this memo is to describe the problem that Marcum solved and to present graphs of more extensive and more accurate computed data in a form which may prove more useful for most applications. Nothing new is added from the statistical viewpoint. Those interested in the mathematical development are referred to Reference (a).

---

* Reference (a) Marcum, J.I. and Swerling, P.; "Studies of Target Detection by Pulsed Radar"; IRE Transactions Volume IT-6, No. 2 dtd April 1960. (Also published as Rand Research Memo RM 754 by J.I.Marcum dtd 1 Dec 1947; Rand Memo RM 753 by J.I.Marcum dtd 1 July 1948; and Rand Memo RM 1217 by P.Swerling dtd 17 March 1954.

Swerling's paper in Reference (a) extends Marcum's results to the case of a radar target with an echo of fluctuating strength. Swerling's analytic results have been used in this memo to extend the numerical data beyond that given in Reference (a). The results of these computations are presented below.

The Noise Problem

A pulse radar set is an electronic device which can alternately radiate and receive electromagnetic energy. Limitations are placed on the bandpass of the receiver and also on the time of reception so that any received energy is suspected of being an echo of the radiated energy. The receiver is designed to measure the smallest energy possible to minimize the transmitted energy. As these receivers become more and more sensitive, their measurements become influenced by energy which before had been unnoticed in the background.

Until recently, background discrimination was done principally by people who observed a display attributable to the received energy and thermal noise generated internally. Through the use of very subtle target detection criteria and integration laws, (that are not well understood) trained observers are very effective in detecting targets in the presence of background noise. Marcum's results, in theory, apply at least partially to target detection by people. For applicable numerical results, it would be necessary to interpret their detection criteria in terms of a signal-to-noise ratio; and also to know the observer's integration law.

Marcum's results apply directly to the performance of an automatic detection system which is based on signal-to-noise ratio. In an automatic system, energy received as noise simultaneously with an echo cannot be rejected on the basis of

frequency without rejecting the echo. This is because noise contains all the frequencies of interest superimposed in random phase. This superposition accounts for the large and random fluctuations in the amplitude of the noise signal.

The ratio of signal energy to noise energy is of fundamental concern in attempting to make radar detections. When signal energy is measured over the same time interval as noise energy, the energy ratio is identical to the power ratio. Since the times are usually the same, equations below will be written in terms of power. It should be remembered, however, that in the general case the time interval for measuring signal and noise energy might not be the same and due account of this fact must then be taken.

The power, P_e, of the target echo, which we would like to measure is:

$$P_e = \left(\frac{P_t G_t}{4\pi R^2}\right)\left(\frac{\sigma}{4\pi R^2}\right)\left(\frac{G_R \lambda^2}{4\pi}\right) L \qquad (1)$$

where
- P_e is the power of the echo at the input to the receiver
- P_t is the power transmitted
- G_t is the gain of the transmitting antenna
- σ is the scattering cross section of the target
- G_R is the gain of the receiving antenna
- λ is the carrier wave length
- L is a factor to account for two-way losses due to such causes as propagation through the medium, antenna, beam shape and plumbing, and
- R is the range to the target.

The first term of equation (1) in parenthesis describes the radial distribution of power density from the transmitting (illuminating) antenna. The second term accounts for the power reradiated from the target. The third defines the fraction of the reradiated power captured by the receiving antenna. The product of these terms defines a mean echo power that would be measured were it not for the large fluctuations in noise power. Consequently, what is needed is a criterion for deciding whether the measured power indicates the presence of a target or not. A very useful decision criterion is used in statistics called the Neyman-Pearson Observer. This criterion requires a fixed value of signal-to-noise ratio (i.e. threshold) for comparison to the signal-to-noise ratio being measured. If the measured value is larger than the threshold, a target is reported. Noise will, at times, cause reports of targets when no targets are present. Some detections will be missed because noise happens to be low during the echo. If false alarms prove bothersome, either the threshold value of signal-to-noise ratio must be increased at the expense of missed detections or more radiated power; or more sophisticated decision criteria must be instrumented. This latter alternative is outside the scope of the present paper.

The problem of target detection by continuous-wave radar can be treated in the same way if the observed sample of the continuous return from the target is interpreted as a pulse.

False Alarm Number

Marcum defined the complex relationship between a threshold value of signal-to-noise ratio and the probability that values in excess of the threshold will exist in the

presence of both noise and echoes. These excesses will be reported as target detections and as mentioned above, will include both false and real reports of targets.

The problem starts with noise. Suppose that the voltage due to noise alone varies with time like this:

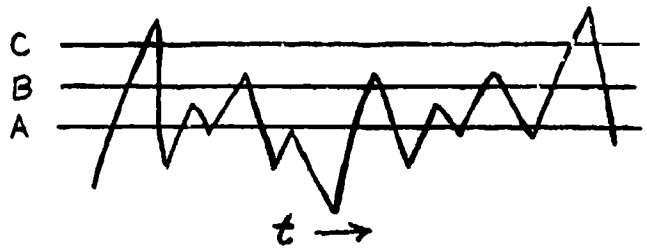

During the period shown the noise would have exceeded threshold voltage level A 7 times, level B 5 times and level C only twice. Obviously, the higher the threshold, the longer will be the average time between occasions when noise alone exceeds the threshold. This time is of considerable concern because if too short, we will be faced with too frequent false alarms; and if too long, excessive radiated energy will be required to achieve reasonable probabilities of target detection. To get a mathematical handle on this time, it is defined as follows: the false alarm time is the time during which the probability is P_o that there will not be a false alarm. For purposes of standarization, P_o is taken to be 0.5.

P_N is the probability that a false alarm is obtained each time there is an opportunity. The false alarm number, n', is the number of independent opportunities for a false alarm in the false alarm time. Then as standardized

$$P_o = (1 - P_N)^{n'} = 0.5 \text{ (Marcum eq. 10)*} \qquad (2)$$

---

* These references are to equations in RM-753 of Reference (a) but they are not necessarily quoted verbatum.

where P_o is the probability of no false alarm during the false alarm time

P_N is the probability of a false alarm on each opportunity, and

n' is the false alarm number.

When the number of opportunities for a false alarm, i.e., the false alarm number, is very large, an approximation to equation (2) gives accurate values of the probability of a false alarm, namely,

$$P_N \approx \frac{1}{n'} \log_e \frac{1}{P_o} \quad \text{(Marcum eq. 21)} \qquad (3)$$

The values of false-alarm probability in Table I apply when $P_o = 0.5$.

TABLE I

PROBABILITY OF A FALSE ALARM IN THE ABSENCE OF TARGET ECHOES

False Alarm Number, n'	False Alarm Probability, P_N
10^2	6.93×10^{-3}
10^3	6.93×10^{-4}
10^6	6.93×10^{-7}
10^8	6.93×10^{-9}
10^{10}	6.93×10^{-11}

The choise of false alarm number associated with a particular radar depends on the function it performs. Search radars usually are designed to have very large false alarm numbers, e.g., 10^6, to minimize the time wasted in reacting to false detections. On the other hand, track radars can use

small false alarm numbers because the tracking antenna is not unduly distracted by an occasional false detection during acquisition of the target; and, during tracking, the distraction is completely negligible.

The number of opportunities for a false alarm may be calculated in terms of the pulse repetition frequency (PRF), the number of range gates per range sweep, and the method of signal processing. Common processing techniques are the coherent and incoherent integration of pulses; coherency refers to the preservation of phase in the pulse-summing process. Range gates are switches that open and close at specified times so that a target echo, if any, can be admitted from a predetermined element of space, referred to as a cell.

Since a decision must be made each time a gate is open, whether a target is present or not, noise pulses that enter can be interpreted as a target if their sum is strong enough. The number of pulses actually processed per unit time is the number of range gates per sweep multiplied by the pulse repetition frequency. If, prior to the decision, m pulses are integrated coherently, and then N of the resulting signals are integrated incoherently, the opportunities for a false alarm are reduced proportionally at the expense of reducing the number of cells that may be searched per unit time.

The false alarm number is related to the false alarm time as follows:

$$t_F = \frac{mNn'}{(PRF)G} \tag{4}$$

where t_F is the false alarm time

m is the number of pulses integrated coherently

N is the number of signals integrated incoherently, and

G is the number of range gates per range sweep.

Bias Level

The probability, P_N, that noise alone will exceed a given bias level of voltage is obviously a function of the bias level. The nature of the function depends on the combined law of the detector and integrator and the characteristics of the noise. The detector referred to here is the envelope detector, the output of which is a given function of the envelope of the carrier wave. This function is called the law of the detector. The integrator affects the statistical problem in the same way as the detector. The function of the signal voltage which is integrated is called the law of the integrator, e.g. the square of the pulse voltage might be integrated over N pulses. So long as the same weight is applied to each of the N pulses the integrator is called linear, e.g., we could have a linear square-law integrator.

The solutions for the bias level which are obtained are for the combined law of the detector and integrator. The sclution obtained most easily is for a combined square law which is usually thought of as a square-law detector coupled with a linear linear-law integrator.

The bias level for the combined square law case, and for the assumed normal distribution of noise voltage, is given by:

$$P_o^{\frac{1}{n'}} = \int_o^{Y_b} \frac{Y^{N-1} e^{-Y}}{(N-1)!} \, dY \quad \text{(Marcum eq. 39)} \qquad (5)$$

and

$$Y = \sum_1^N y \quad \text{(Marcum eq. 26)} \qquad (6)$$

where Y_b is the bias level normalized to root mean square noise, and

y is the output of the detector normalized to root mean square noise.

The relationships among Y_b, N and n′ are shown in Figure 1 for $P_o = 0.5$. Mean square noise is defined as

$$\psi_o = \int_o^\infty w\,(f)\,df \quad \text{(Marcum eq. 3)} \qquad (7)$$

where ψ_o is mean square noise

$w(f)$ is the power spectral density of the noise output of the receiver (assumed to be a linear filter with gain), and

f is the frequency.

Target Detection

A functional block diagram of an automatic pulse radar may be drawn as follows:

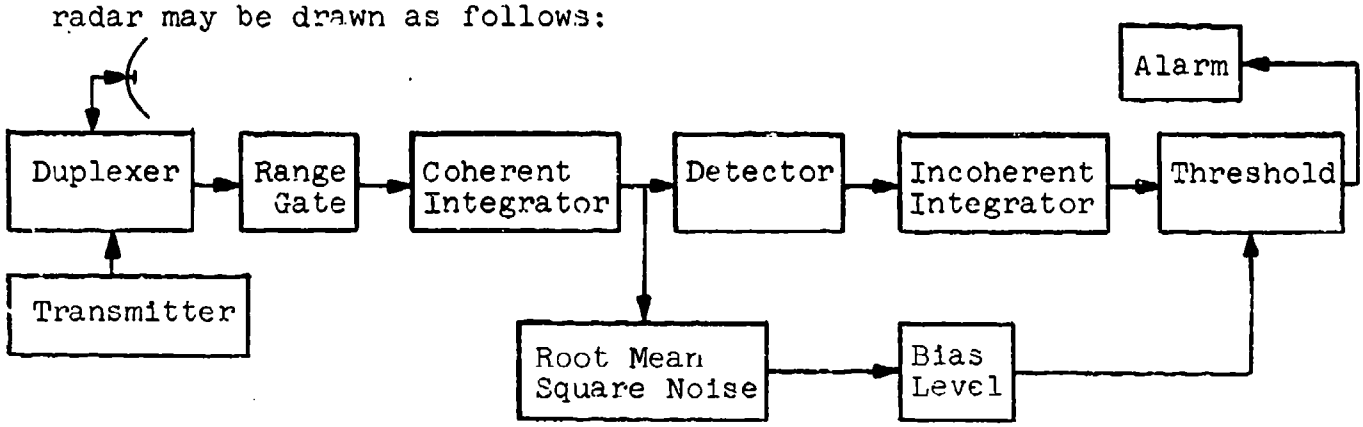

The coherent integrator adds pulses either at carrier frequency or at some intermediate frequency. The output is fed to the envlope detector and also to a device to obtain ψ_o and take the square root. The value obtained for ψ_o must not be unduly influenced by echoes. This value is multiplied by a factor, Y_b,

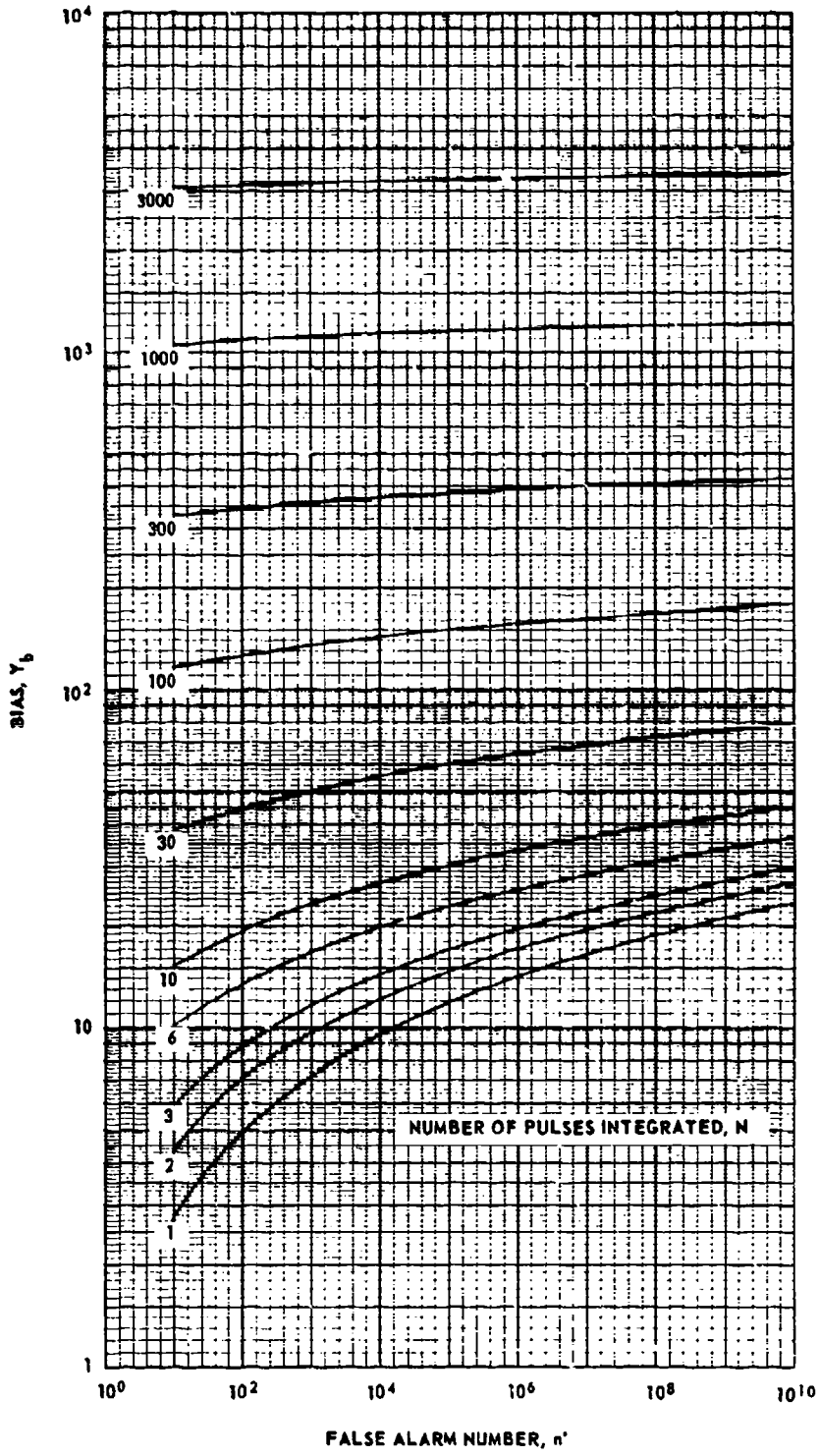

Fig. 1 THE BIAS REQUIRED ON ROOT MEAN SQUARE NOISE TO ESTABLISH A THRESHOLD

to obtain the bias level. The integrated output of the detector is compared to the bias level in the threshold device. If the integrated detector output is larger, the alarm is sounded indicating the probable presence of a target. Marcum's analysis applies to only that part of the functional block diagram downstream of the coherent integrator. If m pulses are integrated coherently, Marcum's data apply to $\frac{1}{m}$ of the transmitted pulses, each of which has m times the energy of a single transmitted pulse.

The probability of detection, i.e. the probability of sounding the alarm in the presence of signal and noise, is given by:

$$P_N = 1 - \int_0^{Y_b} \left(\frac{Y}{Nx}\right)^{\frac{N-1}{2}} e^{-Y-Nx} I_{N-1}\left(2\left[NxY\right]^{1/2}\right) dY \qquad (8)$$

(Marcum eq. 49)

where x is the signal to noise power ratio (later x = S), and
I is the modified Bessel function of the first kind.

Since the relationships have been established among the bias level, Y_b, the false alarm number, n′, and the number of pulses integrated N, by equation (5), the probability of detection can now be related to n′ and N through equation (8). These relationships are shown in Figures 2 through 11.

Range Equation

As mentioned above in connection with equation (1), the signal-to-noise power ratio is available by observing signals and noise over the same period of time. Since Marcum shows the probability of detection as a function of the signal-

to-noise power ratio (equation (8)), all the parameters of interest to the formulation of the range equation are available in consistent units. Noise power from unavoidable sources such as thermal, shot and galactic noise is usually normalized to thermal noise power.

The range equation can now be written. It expresses, among other things, the relationship between the range and the probability that a detection will be made each time the range is sampled. These detections will include false alarms.

$$R^4 = \frac{m \hat{P}_t G_t G_R \lambda^2 \sigma L}{(4\pi)^3 [KT\beta F] S(N, n', P_N)} \qquad (9)$$

where
- R is the range
- m is the number of pulses integrated coherently
- $\hat{P}_t$ is the peak power in relation to the average transmitted power of the radar (actually the average power of each transmitted pulse)
- G_t is the gain of the transmitting antenna
- G_R is the gain of the receiving antenna
- λ is the wave length of the carrier wave
- σ is the scattering cross section of the target
- L is the product of loss factors, e.g. due to medium, plumbing, beam shape, etc.
- K is Boltzmann's constant for thermal noise energy $= 1.38 \times 10^{-23}$ joules/degree Kelvin
- T is the absolute "room" temperature (IRE standard is 290°K)
- β is the receiver bandpass
- F is the noise figure of the receiver
- N is the number of pulses integrated incoherently
- n' is the false alarm number
- P_N is the probability of detection for N pulses integrated incoherently, and

S is the signal to noise power ratio (given as x by Marcum as a function of N, n′, and P_N).

The numerator of equation (9) divided by $\left[(4\pi)^3 R^4\right]$ expresses the summed power of m reflected pulses measured at the input to the receiver. The term in brackets in the denominator expresses the noise power due to the usual source, i.e. the noise of the receiver referred to thermal noise. If other sources of noise are present, such as noise jammers, their power as measured at the input to the receiver must be added to the term in brackets.

Collapsing Loss

The function $S(N, n', P_N)$, which is shown in Figures 2 through 11, has been computed for conditions under which the radar set integrates the same number of noise pulses as signal pulses. If more noise pulses are integrated than signal pulses, a greater signal-to-noise ratio is associated with any given probability of detection than is given by $S(N, n', P_N)$. Marcum defines a collapsing ratio as:

$$\rho = \frac{M + N}{N} \quad \text{(Marcum eq. 226)} \qquad (10)$$

where ρ is the collapsing ratio, and
M is the additional number of noise pulses integrated.

The term "collapsing" stems from an association of this ratio with the superposition, or "collapsing", of data on a radar scope. A collapsing loss is also defined:

$$L_c = \frac{S_1}{S} \quad \text{(Marcum eq. 232)} \qquad (11)$$

where L_c is the collapsing loss factor
S is the signal to noise ratio for $M = 0$, and
S_1 is the signal to noise ratio for $M > 0$.

In cases where collapsing loss applies, the denominator of equation (9) is multiplied by L_c. Note that in so doing, $S(N, n', P_N)$ is merely changed to $S_1(M, N, n', P_{N+M})$.

Values of $S_1(M, N, n', P_{N+M})$ can be found from $S(N, n', P_N)$ through the use of ρ. First find the bias level from Figure 1 using ρN for the parameter N noted on the Figure. Then find a value for S for the desired probability of detection using ρN for N in Figures 2 through 11. Multiply this value of S by ρ to obtain S_1. This value of S_1 can then be used directly in equation (9) for S or used indirectly through equation (11). Symbolically,

$$S_1(M, N, n', P_{N+M}) = \rho S(\rho N, n', P_N) \qquad (12)$$

when $P_{N+M} = P_N$.

Marcum's Other Results

Results which Marcum derived for the square law of the combined detector and integrator have emerged as the standard for radar calculations. This is partly because the square law permits the easiest solution of the statistical problem and partly because changing the law doesn't make much difference. However, this is not Marcum's only result.

Linear Law - Marcum made a limited number of calculations for a combined linear law. A comparison with the square law results show that the differences are very small. For example, at a detection probability of 0.5, the required signal-to-noise ratio is the same for both laws for N = 1 and

N = 70. For N = 10, the square law requires about 1.3% more power ratio than the linear law. For N very large, the linear law approaches a requirement of about 2.2% more signal-to-noise ratio than the square law. These results are ample justification for preferring the more easily obtained square law data.

Signal Plus Noise Minus Noise - Marcum obtained results for systems which integrate composite pulses formed by subtracting one noise pulse from each signal-plus-noise pulse. Quoting his own analysis of the results, "There appears to be no significant difference in the probabilities of detection for N between 1 and 10. For N between 100 and 1000, the composite case gives an effective signal to noise ratio about 1 db lower than the ordinary case". An advantage of this scheme is that substantially lower bias levels pertain when N is large.

Alternate Detection Criteria - Another method of detection is based on the probability of signal-plus-noise exceeding noise alone over a period of time. This time is taken to be the false alarm time. Marcum obtained limited numerical results for this criterion. He points out that this criterion is not useful for search because of the difficulty of picking out the largest signal over a period of time and because of the difficulty of what to do when many signals are present. However, this criterion is useful for determining the probability that an automatic tracking beam will lose its target due to noise. See (Marcum eq. 185).

Another detection criterion is based on the shift in average value of a distribution of signal plus noise from that of noise alone divided by the standard deviation of noise alone. This is called the deflection criterion. Marcum

shows that this criterion makes detection a function of $N^{1/2}$ whereas the bias level criterion takes advantage of making detection a function of N raised to powers from 1 to about 0.75 depending on the size of N. Thus, the deflection criterion is not preferable. Marcum uses the deflection criterion, however, for a special proof that the square law for the detector-integrator is the best possible law for sufficiently small signal-to-noise ratios (Marcum eq. 225).

Best Possible Detector Law - Marcum proves rigorously that there is a best possible detector law for each signal strength (Marcum eq. 217). For small signals the best possible law closely approximates the square law. For large signals, it is the linear law. However, the numerical results for these extreme cases are not very different, so that if faced with a choice, there is not much reason to prefer one to the other on the basis of detection probability. However, the linear law has one practical advantage in that a linear detector would be less subject to saturation by large signals.

Antenna Beam Shape Loss - Marcum points out the obvious fact that in the static case, one should use the antenna gain which is associated with the target's position in the beam pattern. However, in the scanning case the target's position moves through the beam pattern causing different gains to apply each time the range is sampled. The question arises as to how long the echo pulses can be integrated while the beam is on the target. Marcum states, as the result of his analysis, that integration should be carried out to about 1.1 times the half-power beamwidth, practically independent of the range and the number of pulses per half-power beamwidth. If this is done, the average loss factor referred to the ideal case of constant gain is about 0.84 (i.e. 1.5 db). This result

does not apply when scanning is so fast that only one target hit is achieved per beamwidth. For cases where fast scanning results in successive echo pulses having different signal strengths Marcum indicates the statistical solution, but does not work it out.

Limiting Loss - Through calculations which were not reproduced in Reference (a), Marcum concluded that for N large, the loss due to limiting in the receiver is only a fraction of a db if the limiting ratio is as large as 2 or 3. The limiting ratio is defined as the ratio of the limiting level to the root mean square noise level. If only 1 or 2 pulses are integrated the ratio must be as high as 10 to prevent a serious loss. Integrator limiting can also cause a loss but Marcum says that this loss is small compared to the limiting of the individual pulses.

Fluctuating Target

Swerling extended Marcum's square law results to four different cases in which targets return echoes of fluctuating strength. Cases 1 and 2 apply to targets which can be represented as a number of independently fluctuating reflectors of about equal echoing area. Such is said to be the case for objects which are large compared to a wave length and shaped not too much like a sphere. It is claimed that observed data on aircraft targets agree with the density distribution assumed for cases 1 and 2. This distribution is

$$w(x, \bar{x}) = \frac{1}{\bar{x}} e^{-\frac{x}{\bar{x}}} ; \quad x \geq 0 \qquad (13)$$

where $\bar{x}$ is the average signal to noise ratio over all target fluctuations.

Cases 3 and 4 apply to targets which can be represented as one large reflector together with a number of

small reflectors; or as one large reflector subject to small changes in orientation. The assumed density distribution is:

$$w(x,\bar{x}) = \frac{4x}{\bar{x}^2} e^{-\frac{2x}{\bar{x}}} \quad ; \; x \geq 0 \tag{14}$$

Cases 1 and 3 apply when echo fluctuations occur from scan to scan. During a scan the echo strength is assumed constant. Cases 2 and 4 apply when fluctuations occur from pulse to pulse. Swerling's formulas are as follows:

CASE 1 -

For N = 1:

$$P_1 = e^{\frac{-Y_b}{1+\bar{x}}} \tag{15}$$

For N > 1:

$$P_N = 1 - \int_0^{Y_b} \frac{e^{-Y_Y N-2}}{(N-2)!} \, dY + \left(1+\frac{1}{N\bar{x}}\right)^{N-1} e^{\frac{-Y_b}{1+N\bar{x}}} \int_0^{\frac{Y_b}{1+\frac{1}{N\bar{x}}}} \frac{e^{-Y_Y N-2}}{(N-2)!} \, dY \tag{16}$$

CASE 2 -

For any N:

$$P_N = 1 - \int_0^{\frac{Y_b}{1+\bar{x}}} \frac{e^{-Y_Y N-1}}{(N-1)!}\, dY \qquad (17)$$

CASE 3 -

For N = 1:

$$P_1 = \left(1 + \frac{Y_b}{\left(1 + \frac{\bar{x}}{2}\right)\left(1 + \frac{2}{\bar{x}}\right)}\right) e^{\frac{-Y_b}{1 + \frac{\bar{x}}{2}}} \qquad (18)$$

For N = 2:

$$P_2 = \left(1 + \frac{Y_b}{1 + \bar{x}}\right) e^{\frac{-Y_b}{1 + \bar{x}}} \qquad (19)$$

For N > 2:

$$P_N = 1 - \frac{\left(1 + \frac{2}{N\bar{x}}\right)^{N-2}}{\left(1 + \frac{N\bar{x}}{2}\right)^2} \int_0^{Y_b} Y_1 e^{\frac{-Y_1}{1 + \frac{N\bar{x}}{2}}} \int_0^{\frac{Y_1}{1+\frac{2}{N\bar{x}}}} \frac{e^{-Y_Y N-2}}{(N-2)!}\, dY\, dY_1$$

$$+ \frac{(N-2)\left(1 + \frac{2}{N\bar{x}}\right)^{N-1}}{\left(1 + \frac{N\bar{x}}{2}\right)^2} \int_0^{Y_b} e^{\frac{-Y_1}{1 + \frac{N\bar{x}}{2}}} \int_0^{\frac{Y_1}{1+\frac{2}{N\bar{x}}}} \frac{e^{-Y_Y N-2}}{(N-2)!}\, dY\, dY_1$$

$$- \frac{N-1}{\left(1 + \frac{N\bar{x}}{2}\right)^2} \int_0^{Y_b} \frac{e^{-Y_Y N-1}}{(N-1)!}\, dY \qquad (20)$$

CASE 4 -

For any N;

$$P_N = 1 - \frac{1}{\left(1 + \frac{2}{\bar{x}}\right)^N} \sum_{k=0}^{N} \left(\frac{\bar{x}}{2}\right)^{-k} \frac{N!}{k!\,(N-k)!} \int_0^{\frac{Y_b}{1+\frac{\bar{x}}{2}}} \frac{e^{-Y} Y^{2N-1-k}}{(2N-1-k)!}\, dY \qquad (21)$$

For N = 1, this equation reduces to Equation (18).

Swerling did not give the exact expression for P_N for Case 4. Equation (21) was derived by Ronald Roll from the characteristic function for Case 4 given in Reference (a).

The relationships among P_N, $\bar{x}$, N and n' expressed by Equation (5) and Equations (15) through (21) are shown in Figures 12 through 49. Symbolically,

$$\bar{x} = S_2(N, n', P_N) \qquad (22)$$

and values of S_2 are used in Equation (9) in place of S_1 when the detection range of fluctuating targets is desired.

Concluding Remarks

Detection probability, P_N, is related to the bias level, Y_b, through integrals, the values of which are very sensitive to small changes in the limits of integration, especially for large N. To obtain numerical values of P_N as a function of n', the number of significant figures required

for Y_b must be compatible with the sensitivity of the functions to be integrated. Accordingly, the bias level, Y_b, was found from Equation (5) using the numerical methods described in the Appendix and double precision arithmetic on the IBM 7090 computer. Various values of n' between 10 and 10^{10} were used and P_o was taken to be 0.5.

The values of Y_b thus determined were used as the upper limit of integration in Equation (8) and in Equations (15) through (21). The number of pulses integrated, N, was varied from 1 to 3000. The signal-to-noise ratio x or $\bar{x}$, was varied over sufficient range to define a graph for a range of P_N between approximately 0.001 and 0.999. Values of P_N were obtained by numerical methods described in the Appendix.

The signficant figures which can be read from Figures 1 through 49 are sufficient for most purposes. However, if more significance is required for any particular problem, the tabulated data will be kept on file in BPD. These data are exact to six significant digits. A comparison with the data presented in Reference (a) indicates that the accuracy of Marcum's data for non-fluctuating targets is at least as good as the accuracy of reading his graphs. Swerling's data for all cases, however, are substantially in error for large N, the number of pulses integrated. The exact data indicate lower probabilities of detection for the same signal-to-noise ratio.

Leo F. Fehlner

LFF:ls

APPENDIX A

Methods for Digital Machine Computation of Detection Probability by R. G. Roll and G. T. Trotter

Swerling expressed the detection probability, P_N, for case 1 in terms of two incomplete gamma functions and for case 2 in terms of only one. Marcum's expression of the bias level, Y_b, is also a single incomplete gamma function. Numerical values of P_N for cases 1 and 2 and of Y_b can be computed from these expressions as given. To facilitate the evaluation of incomplete gamma functions, a recursion relation has been used to express them as series which can be computed to any precision, given enough time.

The best method of computing Swerling's cases 3 and 4 and Marcum's case (which we will call case 0) is not obvious through inspection of the expressions as they gave them. Therefore, the probability distribution functions were rederived from the characteristic functions to produce series which can be computed to any precision. These series, and the method of programming them for digital computation, are given below.

Incomplete Gamma Function

The incomplete gamma functions are of the form:

$$f(a,p) = \int_0^a \frac{e^{-u}\, u^p}{p!}\, du \qquad \text{(A-1a)}$$

$$= 1 - \int_a^\infty \frac{e^{-u}\, u^p}{p!}\, du \qquad \text{(A-1b)}$$

Appendix A

Integration by parts yield:

$$f(a,p) = - \frac{e^{-u}\, u^p}{p!} + \int_0^a \frac{e^{-u}\, u^{p-1}}{(p-1)!}\, du \qquad \text{(A-2)}$$

which is a recursion relation expressible as:

$$f(a,p) = 1 - \sum_{k=0}^{p} \frac{e^{-a}\, a^k}{k!} \qquad \text{(A-3a)}$$

$$= \sum_{k=p+1}^{\infty} \frac{e^{-a}\, a^k}{k!} \quad . \qquad \text{(A-3b)}$$

If $a > p$, Equation (A-3a) converges faster and is therefore preferable for computation. If $a < p$, Equation (A-3b) is preferable.

Non-fluctuating Target - Case 0

The characteristic function for case 0 as given by Marcum is:

$$C_N(p) = \frac{e^{-Nx}\, e^{\frac{Nx}{p+1}}}{(p+1)^N} \quad . \qquad \text{(A-4)}$$

The density function is obtained by contour integration.

$$f(t) = \frac{1}{2\pi i} \int_{-i\infty}^{+i\infty} \frac{e^{-Nx}\, e^{\frac{Nx}{p+1}}\, e^{(p+1-1)t}}{(p+1)^N}\, dp \quad , \qquad \text{(A-5a)}$$

$$= \frac{e^{-Nx}\, e^{-t}}{2\pi i} \int_{-i\infty}^{+i\infty} \frac{e^{\frac{Nx}{p+1}}\, e^{t(p+1)}}{(p+1)^N}\, dp \quad , \tag{A-5b}$$

$$= e^{-Nx} \sum_{k=0}^{\infty} \frac{(Nx)^k}{k!} \frac{t^{N-1+k}}{(N-1+k)!} \quad . \tag{A-5c}$$

The probability distribution function is given by:

$$P_N(Y_b) = 1 - \int_0^{Y_b} f(t)\, dt = \int_{Y_b}^{\infty} f(t)\, dt \quad . \tag{A-6}$$

$$P_N(x, Y_b) = e^{-Nx} \sum_{k=0}^{\infty} \frac{(Nx)^k}{k!} \sum_{j=0}^{N-1+k} \frac{e^{-Y_b}\, Y_b{}^j}{j!} \tag{A-7a}$$

$$= 1 - e^{-Nx} \sum_{k=0}^{\infty} \frac{(Nx)^k}{k!} \sum_{j=N+k}^{\infty} \frac{e^{-Y_b}\, Y_b{}^j}{j!} \quad . \tag{A-7b}$$

If $Y_b > N(x+1)$, Equation (A-7a) should converge faster and is therefore preferable for computation. The maximum term is identified by that value of k that makes:

$$\frac{(Nx)^k}{k!} \frac{Y_b{}^{N-1+k}}{(N-1+k)!}$$

a maximum. The summation is then carried out around this point.

If $Y_b < N(x + 1)$, Equation (A-7b) is preferable. The maximum term is identified by the value of k that makes:

$$\frac{(Nx)^k}{k!} \quad \frac{Y_b^{N+k}}{(N + k)!}$$

a maximum and the summation is carried out around this point.

Fluctuating Target - Case 3

For case 3, the characteristic function, as given by Swerling, is:

$$\bar{C}_N(p) = \frac{1}{(1 + p)^{N-2}\left[1 + p\left(1 + \frac{N\bar{x}}{2}\right)\right]^2} \quad . \tag{A-8}$$

$$\text{Let } c = \frac{1}{1 + \frac{N\bar{x}}{2}} \tag{A-9}$$

The density function may be obtained from

$$f(t) = \frac{1}{2\pi i}\int_{-i\infty}^{+i\infty} \frac{e^{pt}}{(1 + p)^{N-2}\left(1 + \frac{1}{c}p\right)^2}\, dp \quad . \tag{A-10}$$

By contour integration, we obtain

Appendix A

$$f(t) = -\frac{(N-2)\, c^2\, e^{-ct}}{(1-c)^{N-1}} + \frac{c^2\, t\, e^{-ct}}{(1-c)^{N-2}}$$

$$+ c^2\, e^{-t} \sum_{k=0}^{N-3} \frac{(k+1)\, t^{N-3-k}}{(N-3-k)!\,(1-c)^{k+2}} \qquad \text{(A-11)}$$

The probability distribution function is given by:

$$P_N(c, Y_b) = \frac{Y_b{}^{N-1}\, e^{-Y_b c}}{(N-2)!} + \sum_{j=0}^{N-2} \frac{e^{-Y_b}\, Y_b{}^{j}}{j!}$$

$$+ \frac{e^{-cY_b}}{(1-c)^{N-2}} \left[1 - \frac{(N-2)c}{1-c} + cY_b\right] \left[1 - \sum_{j=0}^{N-2} \frac{e^{-Y_b(1-c)} \left[Y_b(1-c)\right]^{j}}{j!}\right] \qquad \text{(A-12)}$$

The summations are incomplete gamma functions which can be evaluated as shown in Equations (A-3).

Fluctuating Target - Case 4

For case 4, the characteristic function as given by Swerling is:

$$\bar{C}_N(p) = \frac{(1+p)^N}{\left[1 + (1 + \frac{\bar{x}}{2})\, p\right]^{2N}} \qquad \text{(A-13)}$$

Appendix A

Let

$$c = \frac{1}{1 + \frac{\bar{x}}{2}} \tag{A-14}$$

then

$$\bar{C}_N(p) = \frac{c^{2N}\,(1 + p)^N}{(c + p)^{2N}} \quad . \tag{A-15}$$

The density function is obtained from

$$f(t) = \frac{1}{2\pi i} \int_{-i\infty}^{+i\infty} \frac{e^{pt}\, c^{2N}\, (1 + p)^N}{(c + p)^{2N}}\, dp \quad . \tag{A-16}$$

By contour integration we obtain

$$f(t) = e^{-ct}\, c^{2N} \sum_{k=0}^{2N-1} \frac{N!}{k!\,(N-k)!}\, (1 - c)^{N-k}\, \frac{t^{2N-1-k}}{(2N - 1 - k)!} \tag{A-17}$$

The probability distribution function is:

$$P_N(c, Y_b) = C^N \sum_{k=0}^{N} \frac{N!}{k!\,(N - k)!} \left(\frac{1 - c}{c}\right)^{N-k} \sum_{j=0}^{2N-1-k} \frac{e^{-cY_b}\,(cY_b)^j}{j!} \tag{A-18a}$$

$$= 1 - C^N \sum_{k=0}^{N} \frac{N!}{k!\,(N - k)!} \left(\frac{1 - c}{c}\right)^{N-k} \sum_{j=2N-k}^{\infty} \frac{e^{-cY_b}(cY_b)^j}{j!} \tag{A-18b}$$

If $Y_b > N(2 - c)$, Equation (A-18a) is preferable for computation. The maximum term is identified with that value of k that makes

$$\frac{N!}{k!\,(N-k)!}\left(\frac{1-c}{c}\right)^{N-k}\frac{(cY_b)^{2N-1-k}}{(2N-1-k)!}$$

a maximum. The summation is then carried out around this point. If $Y_b < N(2 - c)$, Equation (A-18b) is preferable. The maximum term is identified by that value of k that makes

$$\frac{N!}{k!\,(N-k)!}\left(\frac{1-c}{c}\right)^{N-k}\frac{(cY_b)^{2N-k}}{(2N-k)!}$$

a maximum. The summation is then carried out around this point.

Computational Problems

The extremely large and extremely small numbers encountered in the computations mentioned above led to some interesting computer programming problems. The IBM 7090 computer, which was used for these computations, can normally handle numbers in the range $10^{-38} < |x| < 10^{38}$, with about eight digits of significance. In several instances it was necessary to employ devious means of handling numbers outside this range, or numbers requiring a higher degree of significance.

First, consider the formula for Y_b in terms of N and n':

$$f(Y) = P_0^{\frac{1}{n'}} = \int_0^Y \frac{u^{N-1}\,e^{-u}}{(N-1)!}\,du, \qquad \text{(A-19)}$$

with $P_0 = 0.5$ and $Y = Y_b$. This equation was reduced to a differential equation of the form:

$$f'(Y) = \frac{Y^{N-1} e^{-Y}}{(N-1)!} , \qquad (A\text{-}20)$$

$$f_0 = f(Y_0) = \int_0^{Y_0} \frac{e^{-u} u^{N-1}}{(N-1)!} \, du \qquad (A\text{-}21)$$

where Y_0 is an initial approximation to Y_b, read to about two significant digits from Marcum's curves. This differential equation was integrated by Heun's method:

$$f_{j+1} = f_j + \frac{h}{2}\left[f'(Y_j) + f'(Y_{j+1})\right] , \quad j = 0, 1, 2, \ldots, \qquad (A\text{-}22)$$

where $Y_{j+1} = Y_j + h$. h was set arbitrarily to 0.01 when $f(Y_0) < f(Y_b)$ or -0.01 when $f(Y_0) > f(Y_b)$. The iteration was carried out up to $j = k$, such that $f(Y_k) \approx f(Y_b)$. Then $Y_b = Y_k$.

Note, for example, that $0.5^{1/10^8}$ and $0.5^{1/10^{10}}$ are identical to eight significant digits. Thus, double precision arithmetic, a programming technique which extends significance to about 16 digits, was used for the Heun integration; the Y_b's thus determined are accurate to at least seven significant digits.

In the above procedure, as well as in the computation of the detection probabilities, it is often necessary to evaluate the expression

$$E(a,p) = \frac{e^{-u} u^p}{p!} . \qquad (A\text{-}23)$$

Appendix A

If p is 3000, say, and u is of that order of magnitude, then numbers such as e^{-3000}, 3000^{3000}, 3000!, which are well outside the limitations of the computer, come into play. This problem may be handled by evaluating

$$\ln E = -u + p \ln u - \sum_{i=1}^{p} (\ln i). \tag{A-24}$$

Then,

$$E = e^{\ln E}. \tag{A-25}$$

Note that E is always less than one, and is generally large enough so that ln E is easily handled.

To evaluate the incomplete gamma function, one first computes the maximum term in this logarithmic fashion, and then sums about that point to the desired degree of significance. Each successive term is computed as the product of the preceding term and the appropriate ratio.

Similar techniques are used in the computation of the detection probabilities. For example, in case 4, the maximum term is computed thus:

$$\ln T_{max} = k \ln c + (N - k) \ln (1 - c) + \sum_{i=1}^{N} (\ln i) - \sum_{i=1}^{k} (\ln i) - \sum_{i=1}^{N-k} (\ln i) + \ln \Gamma_I (cY_b, 2N-1-k), \tag{A-26}$$

$$T_{max} = e^{\ln T_{max}}. \tag{A-27}$$

The sum is then carried out about this point, as with the incomplete gamma function.

Appendix A

The error incurred by truncating the series for the incomplete gamma function is estimated as follows. Equation (A-3a), which is used when a > p can be written:

$$f(a,p) = 1 - \frac{e^{-a}\, a^p}{p!}\left[1 + \frac{p}{a} + \frac{p(p-1)}{a^2} + \ldots \frac{p!}{a^p}\right]. \qquad \text{(A-28)}$$

In the above expression the first K terms of the bracketted sum are used. The criteria for determining K is that the K + 1 term is less than 10^{-8} times the sum of the first K terms. The remainder of the terms are dropped.

The sum, R, of the remaining terms is:

$$R = \left[\frac{p(p-1)(p-2)\ldots(p-K)}{a^{K+1}}\right]$$

$$\left[1 + \frac{p-K-1}{a} + \frac{p-K-1)(p-K-a)}{a^2} + \ldots \frac{(p-K-1)!}{a^K}\right]. \qquad \text{(A-29)}$$

The coefficient of this expression is by definition less than 10^{-8} imes the computed sum, C, therefore

$$R < 10^{-8}\, C\left[1 + \frac{p-K-1}{a} + \frac{(p-K-1)(p-K-2)}{a^2} + \ldots \frac{p-K-1}{a^K}\right] \qquad \text{(A-30)}$$

The ratio of the remainder to the computed value is then bounded by the following:

Appendix A

$$0 < \frac{R}{C} < 10^{-8} \left[\frac{a}{a - p + K} \right] . \qquad \text{(A-31)}$$

If $a < p$ the value of $f(a,p)$ is computed from Equation (A-3b) by a similar method. For this case, the ratio of the remainder to the computed value may be bounded by the expression:

$$0 < \frac{R}{C} < 10^{-8} \left[\frac{p + K + 2}{p + K + 2 - a} \right] . \qquad \text{(A-32)}$$

An estimate of a lower bound on K for $a > p$ may be obtained from:

$$K \approx \frac{1}{4} - \frac{p}{2} \ln \frac{p}{a} + \left[\left(\frac{1}{4} - \frac{p}{2} \ln \frac{p}{a} \right)^2 - p \ln \left(\frac{10^{-8}}{1 - \frac{p}{a}} \right) \right]^{1/2} \qquad \text{(A-33)}$$

for $a < p$

$$K \approx - \frac{1}{4} + \frac{p}{2} \ln \frac{a}{p} + \left[\left(\frac{1}{4} - \frac{p}{2} \ln \frac{a}{p} \right)^2 - p \ln \left(\frac{10^{-8}}{1 - \frac{a}{p}} \right) \right]^{1/2} \qquad \text{(A-34)}$$

Substitution of limiting values of a and p in expressions A-31 and A-32 indicates that the truncation error influences only slightly the value of the seventh significant decimal digit.

The value of K associated with the sums of the series is large when N is large. Since the computed value is the sum of only positive numbers and since truncated arithmetic was used, the computed value is biased to the low side of the true value. An estimate of the size of the computer truncation

error indicates that the sixth significant decimal digit would not be affected in the worst case. The computed data are correct therefore to at least six significant decimal digits.

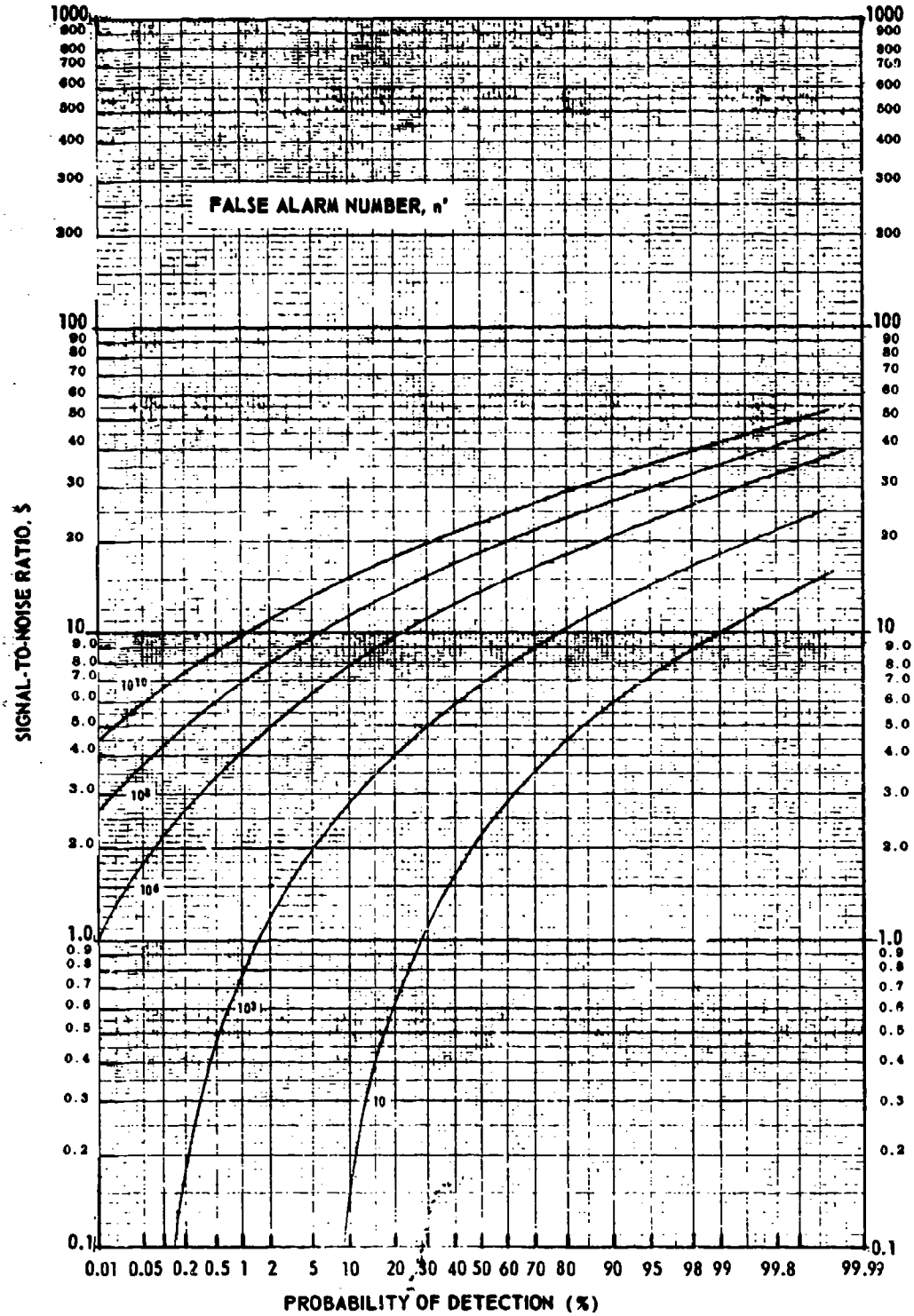

Fig. 2 PROBABILITY OF DETECTING A NON-FLUCTUATING TARGET
Pulses Integrated, N 1

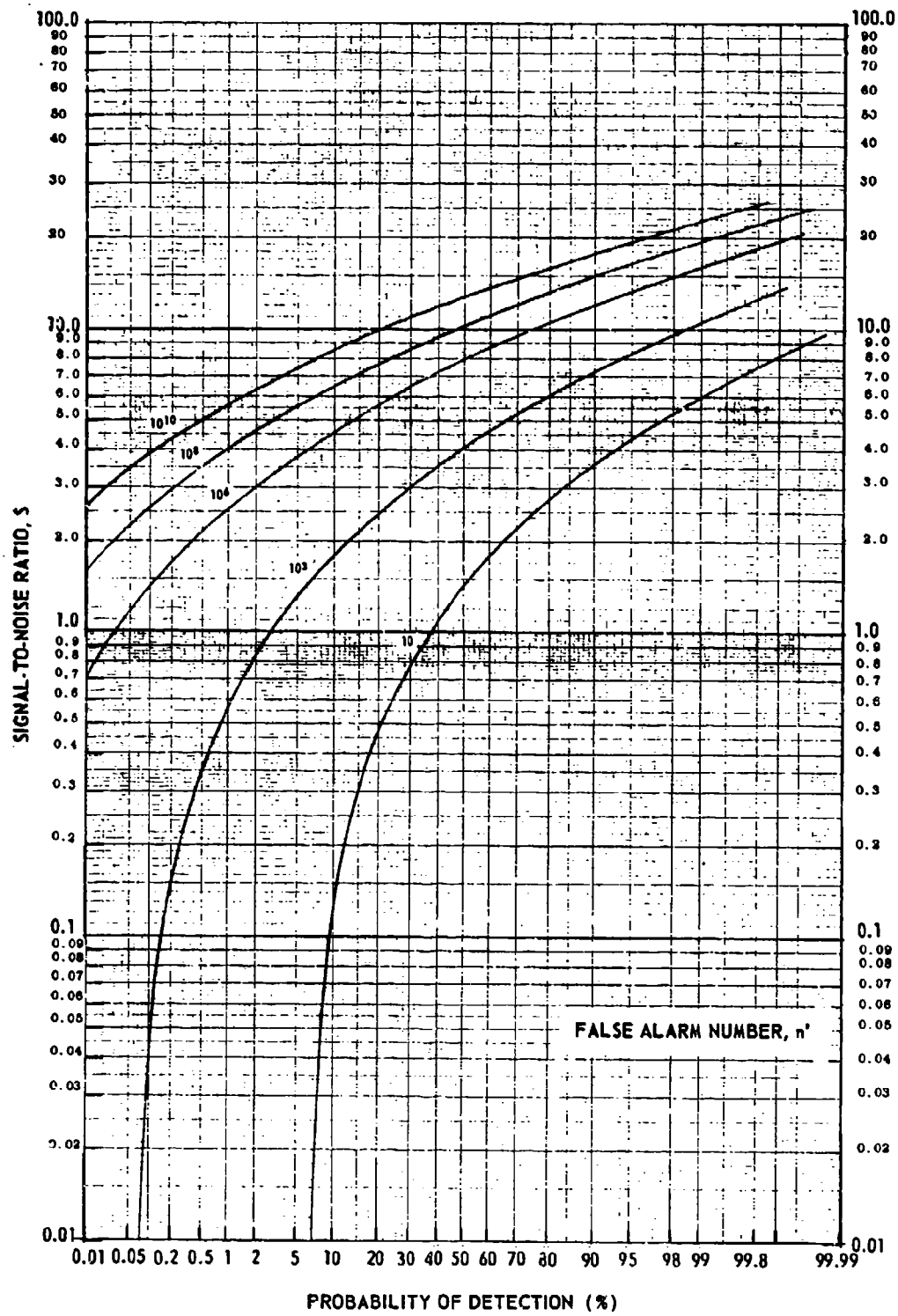

Fig. 3 PROBABILITY OF DETECTING A NON-FLUCTUATING TARGET
Pulses Integrated, N 2

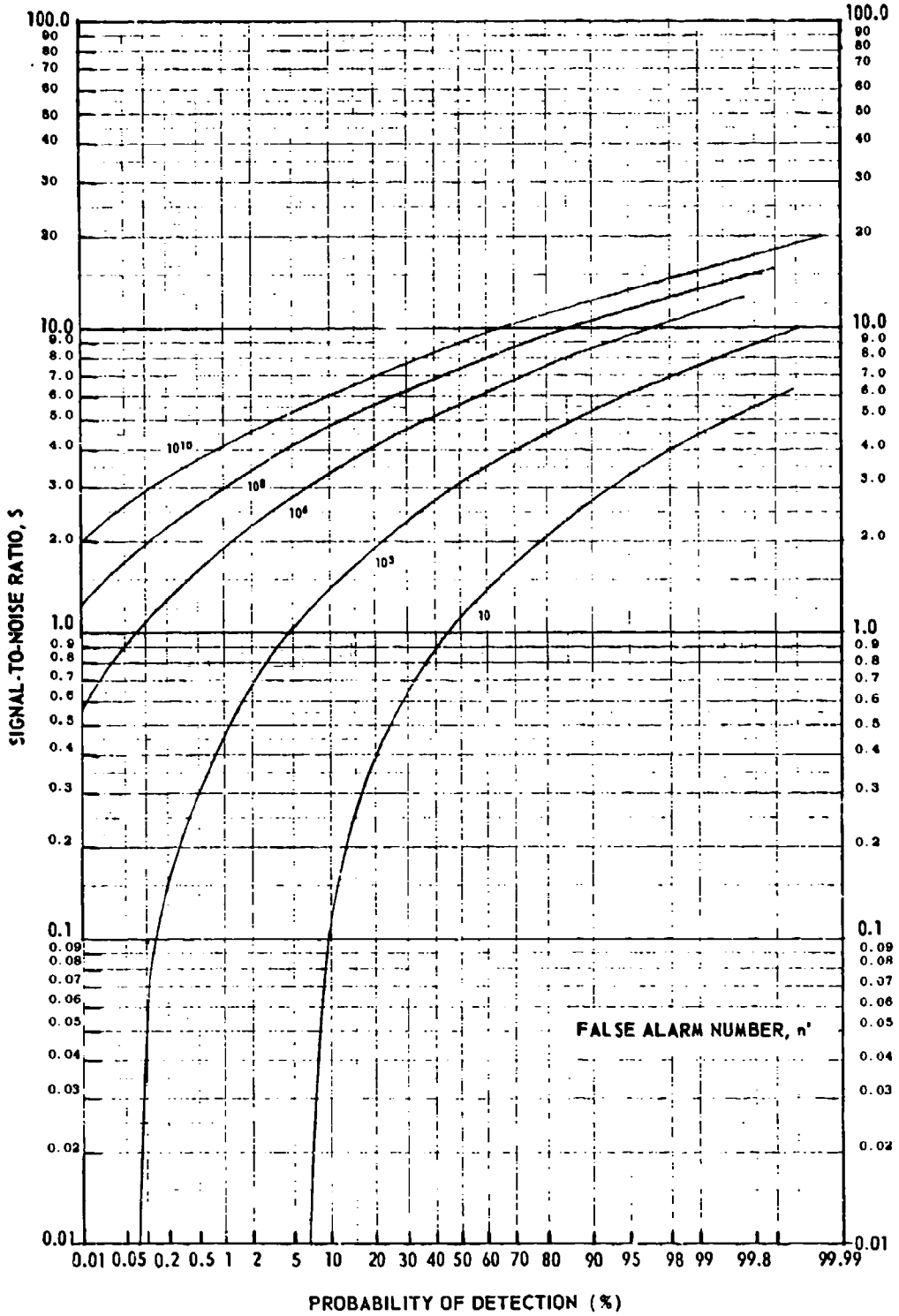

Fig. 4 PROBABILITY OF DETECTING A NON-FLUCTUATING TARGET
Pulses Integrated, N 3

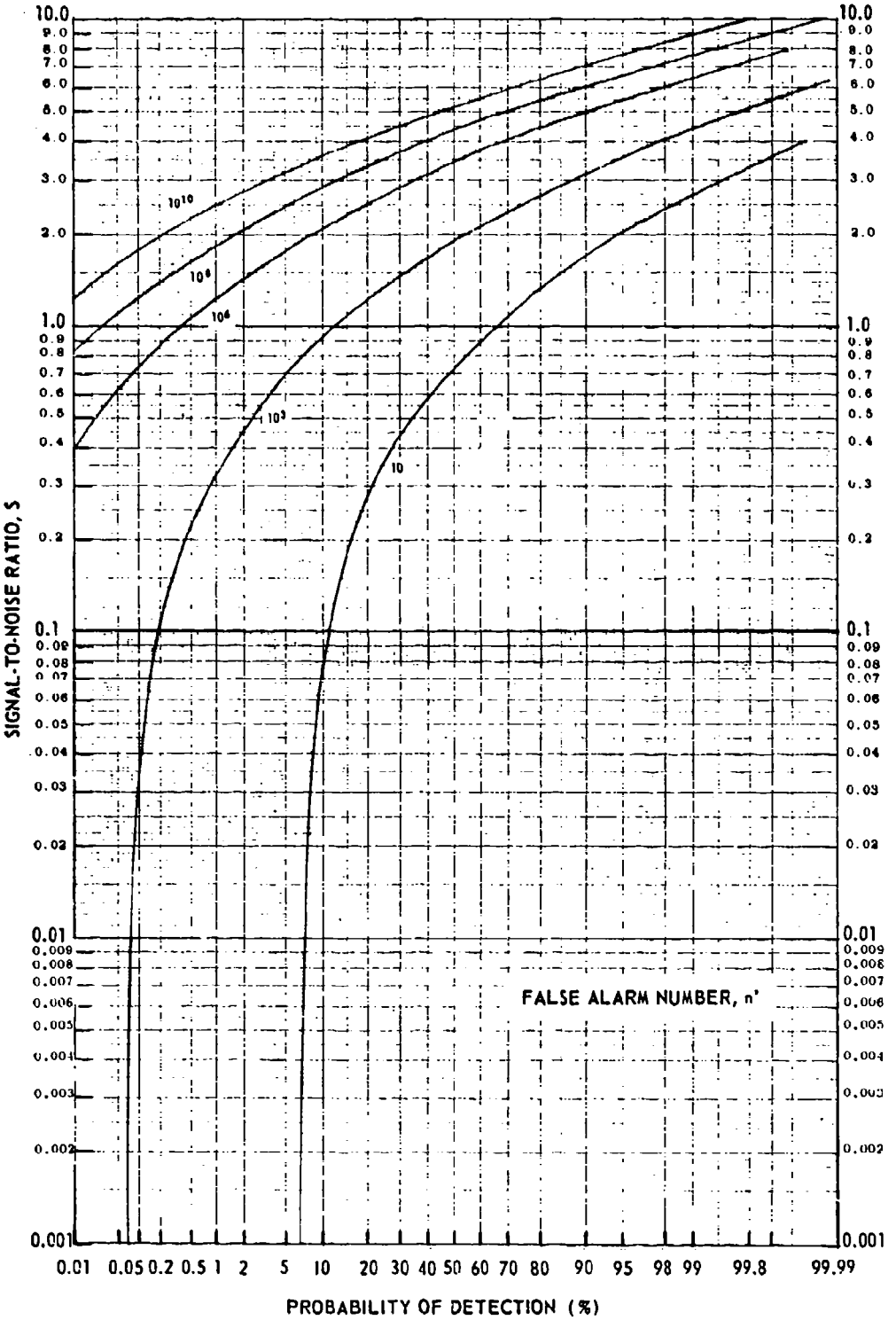

Fig. 5 PROBABILITY OF DETECTING A NON-FLUCTUATING TARGET
Pulses Integrated, N 6

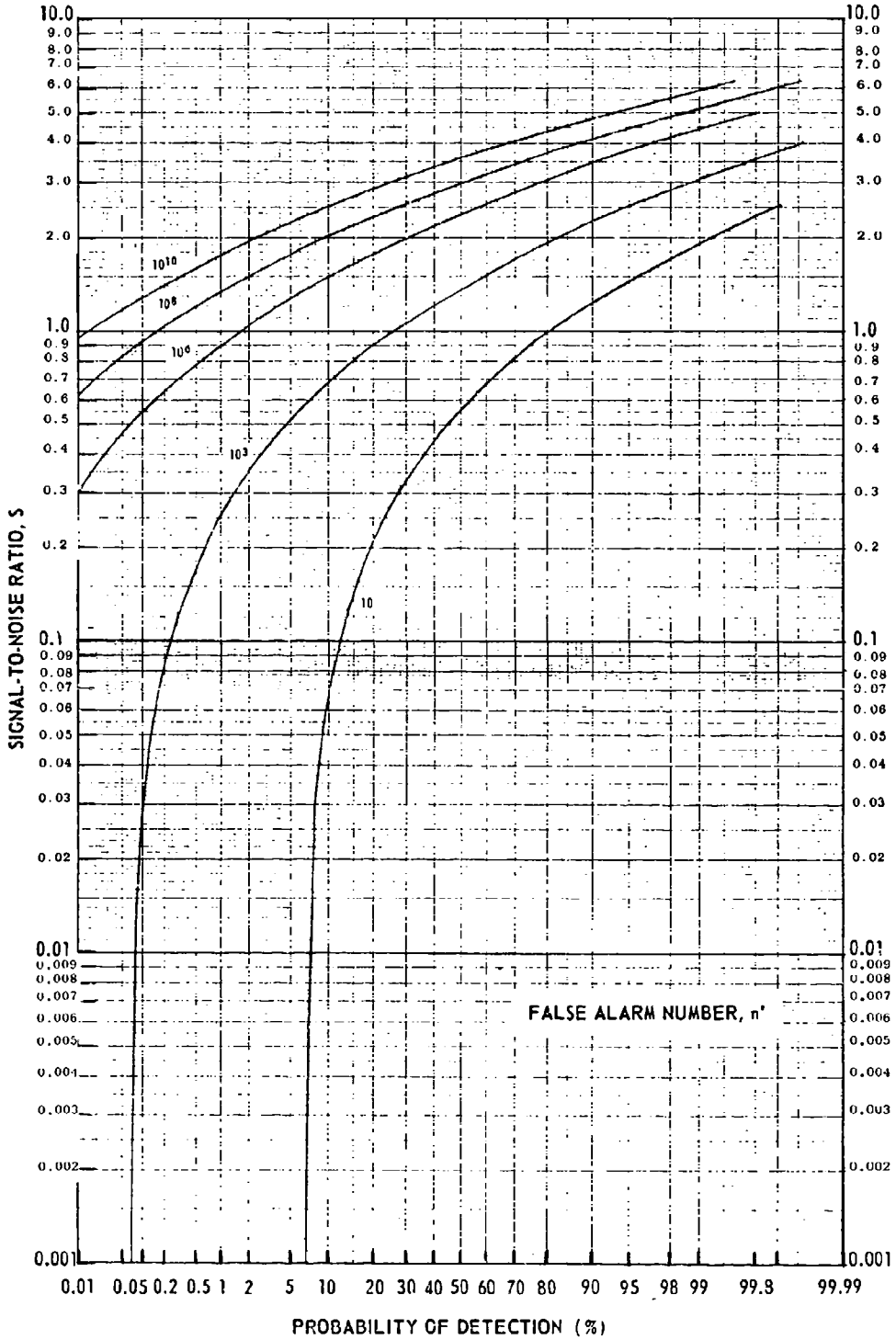

Fig. 6 PROBABILITY OF DETECTING A NON-FLUCTUATING TARGET
Pulses Integrated, 10

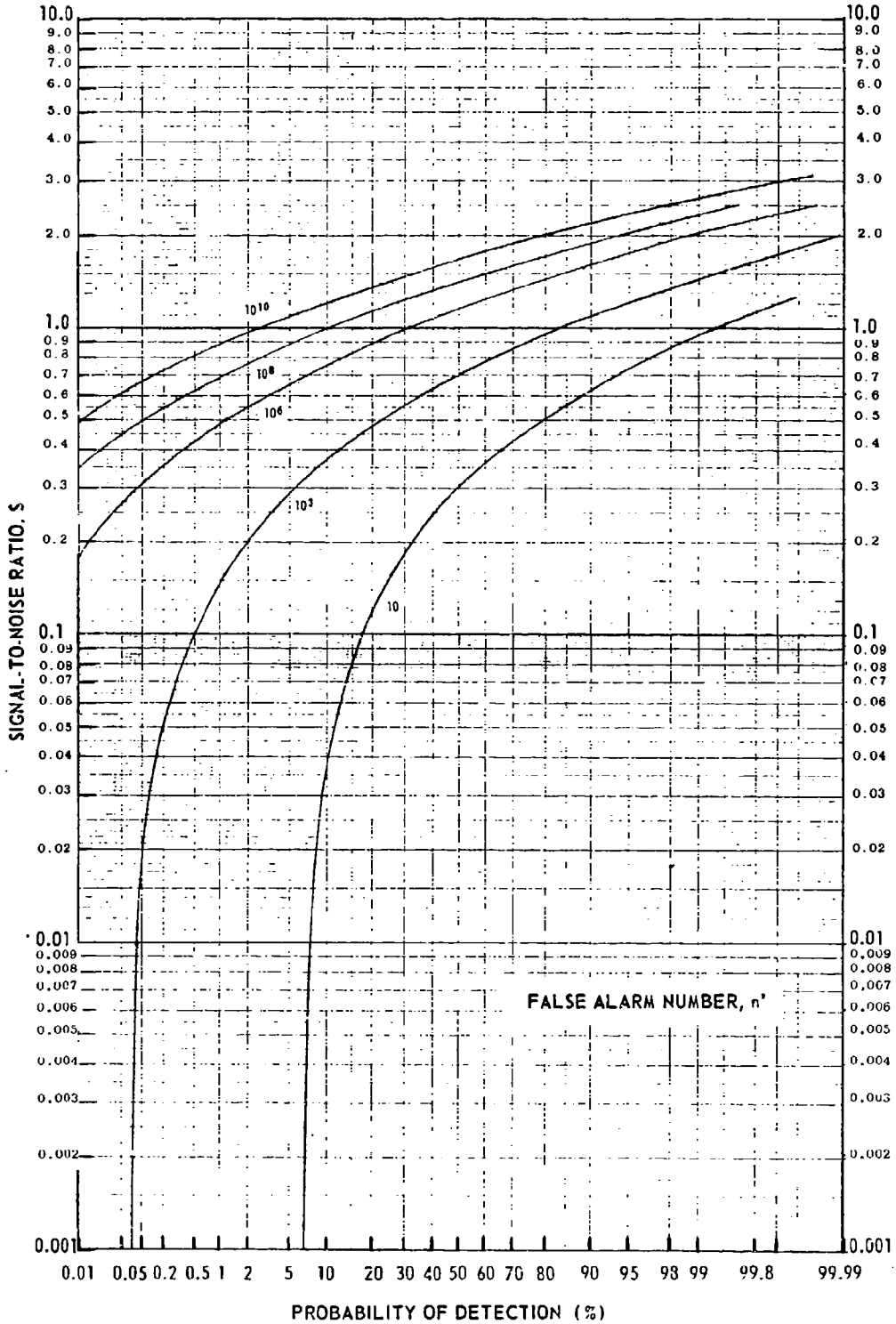

Fig. 7 PROBABILITY OF DETECTING A NON-FLUCTUATING TARGET
Pulses Integrated, N 30

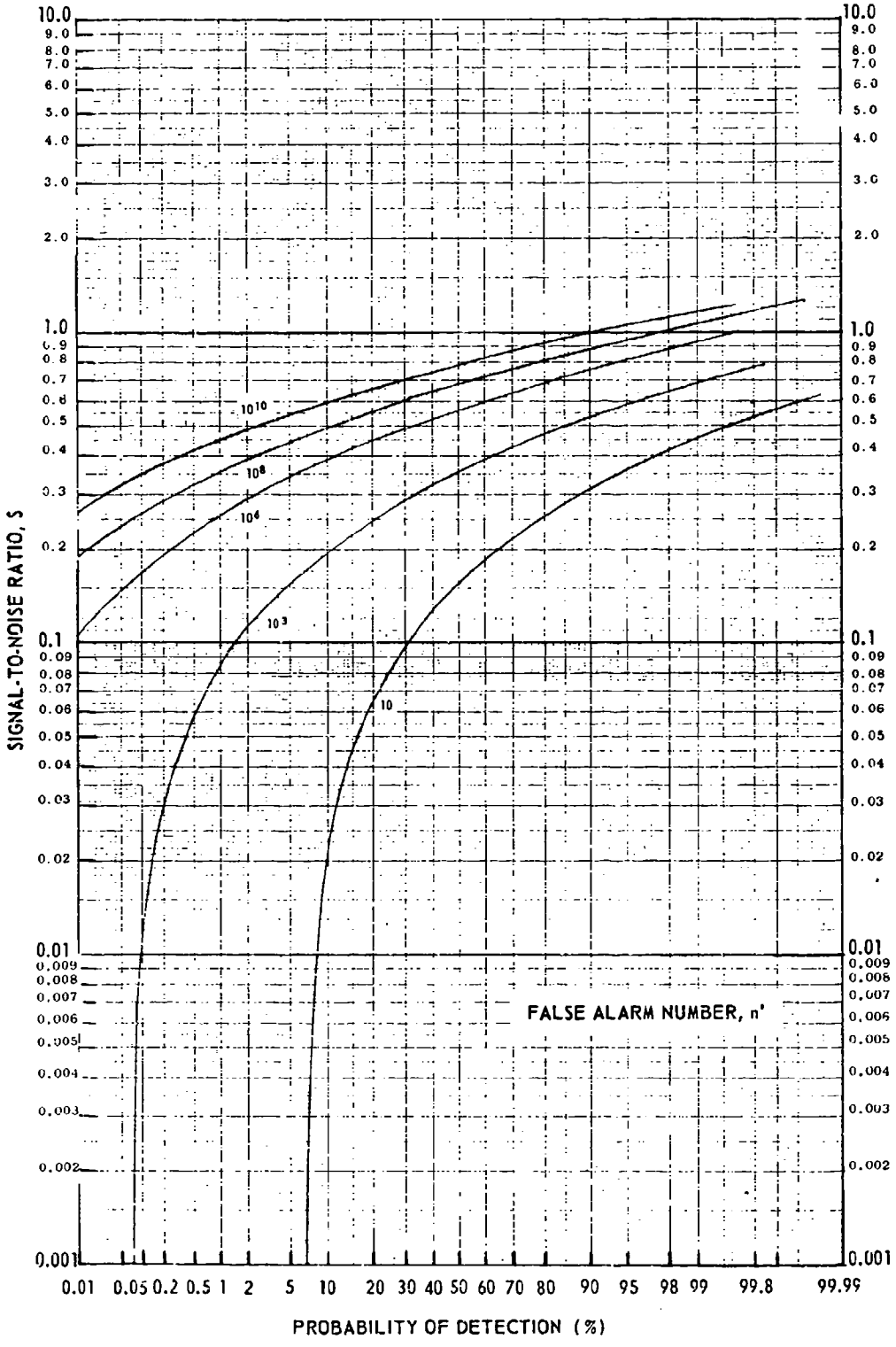

Fig. 8 PROBABILITY OF DETECTING A NON-FLUCTUATING TARGET
Pulses Integrated, N 100

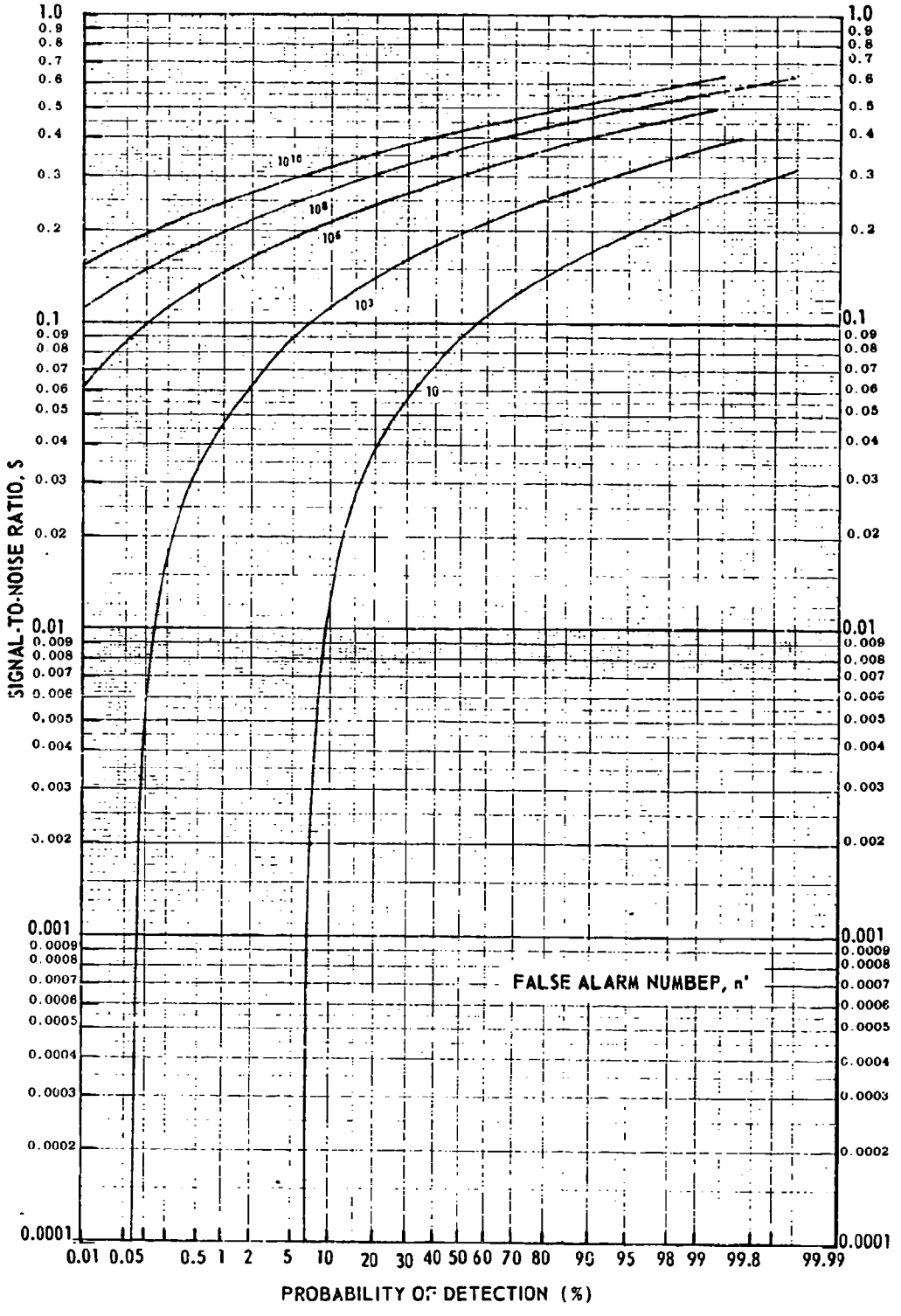

Fig. 9 PROBABILITY OF DETECTING A NON-FLUCTUATING TARGET
Pulses Integrated, N 300

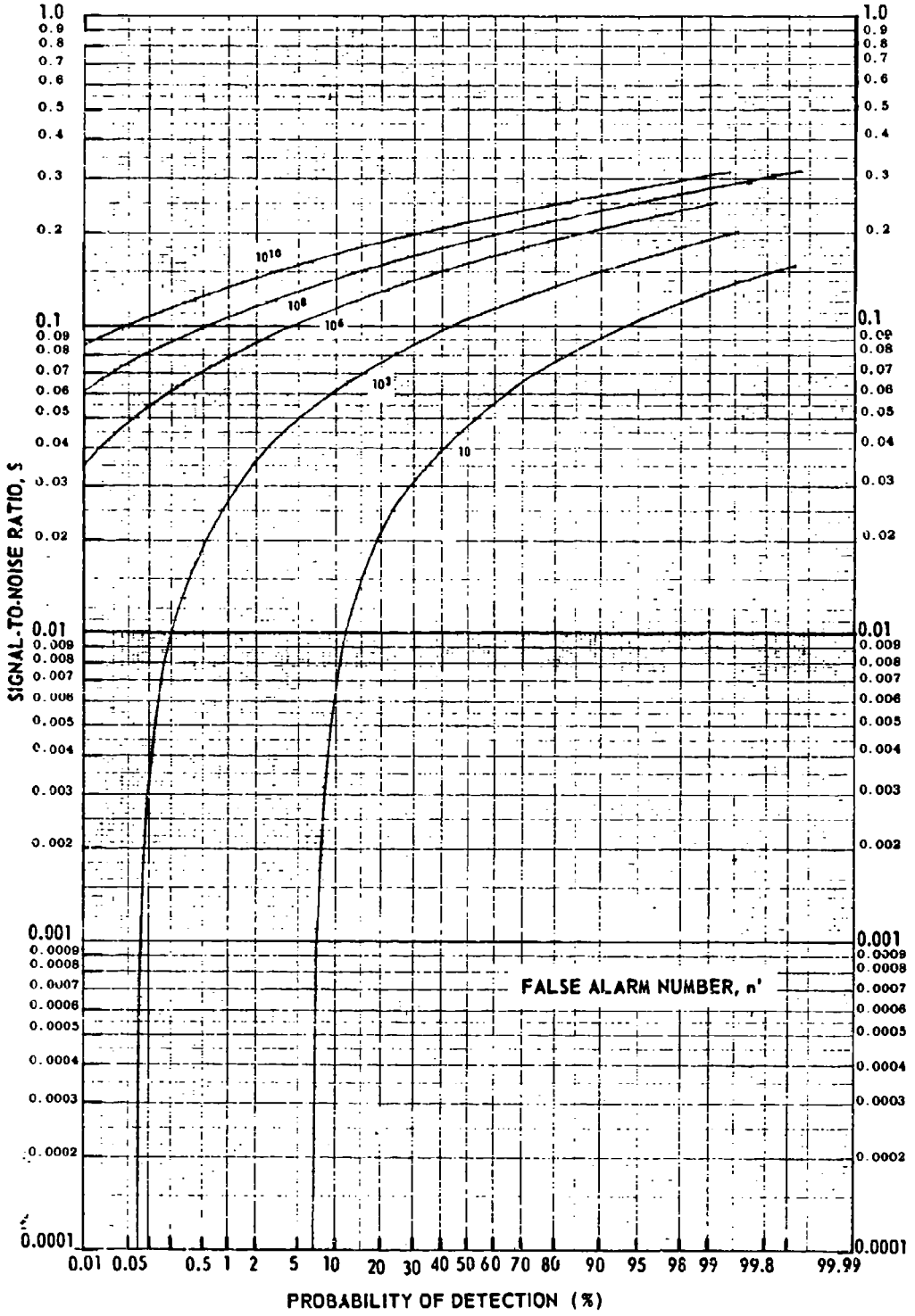

Fig. 10 PROBABILITY OF DETECTING A NON-FLUCTUATING TARGET
Pulses Integrated, N 1000

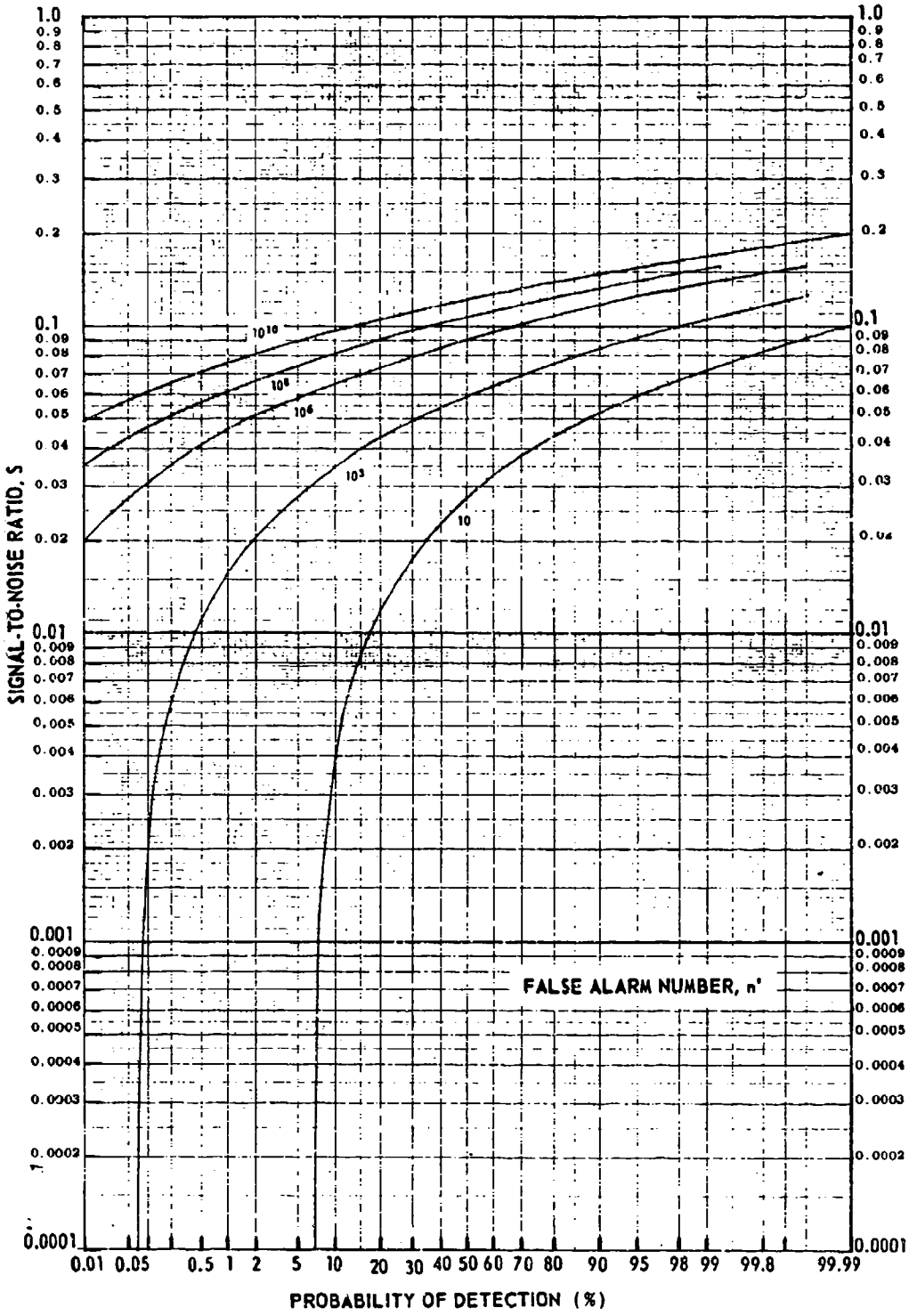

Fig. 11 PROBABILITY OF DETECTING A NON-FLUCTUATING TARGET
Pulses Integrated, N 3000

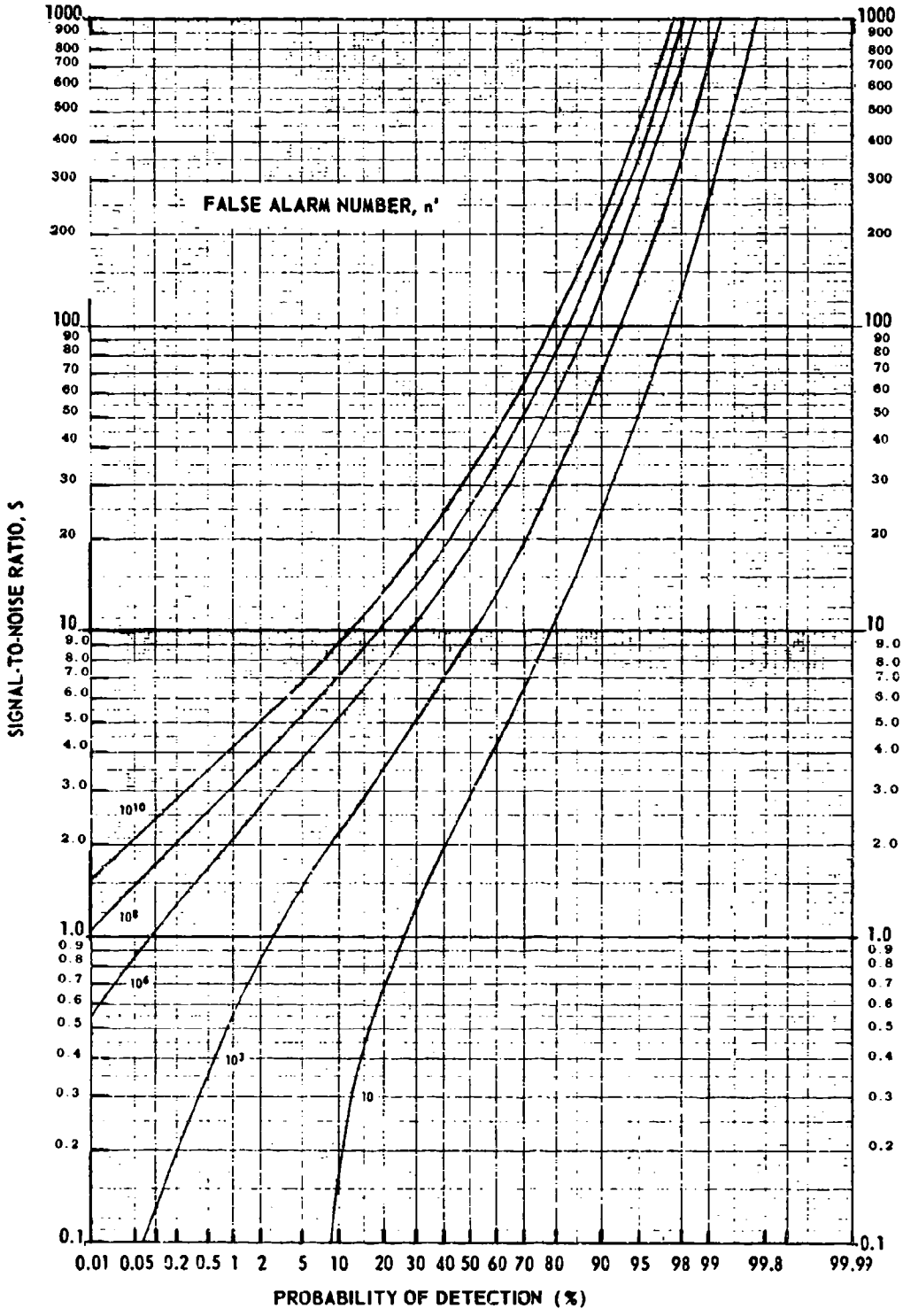

Fig. 12 PROBABILITY OF DETECTING A FLUCTUATING TARGET - CASES 1 AND 2
Pulses Integrated, N 1

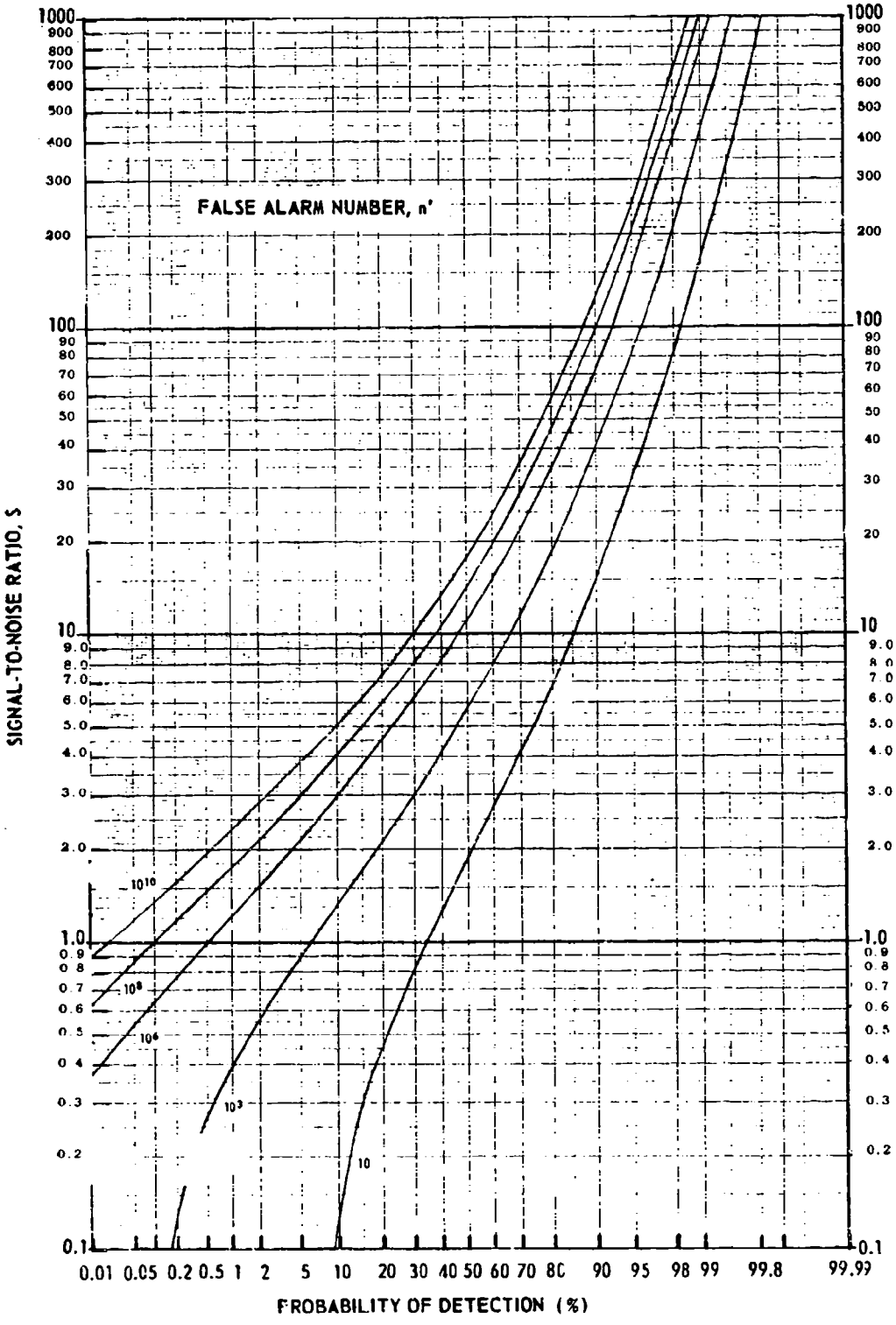

Fig. 13 PROBABILITY OF DETECTING A FLUCTUATING TARGET - CASE 1
Pulses Integrated, N 2

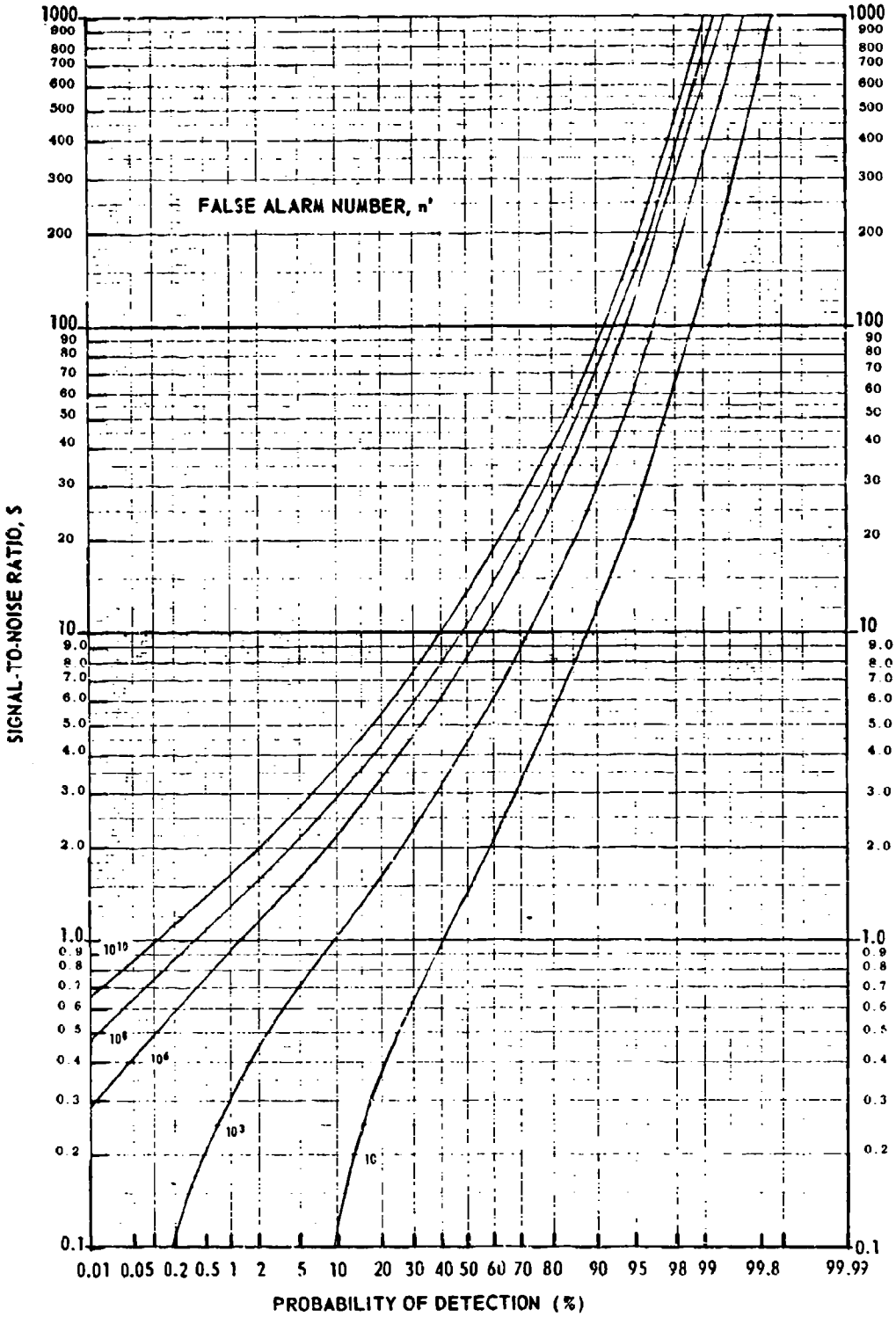

Fig. 14 PROBABILITY OF DETECTING A FLUCTUATING TARGET - CASE 1
Pulses Integrated, N 3

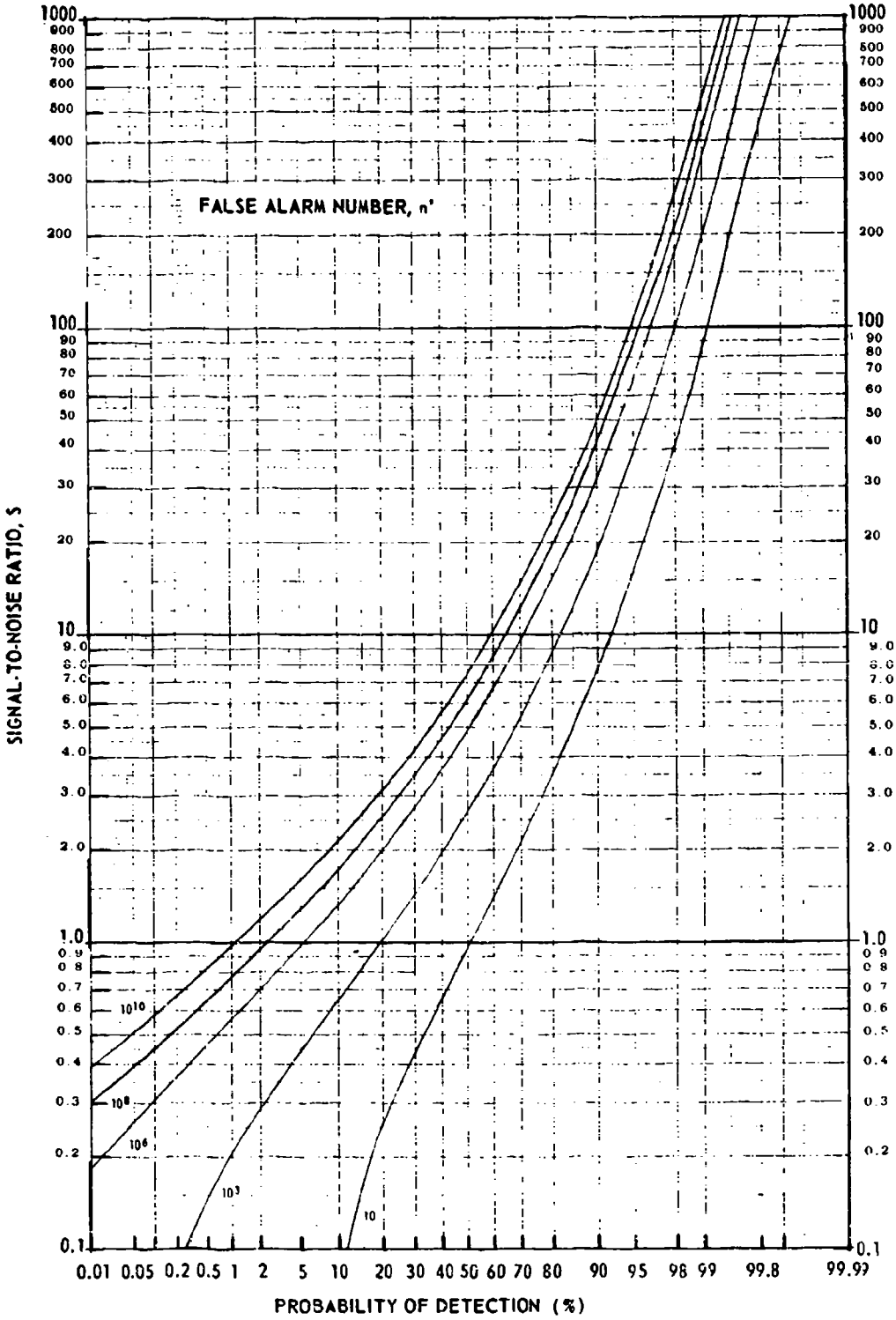

Fig. 15 PROBABILITY OF DETECTING A FLUCTUATING TARGET - CASE 1
Pulses Integrated, N 6

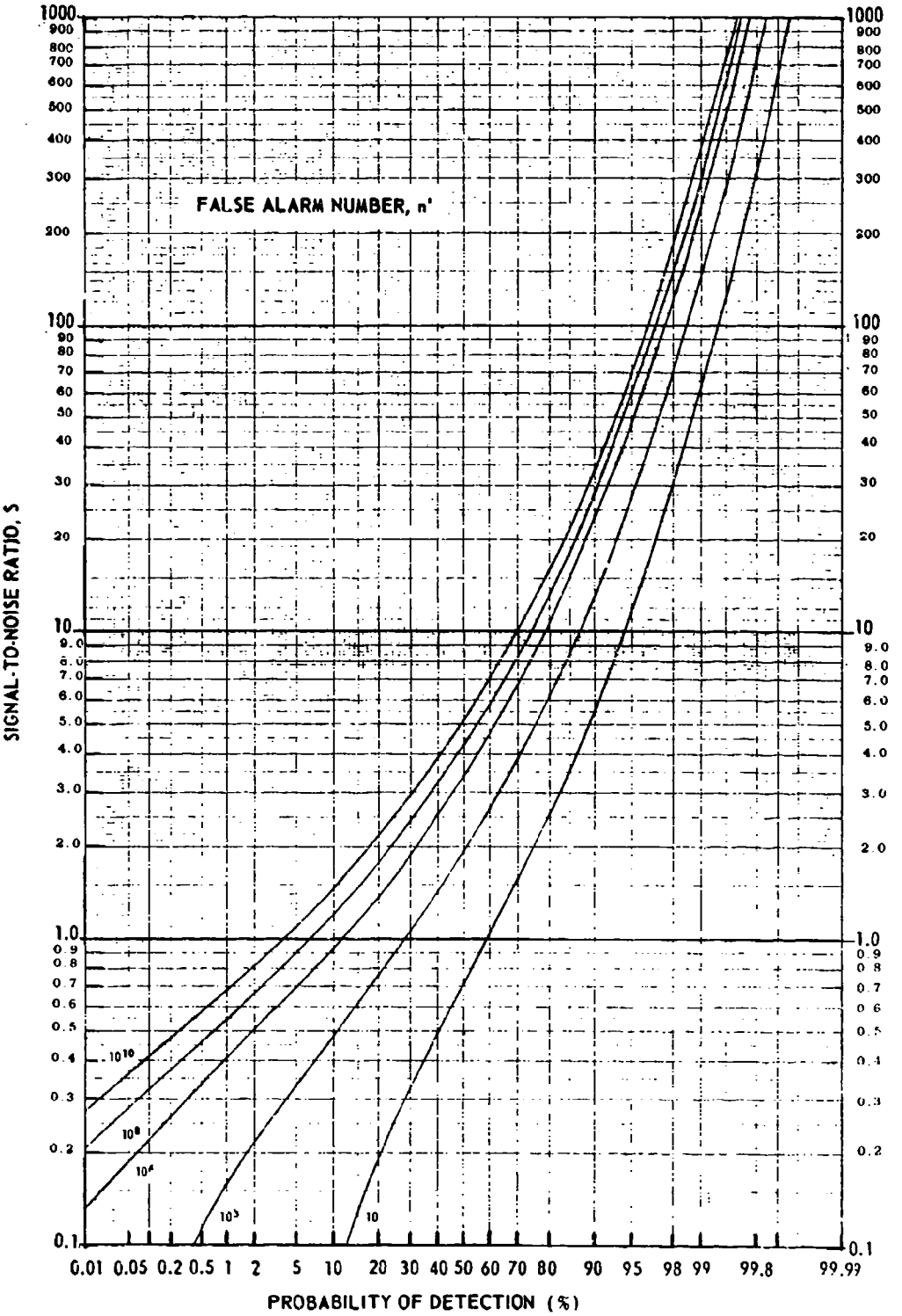

Fig. 16 PROBABILITY OF DETECTING A FLUCTUATING TARGET - CASE 1
Pulses Integrated, N 10

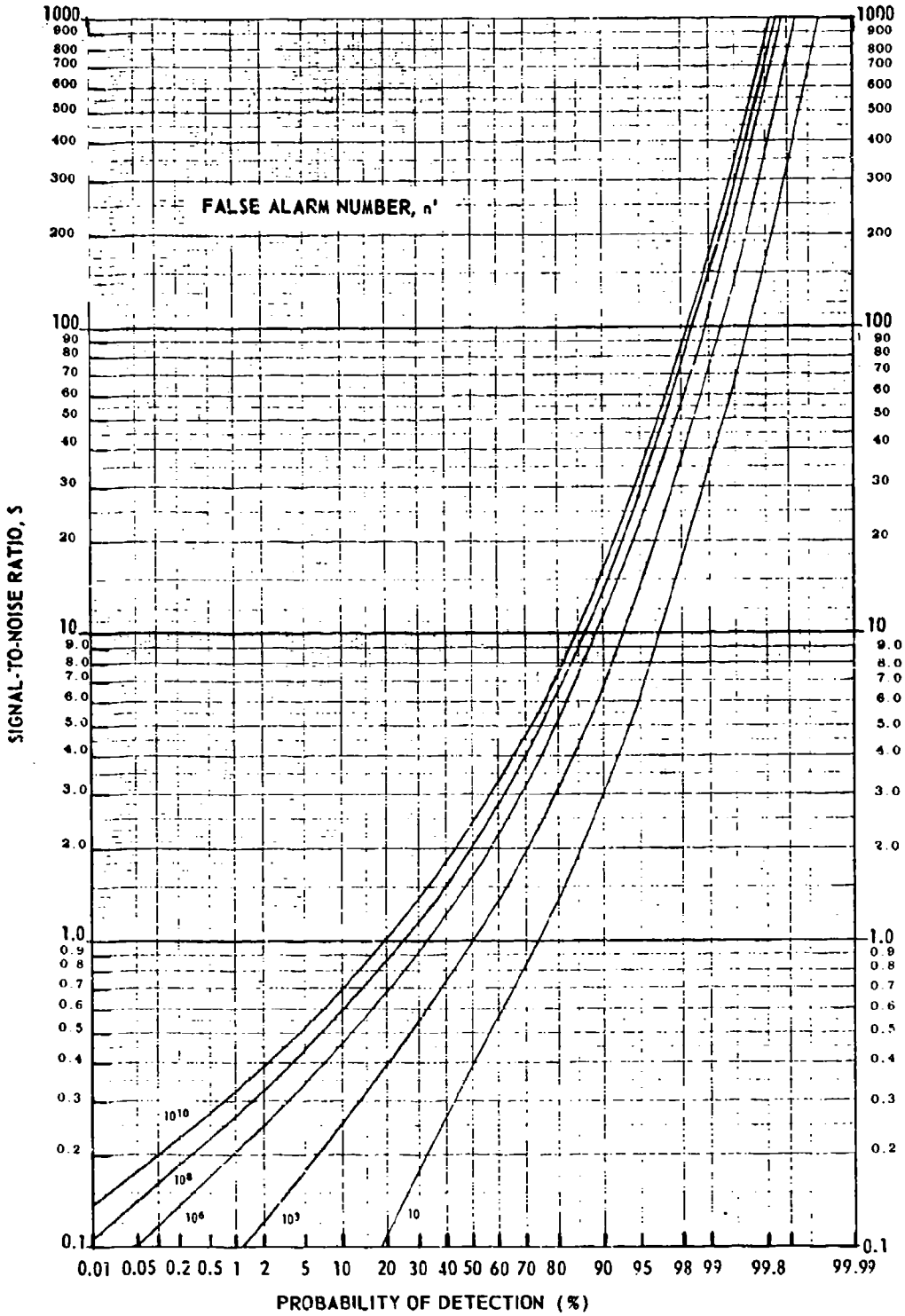

Fig. 17 PROBABILITY OF DETECTING A FLUCTUATING TARGET - CASE 1
Pulses Integrated N 30

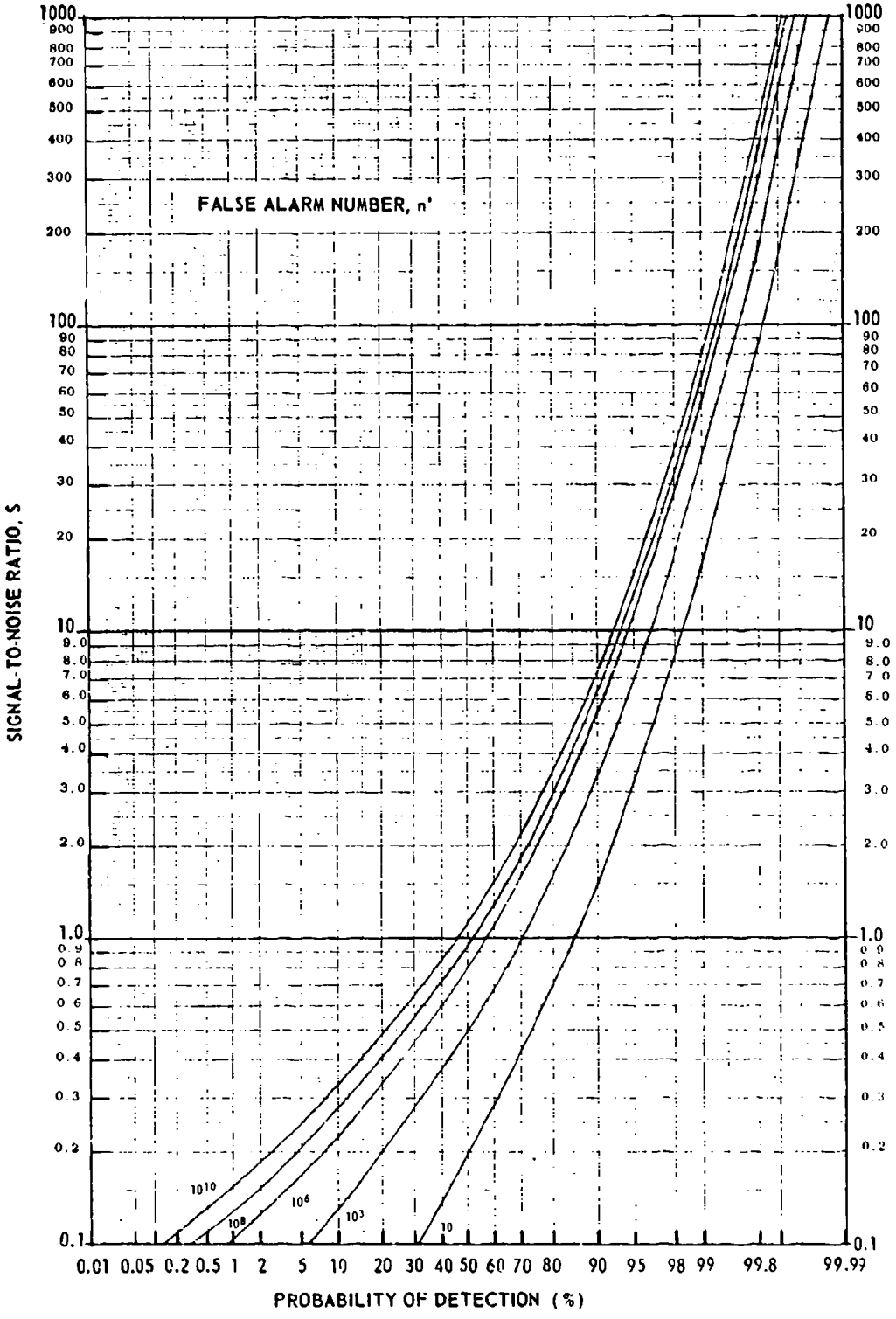

Fig. 18 PROBABILITY OF DETECTING A FLUCTUATING TARGET - CASE 1
Pulses Integrated, N 100

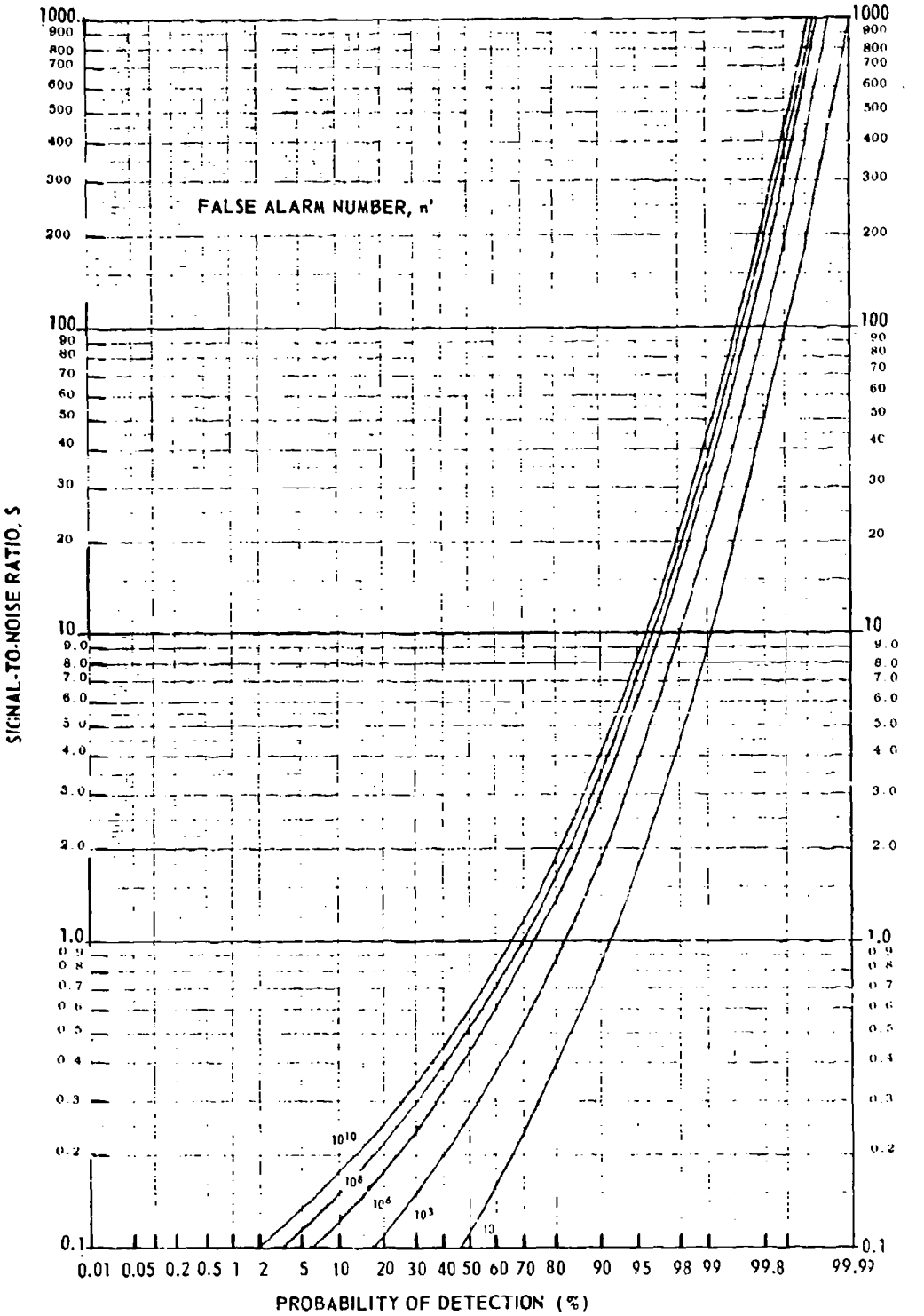

Fig. 19 PROBABILITY OF DETECTING A FLUCTUATING TARGET - CASE 1
Pulses Integrated, N 300

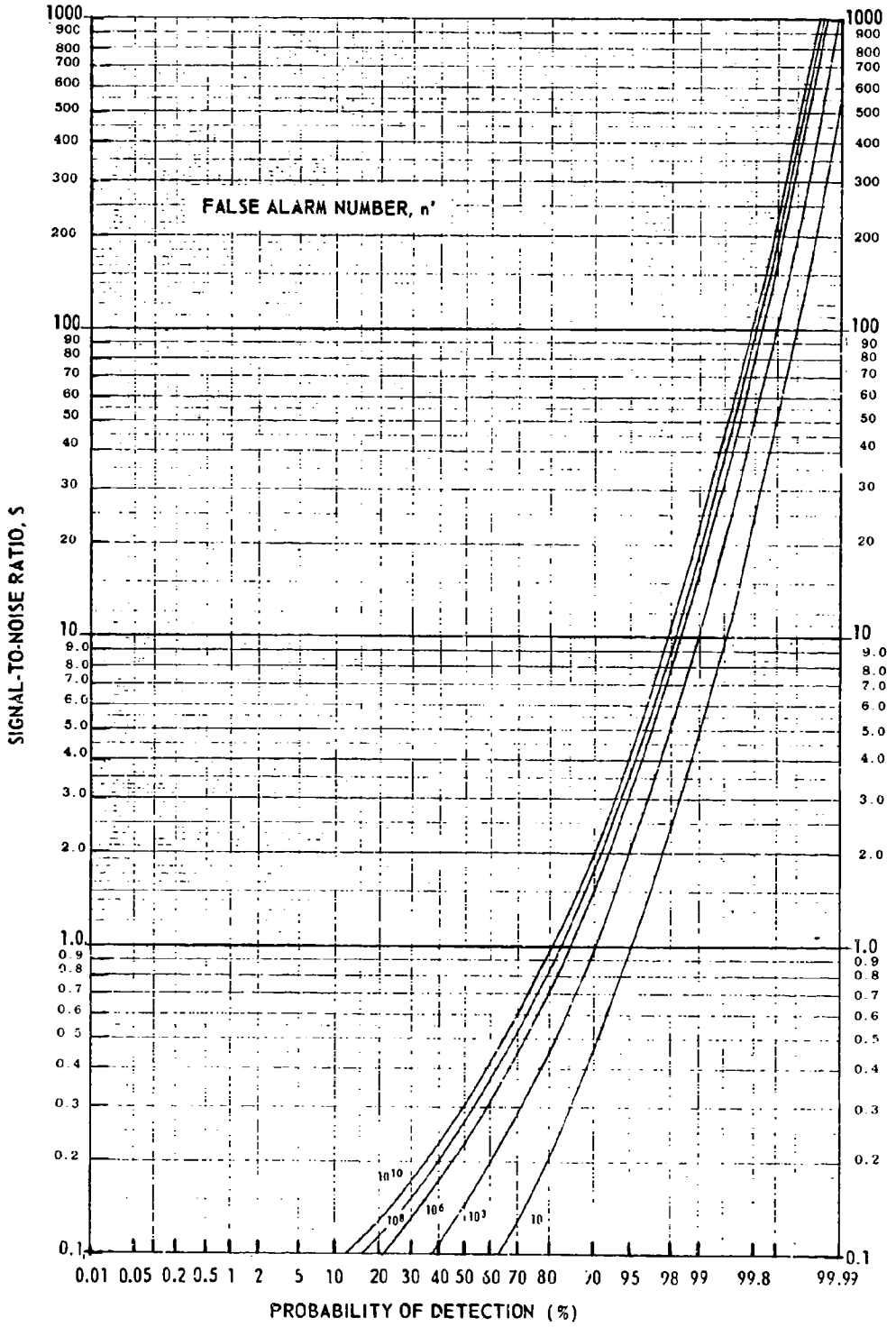

Fig. 20 PROBABILITY OF DETECTING A FLUCTUATING TARGET - CASE 1
Pulses Integrated N 1000

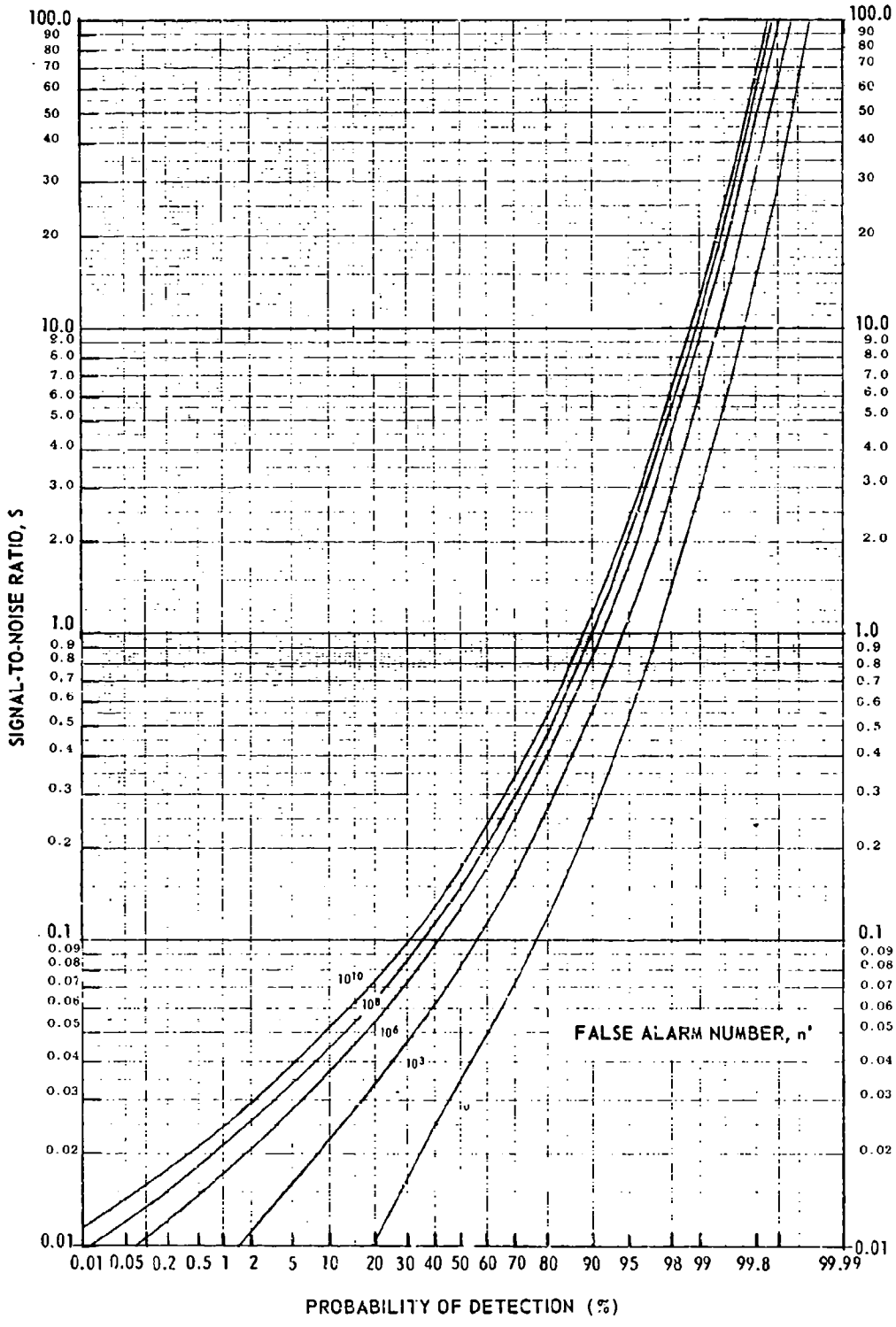

Fig. 21 PROBABILITY OF DETECTING A FLUCTUATING TARGET - CASE 1
Pulses Integrated, N 3000

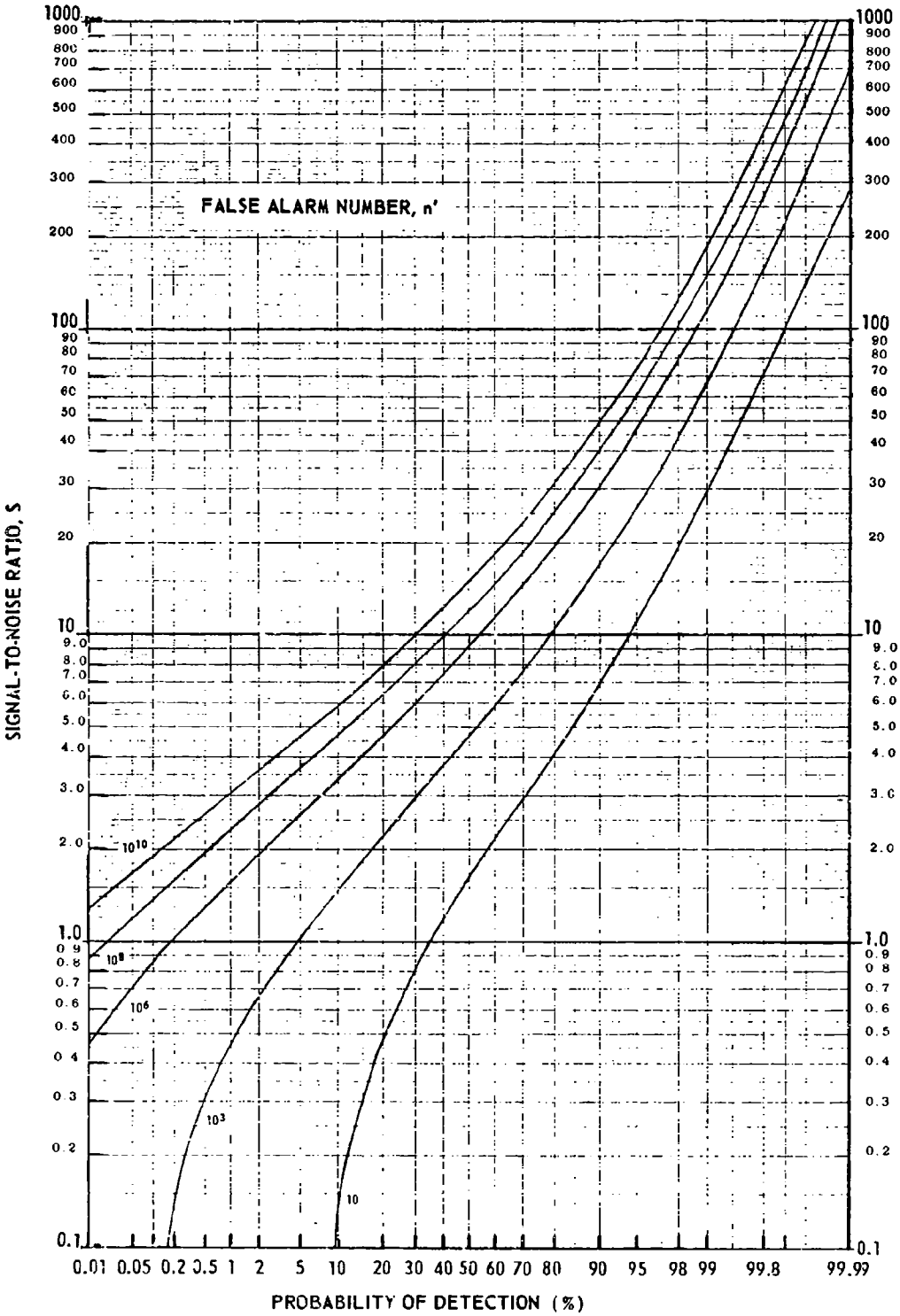

Fig. 22 PROBABILITY OF DETECTING A FLUCTUATING TARGET - CASE 2
Pulses Integrated, N 2

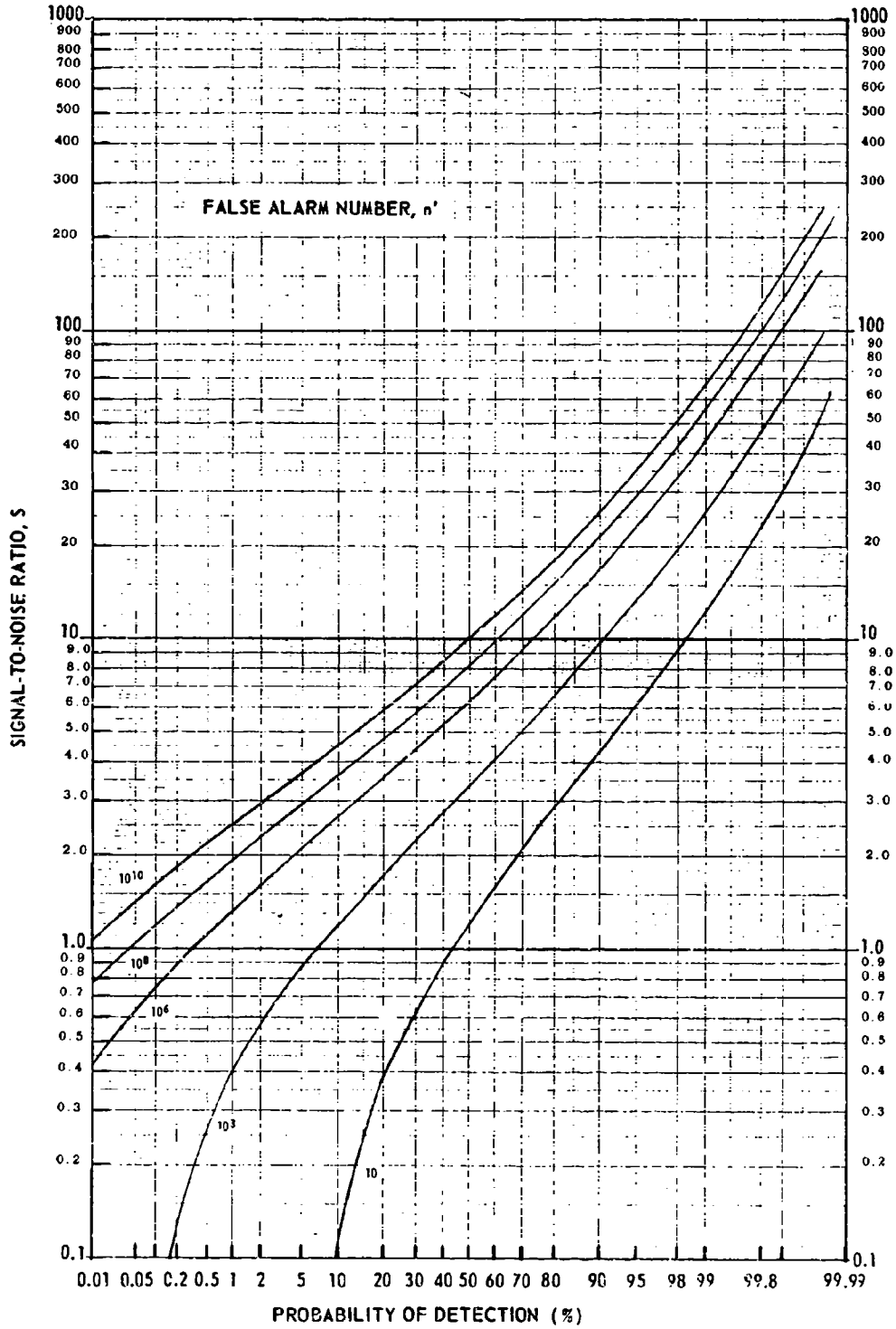

Fig. 23 PROBABILITY OF DETECTING A FLUCTUATING TARGET - CASE 2
Pulses Integrated, N 3

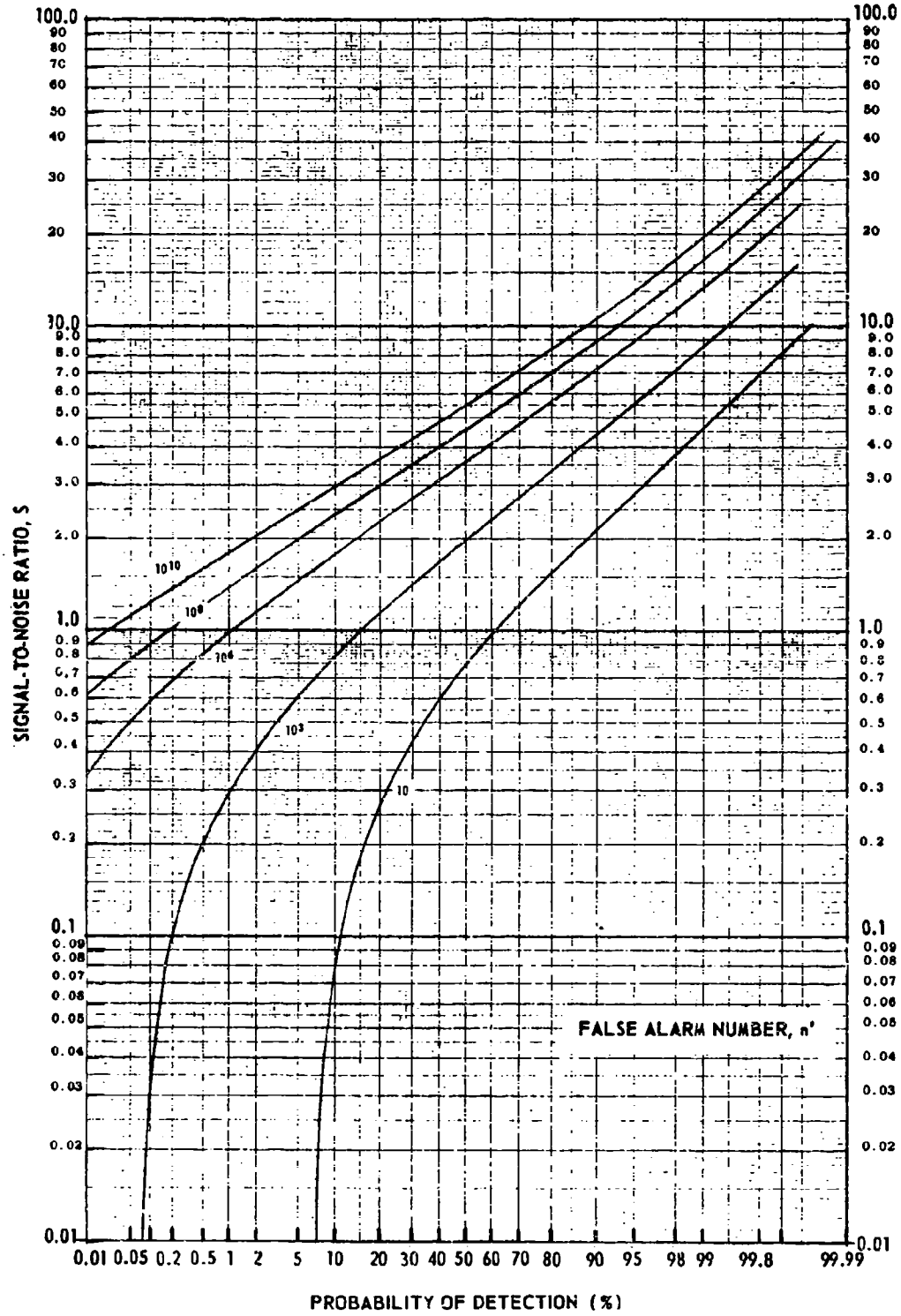

Fig. 24 PROBABILITY OF DETECTING A FLUCTUATING TARGET - CASE 2
Pulses Integrated, N 6

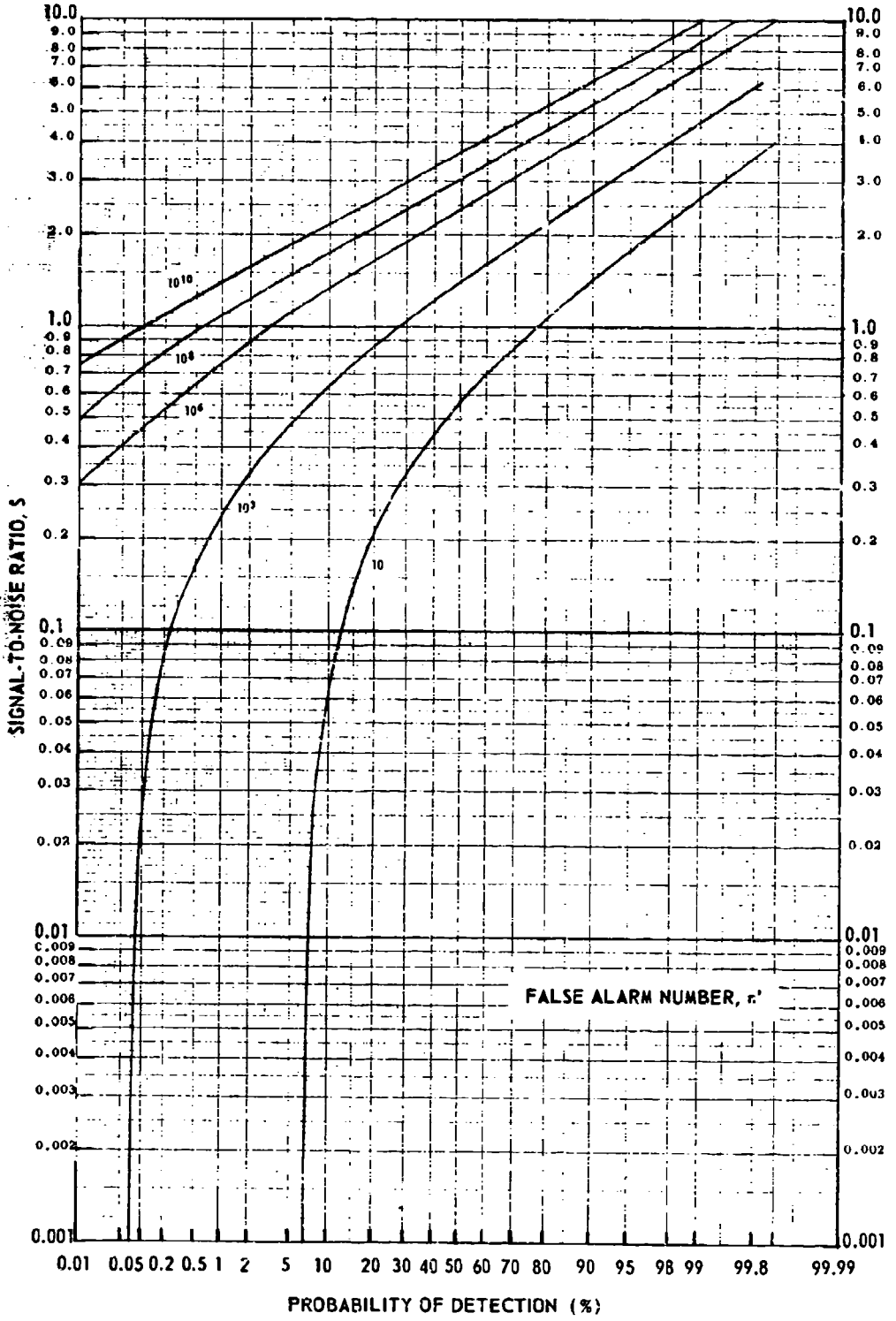

Fig. 25 PROBABILITY OF DETECTING A FLUCTUATING TARGET - CASE 2
Pulses Integrated, N 10

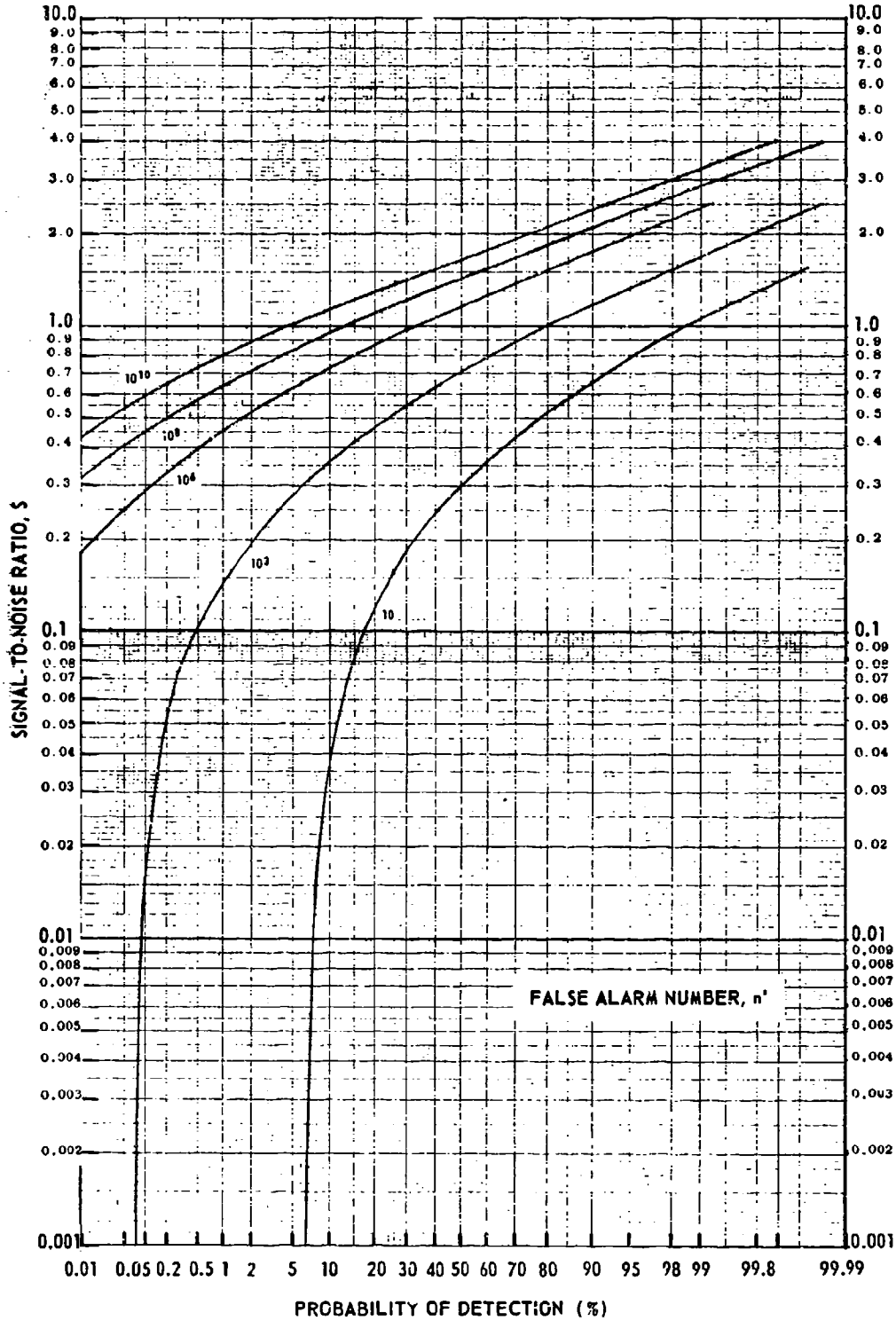

Fig. 26 PROBABILITY OF DETECTING A FLUCTUATING TARGET - CASE 2
Pulses Integrated, N 30

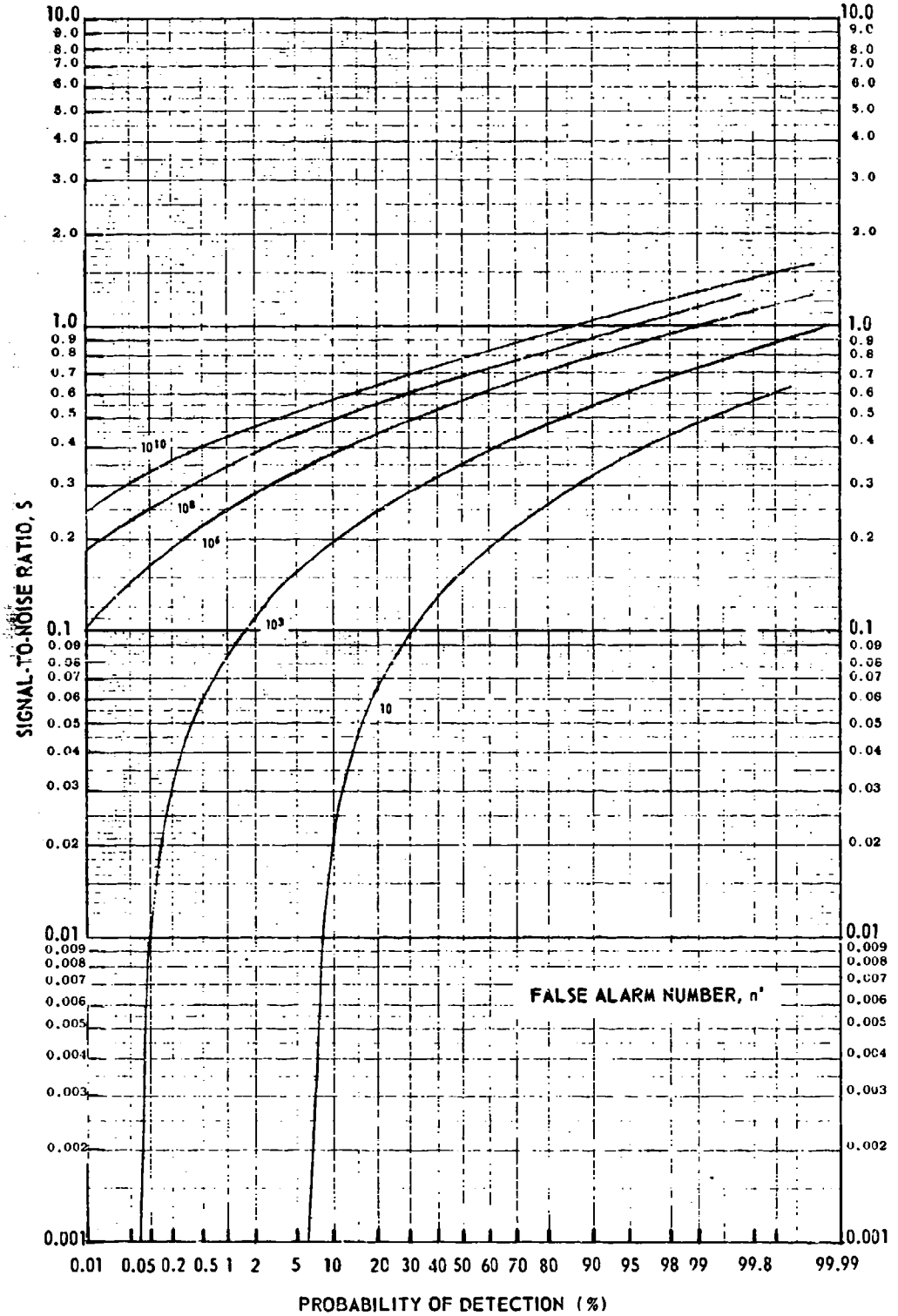

Fig. 27 PROBABILITY OF DETECTING A FLUCTUATING TARGET - CASE 2
Pulses Integrated, N 100

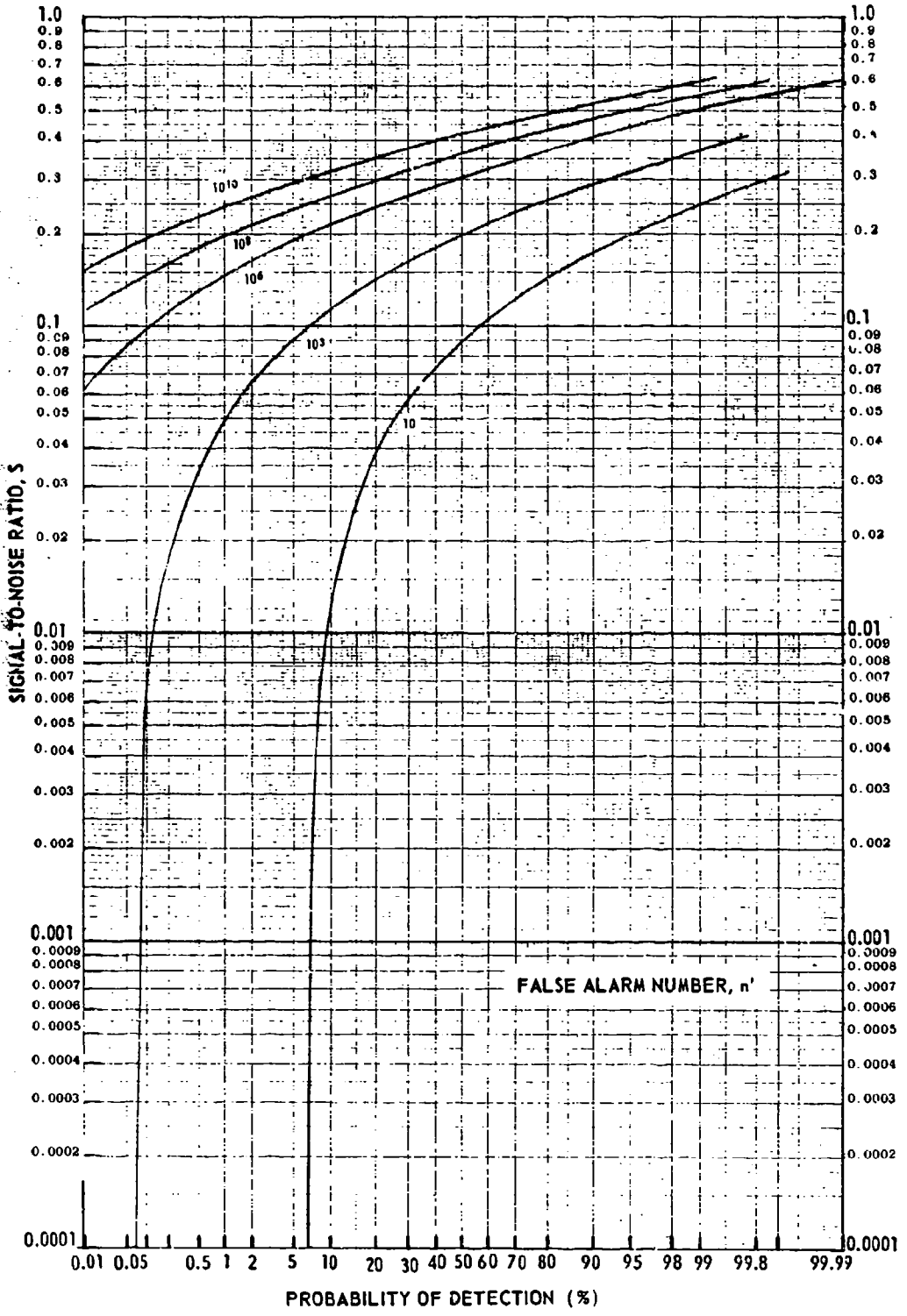

Fig. 28 PROBABILITY OF DETECTING A FLUCTUATING TARGET - CASE 2
Pulses Integrated, N 300

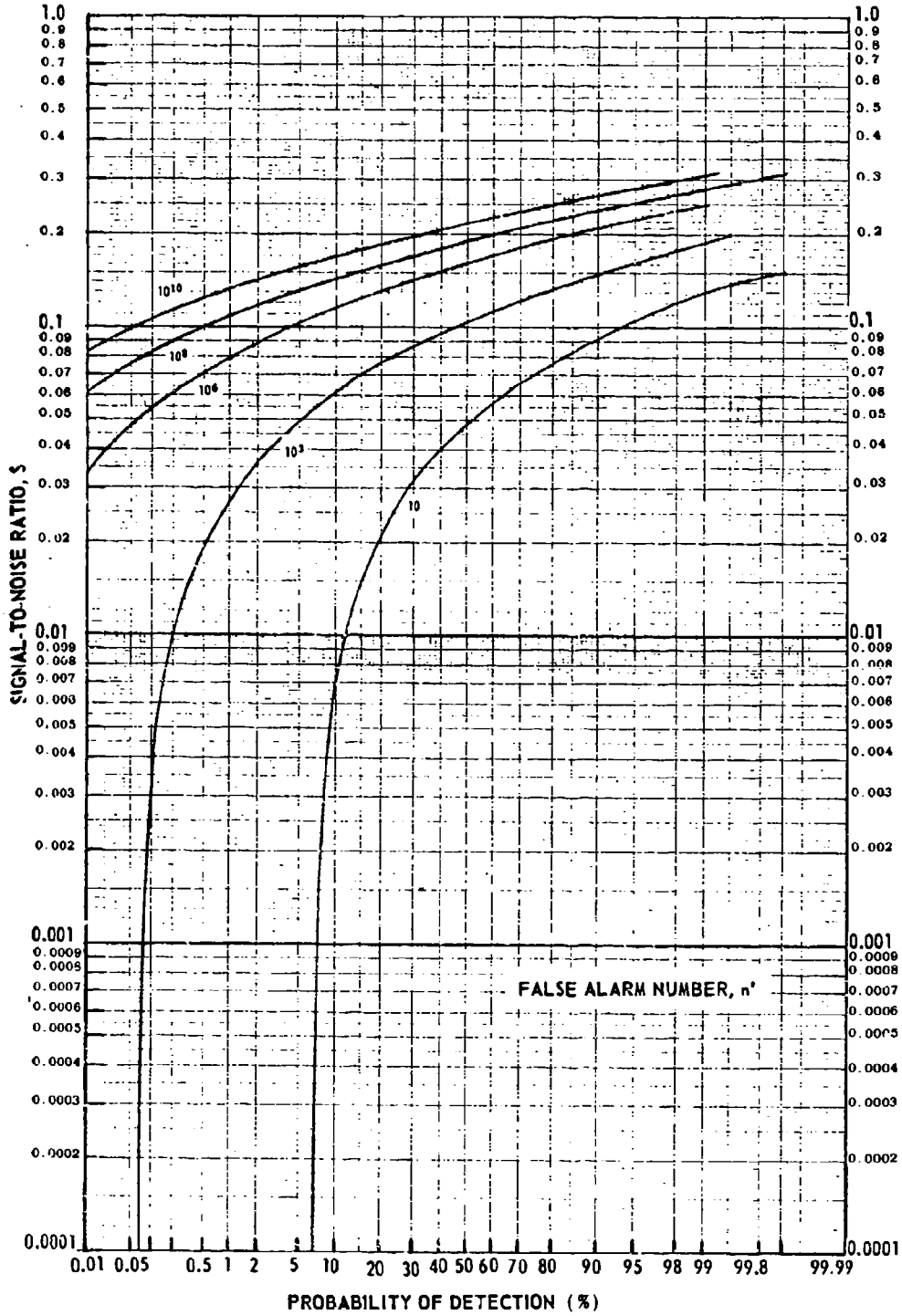

Fig. 29 PROBABILITY OF DETECTING A FLUCTUATING TARGET - CASE 2
Pulses Integrated, N 1000

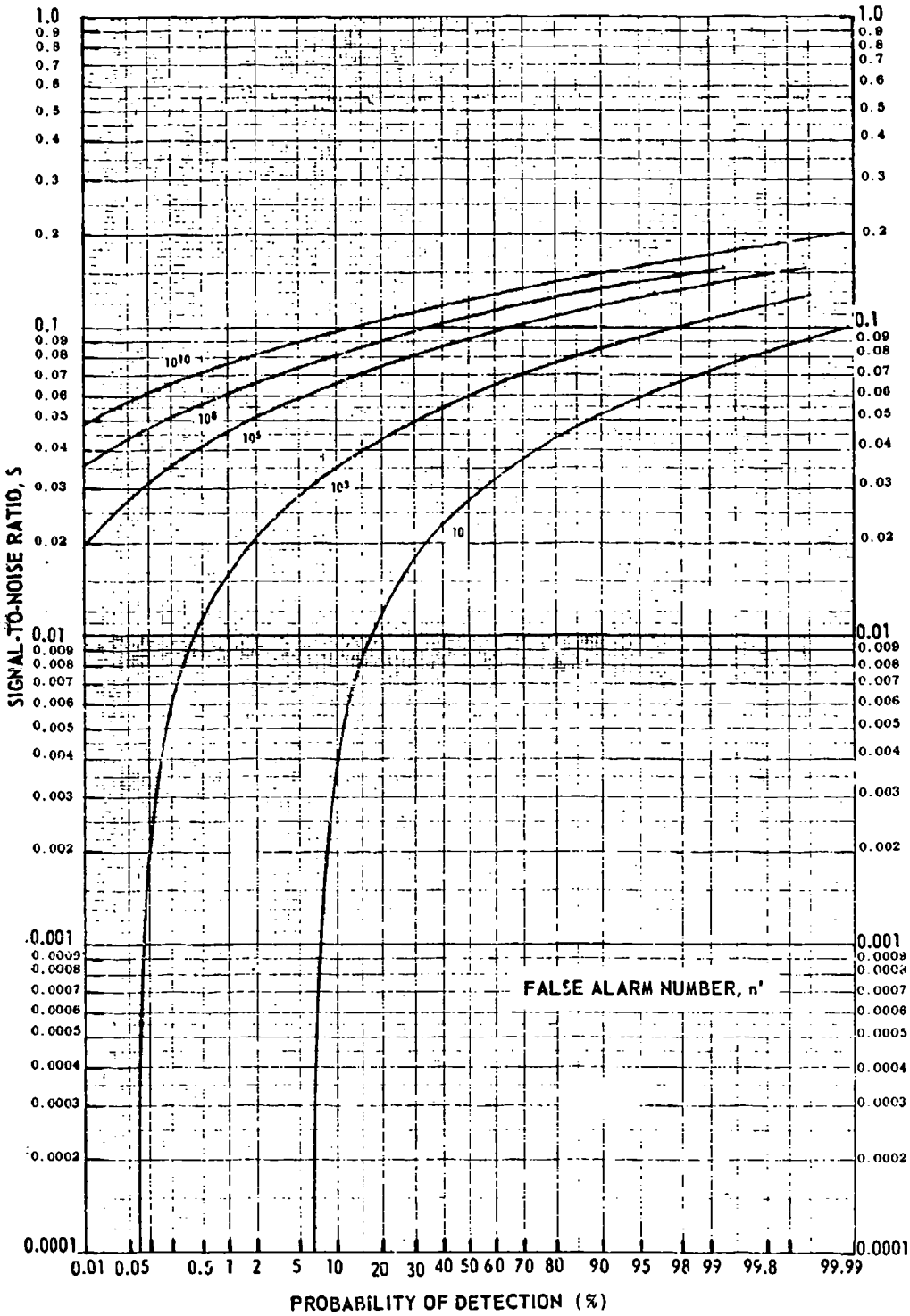

Fig. 30 PROBABILITY OF DETECTING A FLUCTUATING TARGET - CASE 2
Pulses Integrated, N 3000

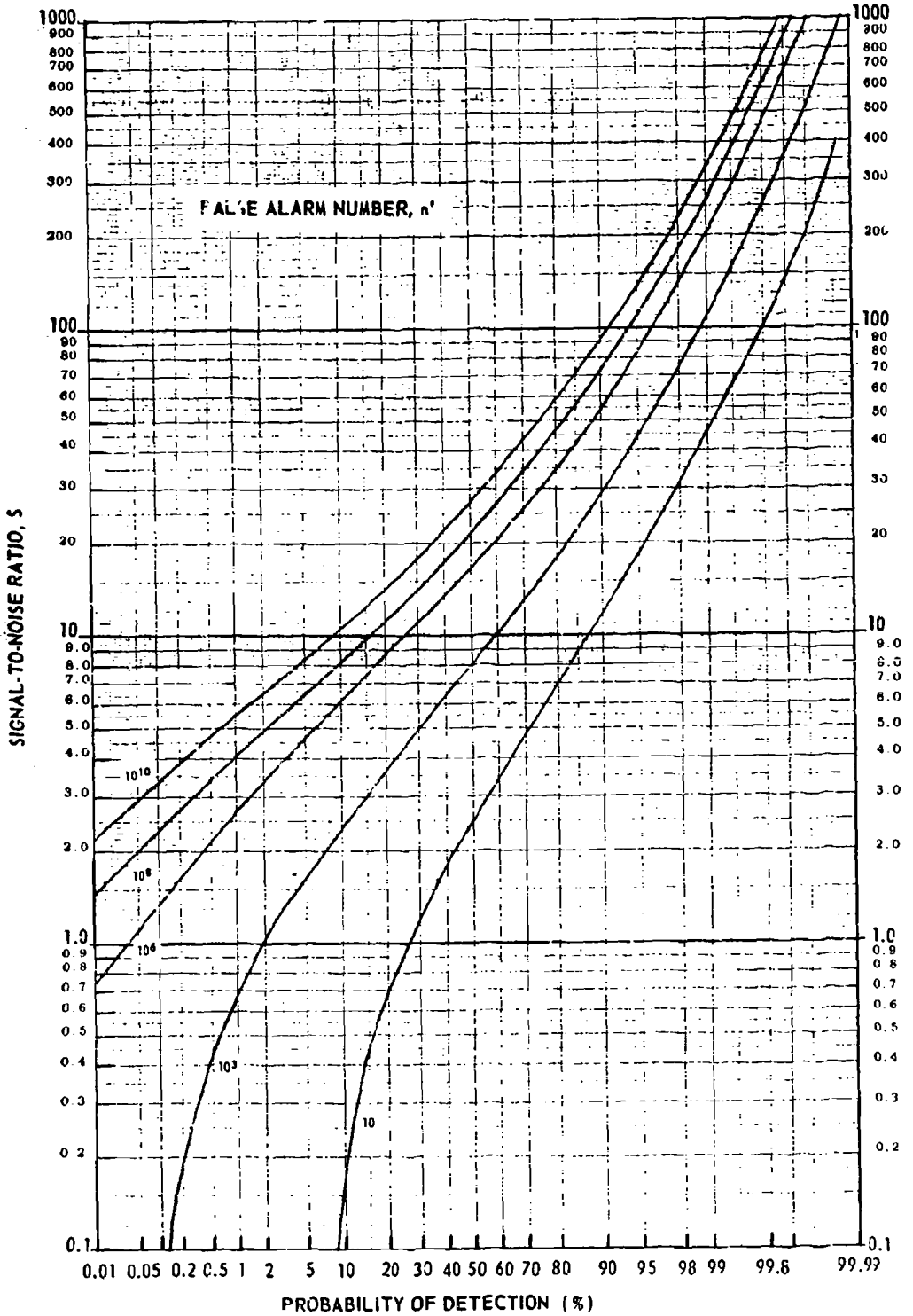

Fig. 31 PROBABILITY OF DETECTING A FLUCTUATING TARGET - CASES 3 AND 4
Pulses Integrated, N 1

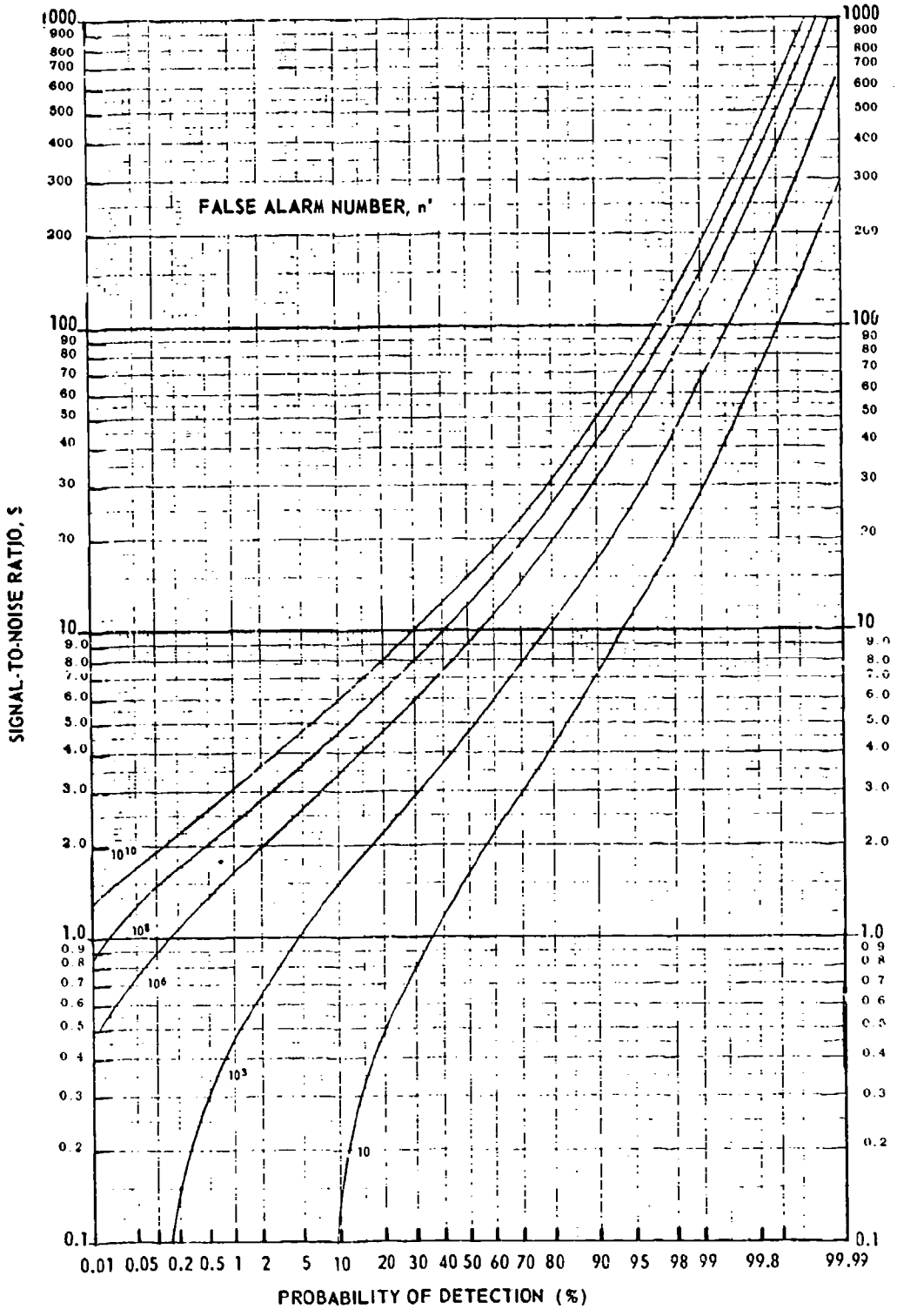

Fig. 32 PROBABILITY OF DETECTING A FLUCTUATING TARGET - CASE 3
Pulses Integrated, N 2

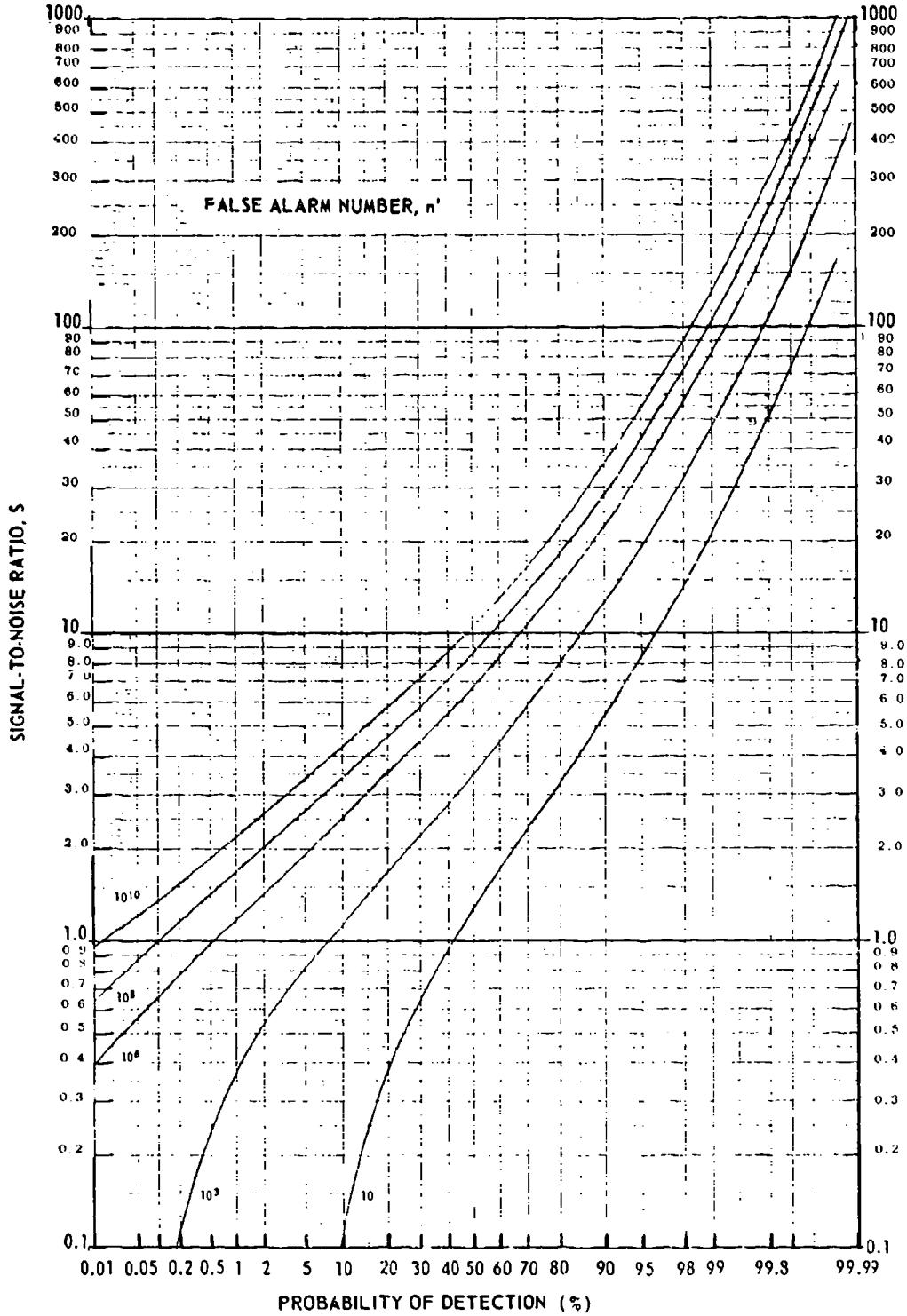

Fig. 33 PROBABILITY OF DETECTING A FLUCTUATING TARGET - CASE 3
Pulses Integrated, N 3

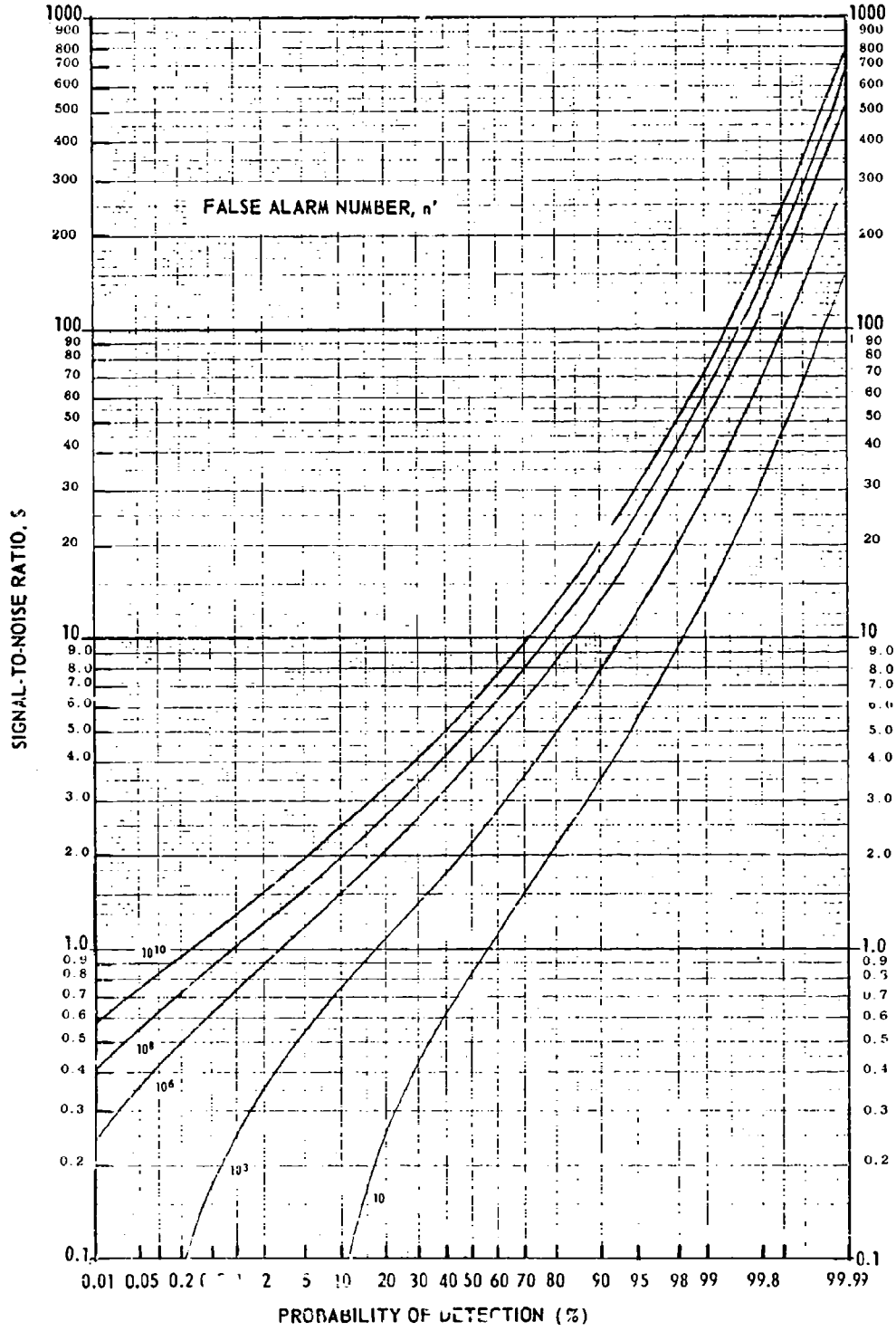

Fig. 34 PROBABILITY OF DETECTING A FLUCTUATING TARGET - CASE 3
Pulses Integrated, N 6

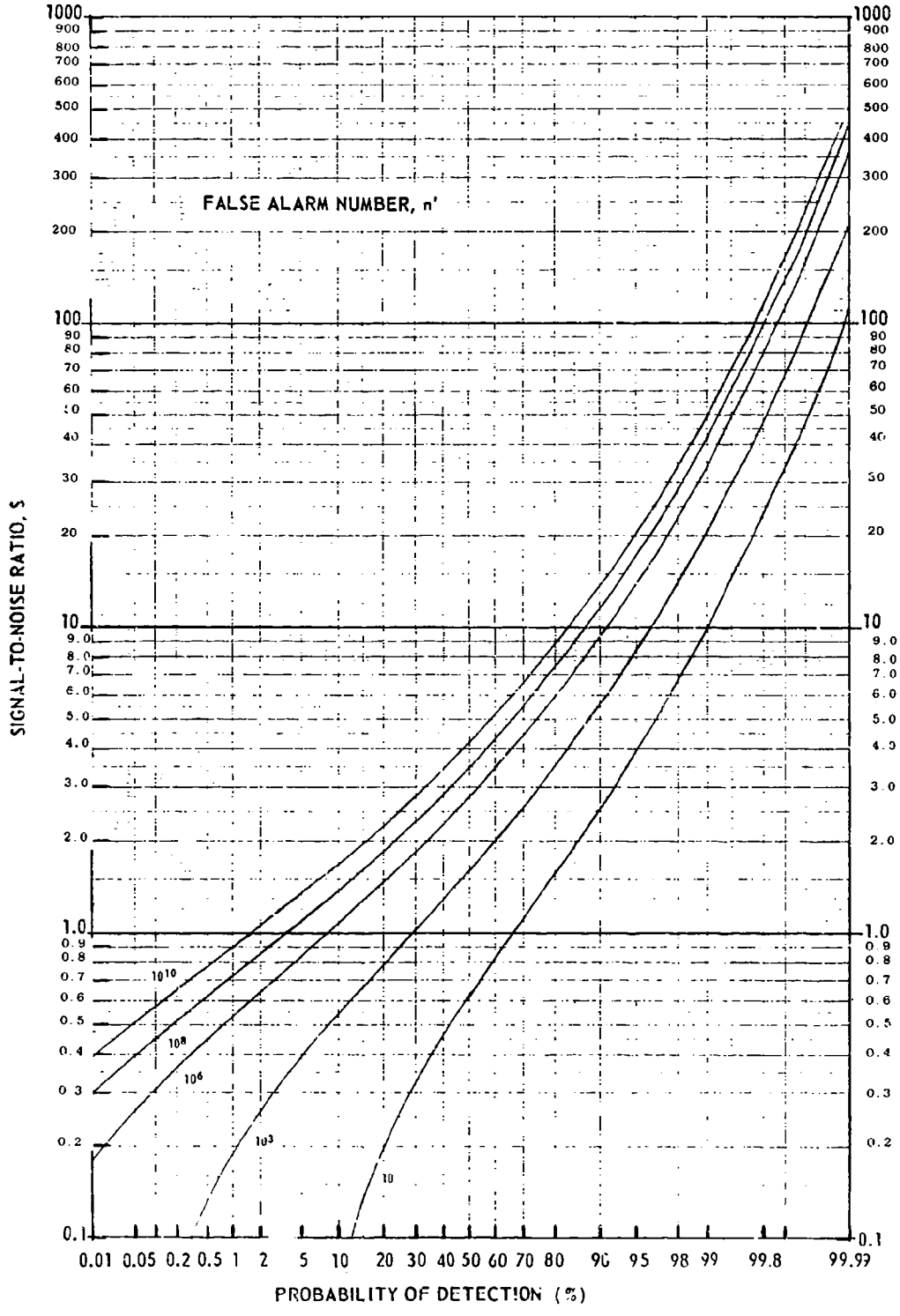

Fig. 35 PROBABILITY OF DETECTING A FLUCTUATING TARGET - CASE 3
Pulses Integrated, N 10

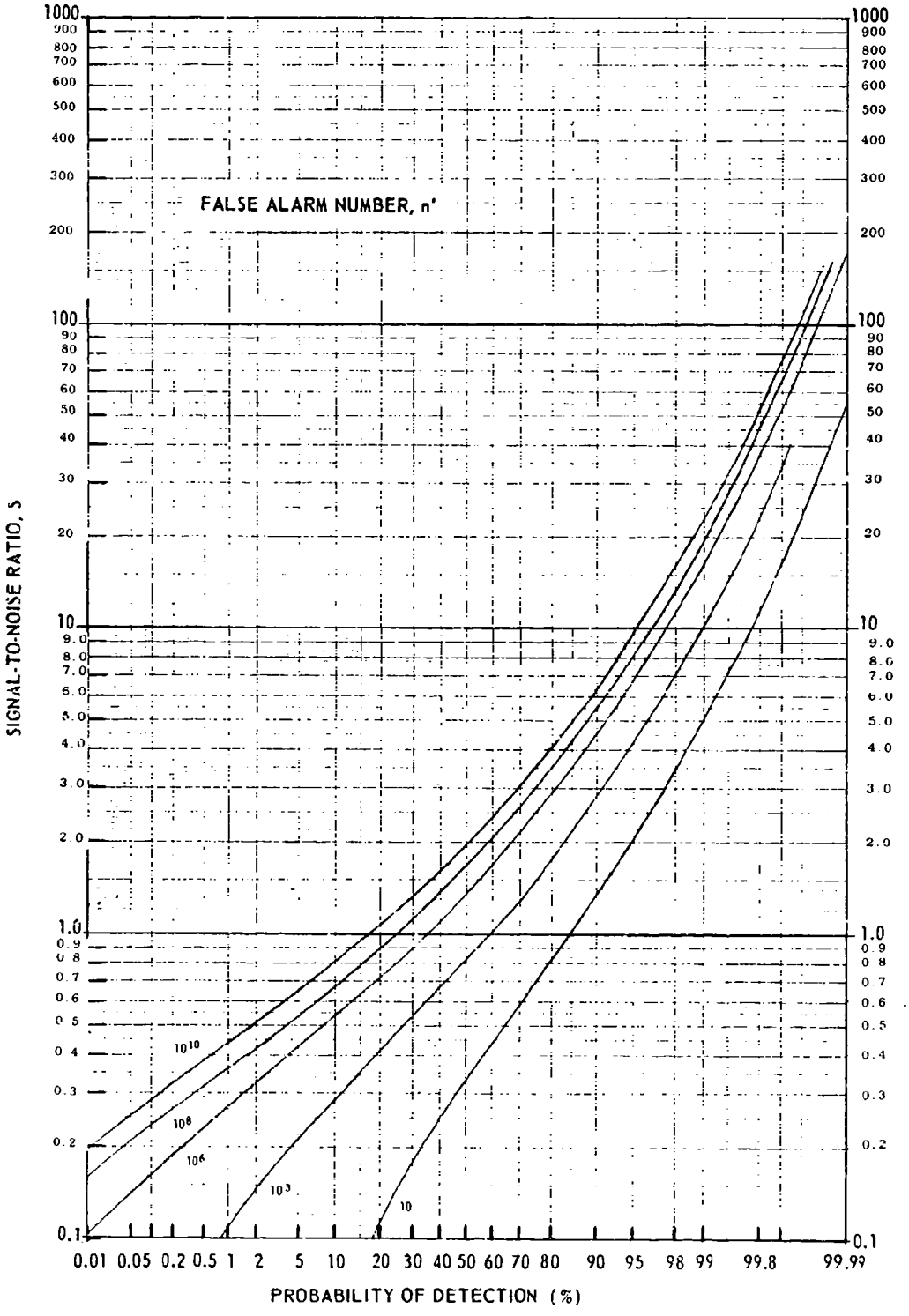

Fig. 36 PROBABILITY OF DETECTING A FLUCTUATING TARGET - CASE 3
Pulses Integrated, N 30

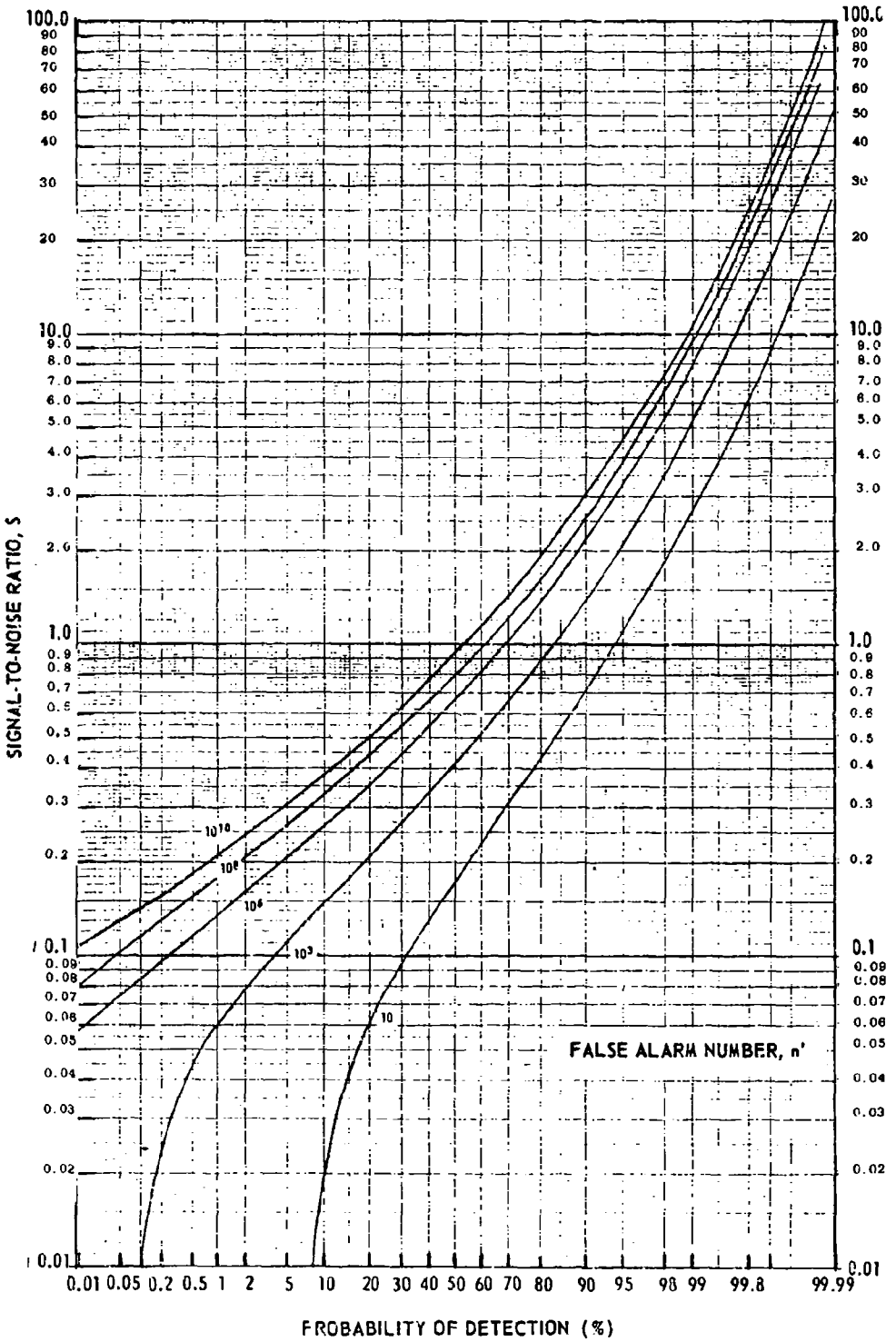

Fig. 37 PROBABILITY OF DETECTING A FLUCTUATING TARGET - CASE 3
Pulses Integrated, N 100

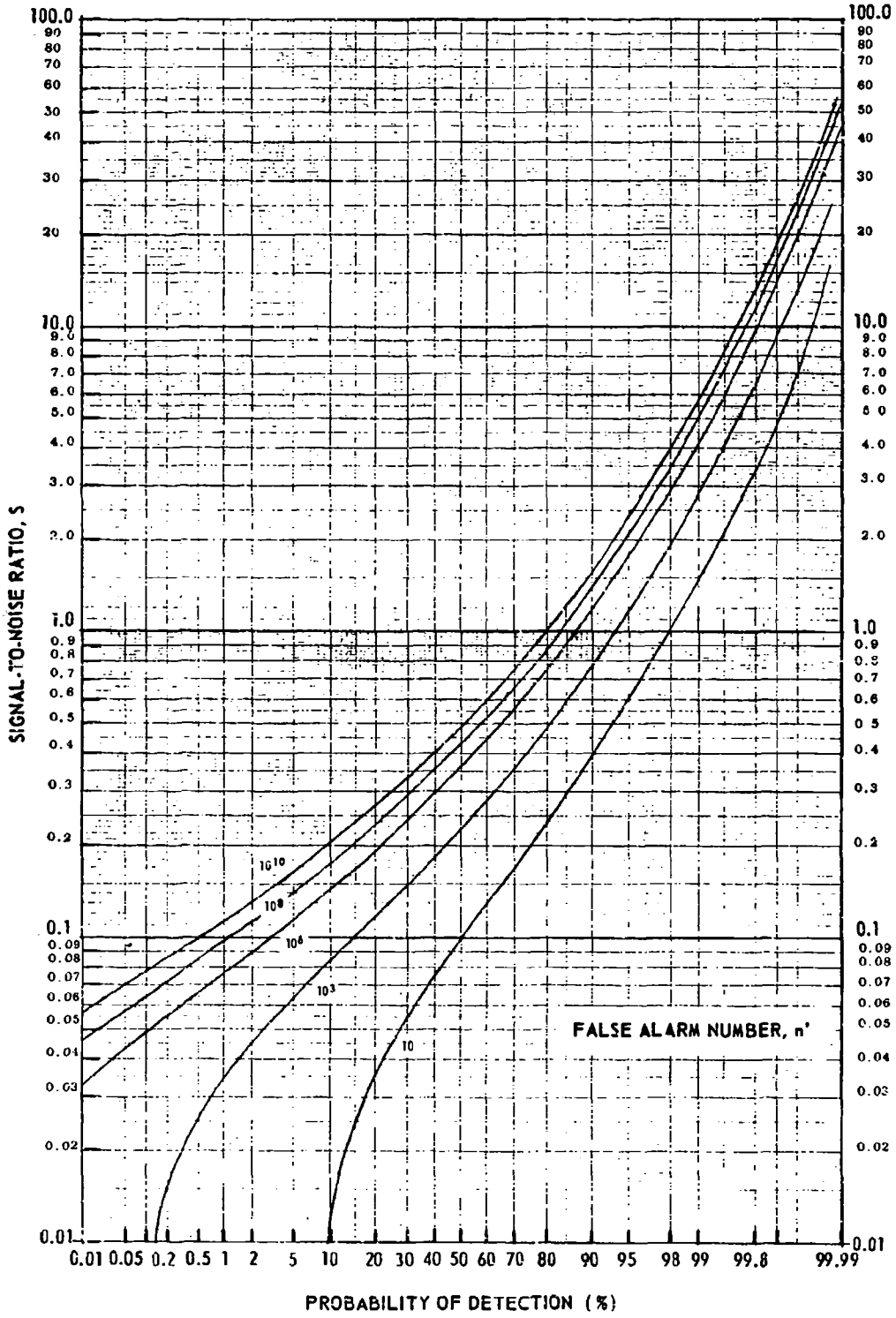

Fig. 38 PROBABILITY OF DETECTING A FLUCTUATING TARGET - CASE 3
Pulses Integrated, N 300

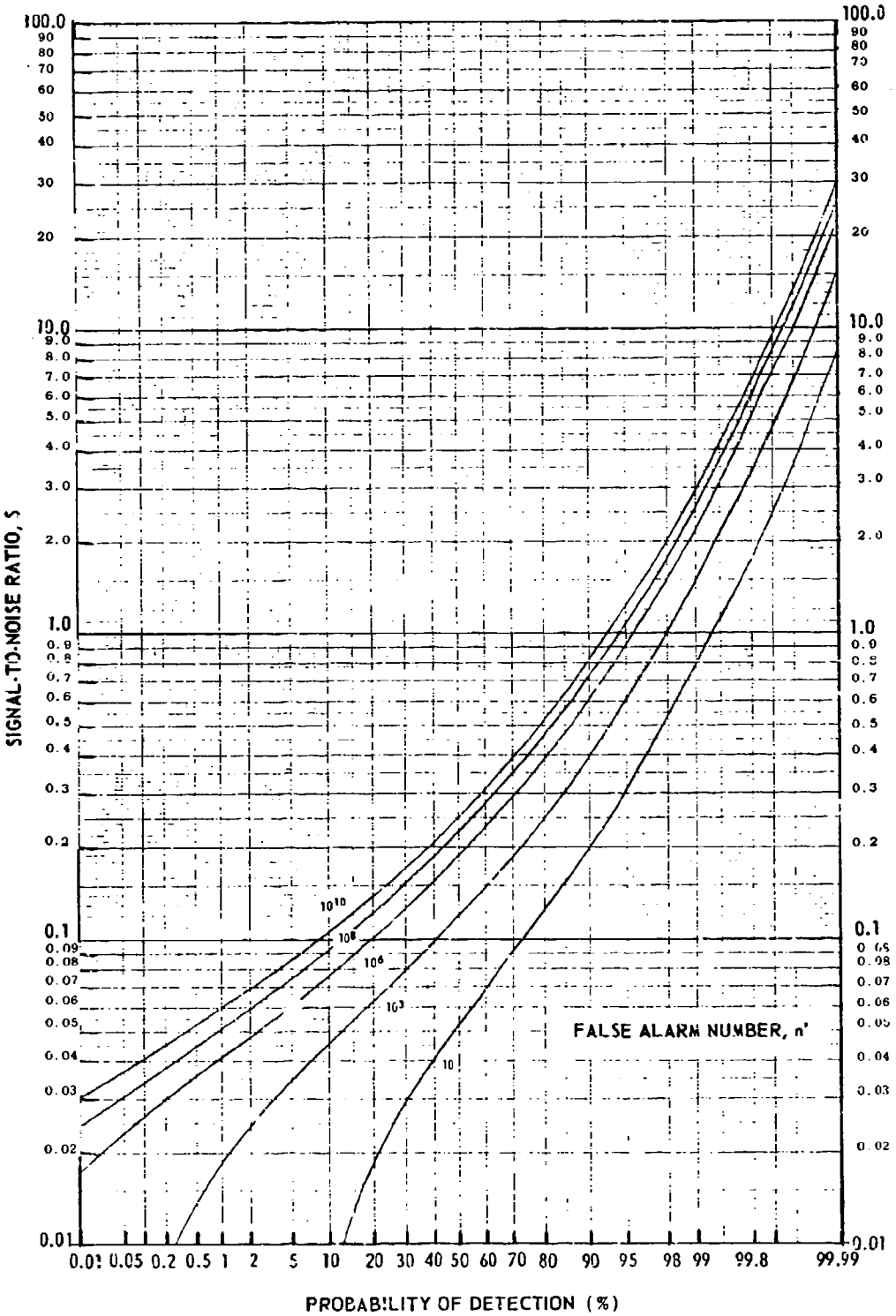

Fig. 39 PROBABILITY OF DETECTING A FLUCTUATING TARGET - CASE 3
Pulses Integrated, N 1000

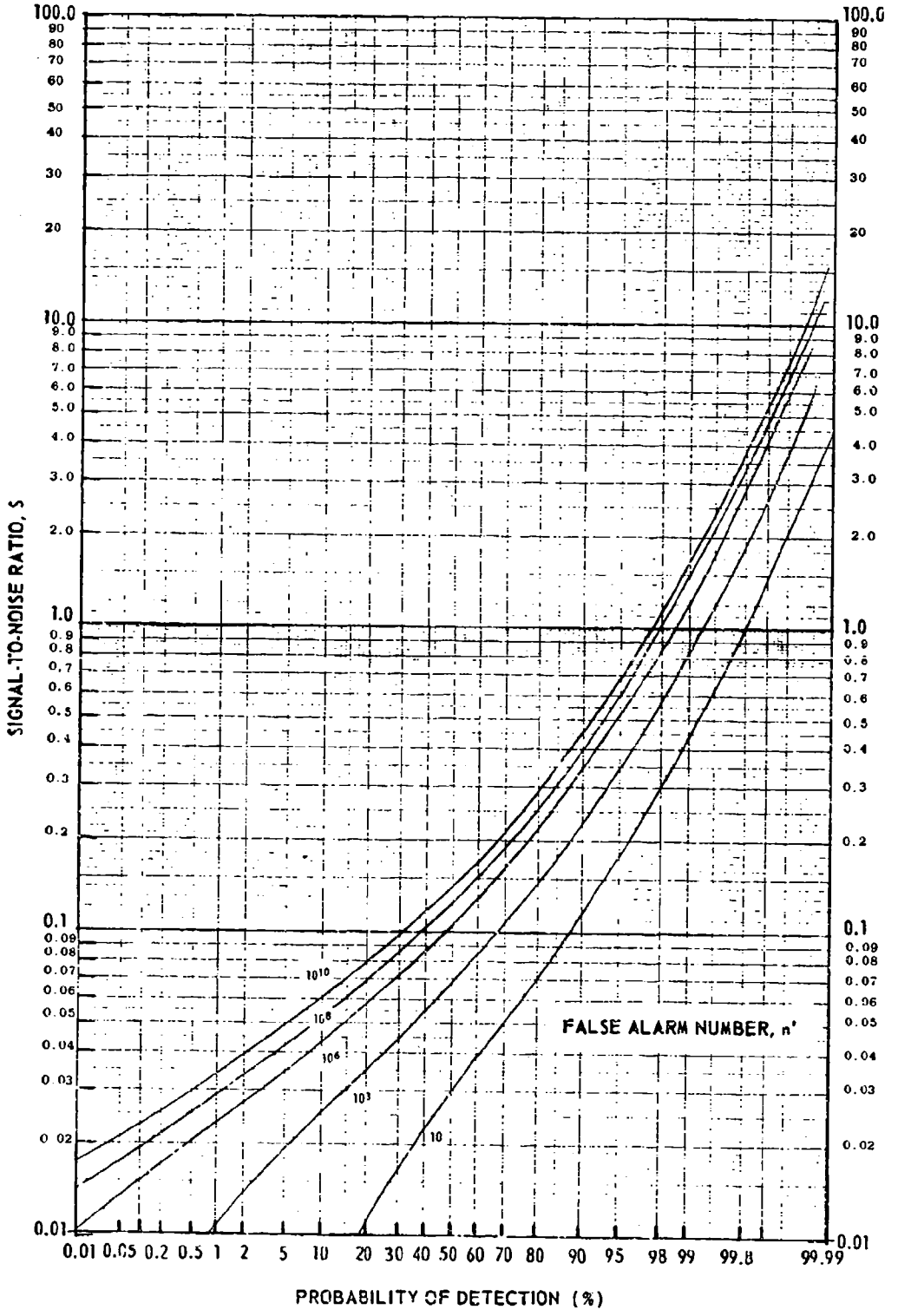

Fig. 40 PROBABILITY OF DETECTING A FLUCTUATING TARGET - CASE 3
Pulses Integrated, N 3000

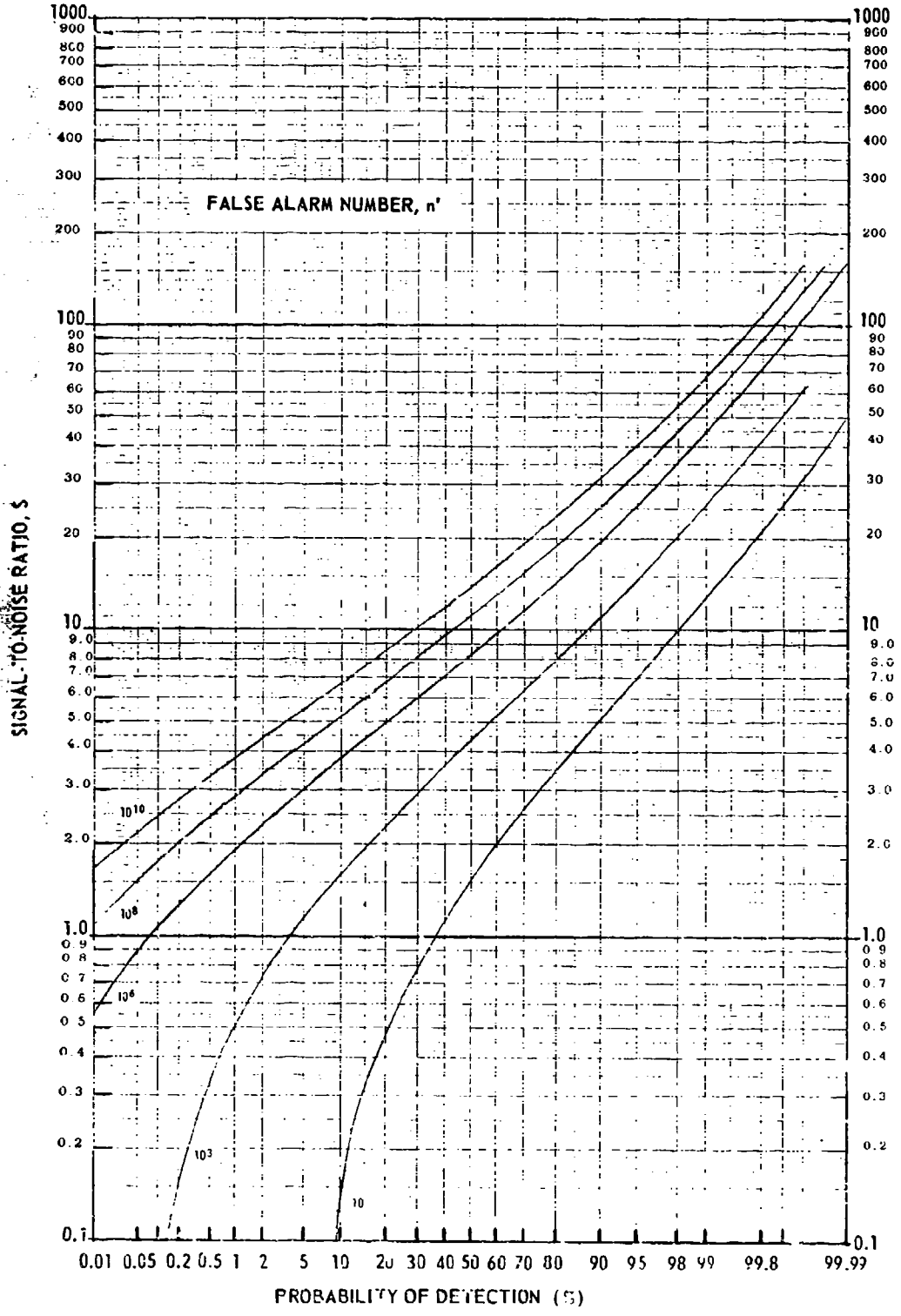

Fig. 41 PROBABILITY OF DETECTING A FLUCTUATING TARGET - CASE 4
Pulses Integrated, N 2

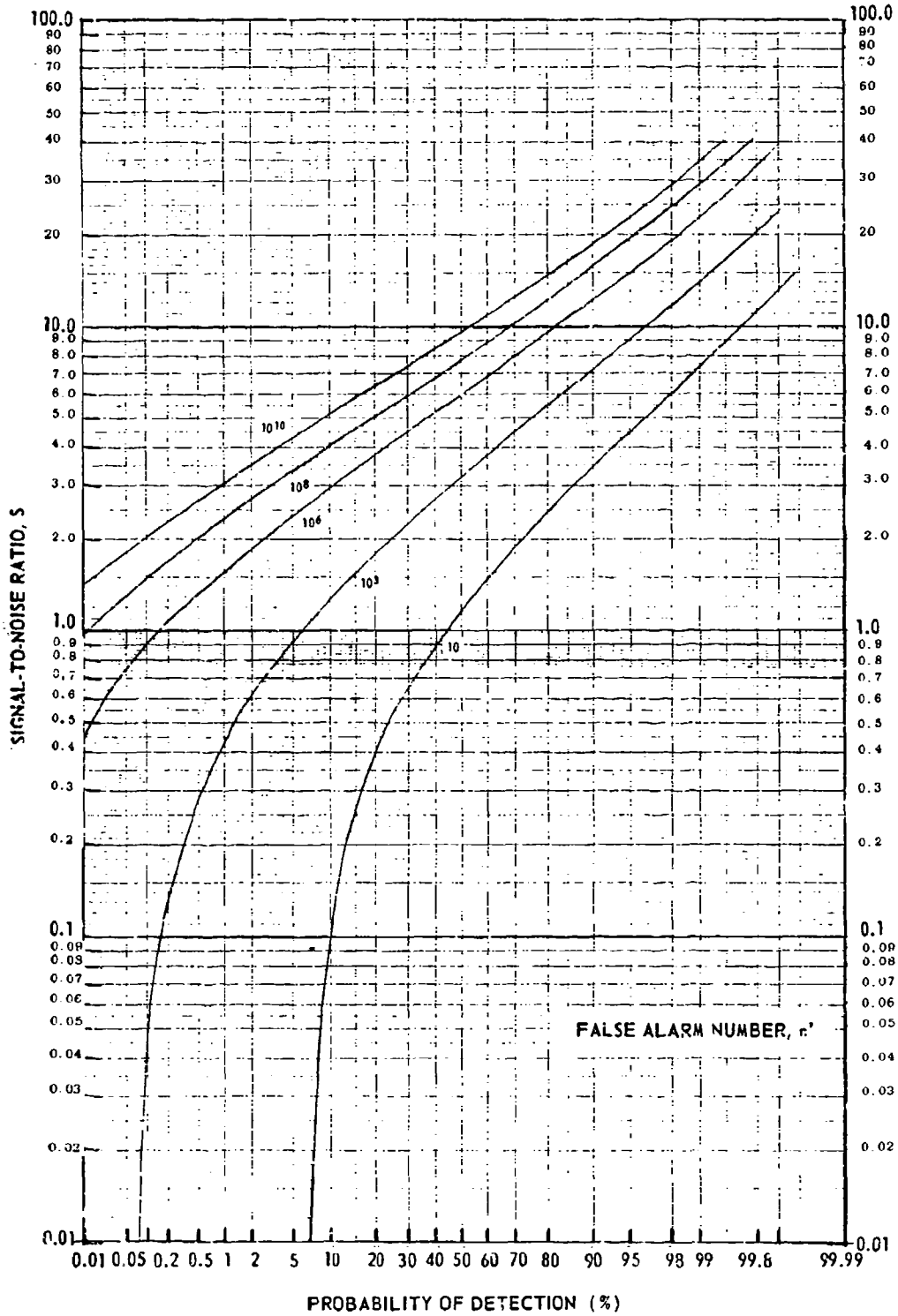

Fig. 42 PROBABILITY OF DETECTING A FLUCTUATING TARGET - CASE 4
Pulses Integrated, N 3

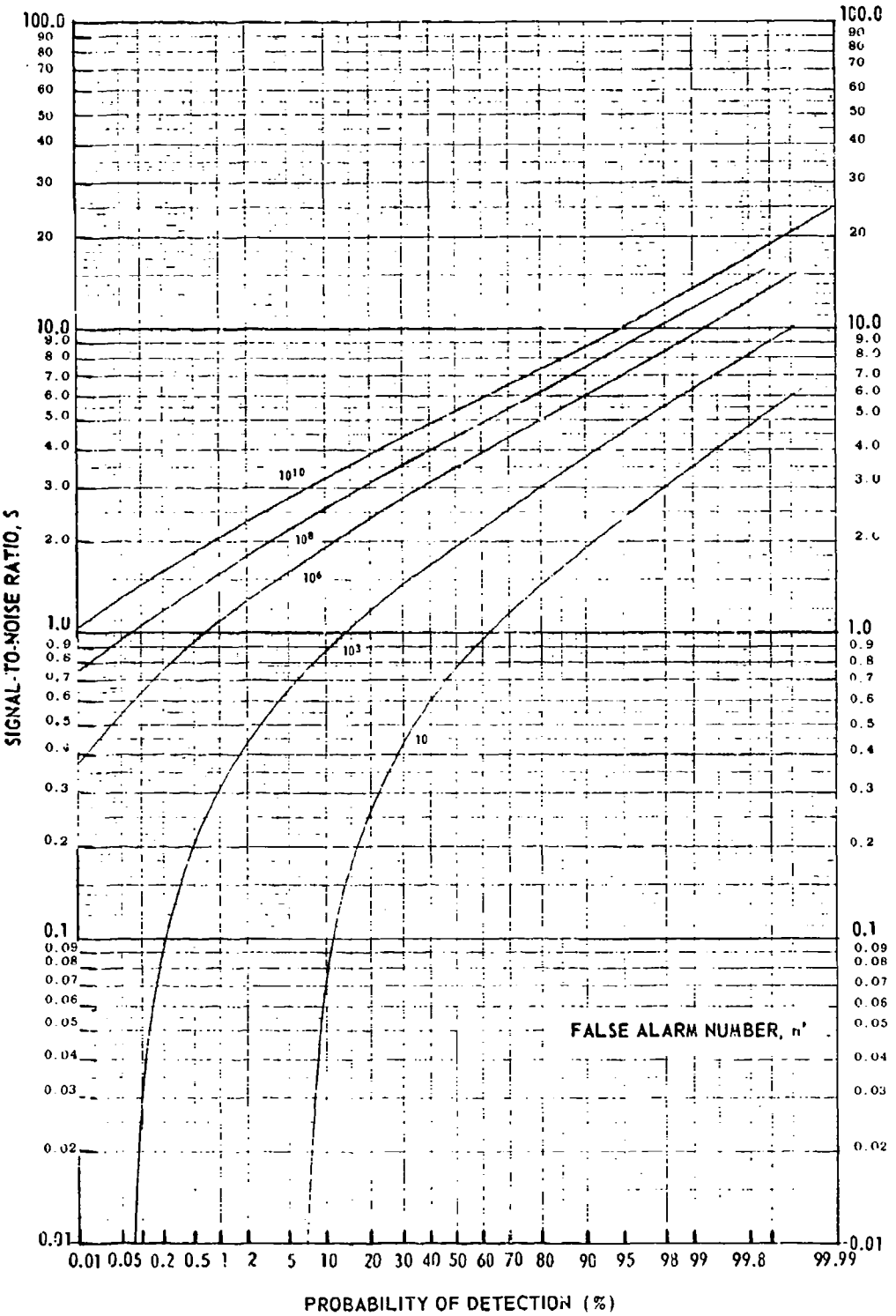

Fig. 43 PROBABILITY OF DETECTING A FLUCTUATING TARGET - CASE 4
Pulses Integrated, N 6

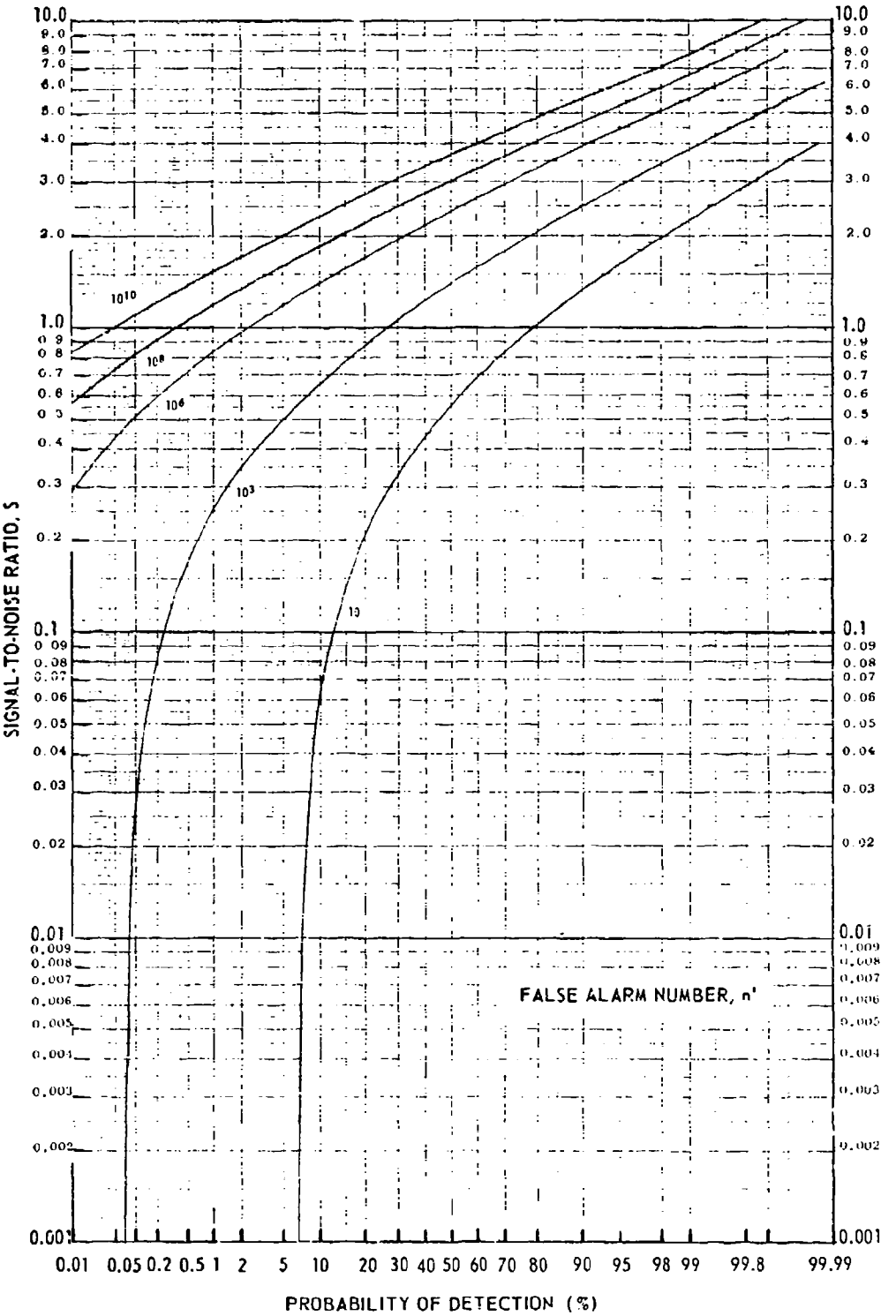

Fig. 44 PROBABILITY OF DETECTING A FLUCTUATING TARGET - CASE 4
Pulses Integrated, N 10

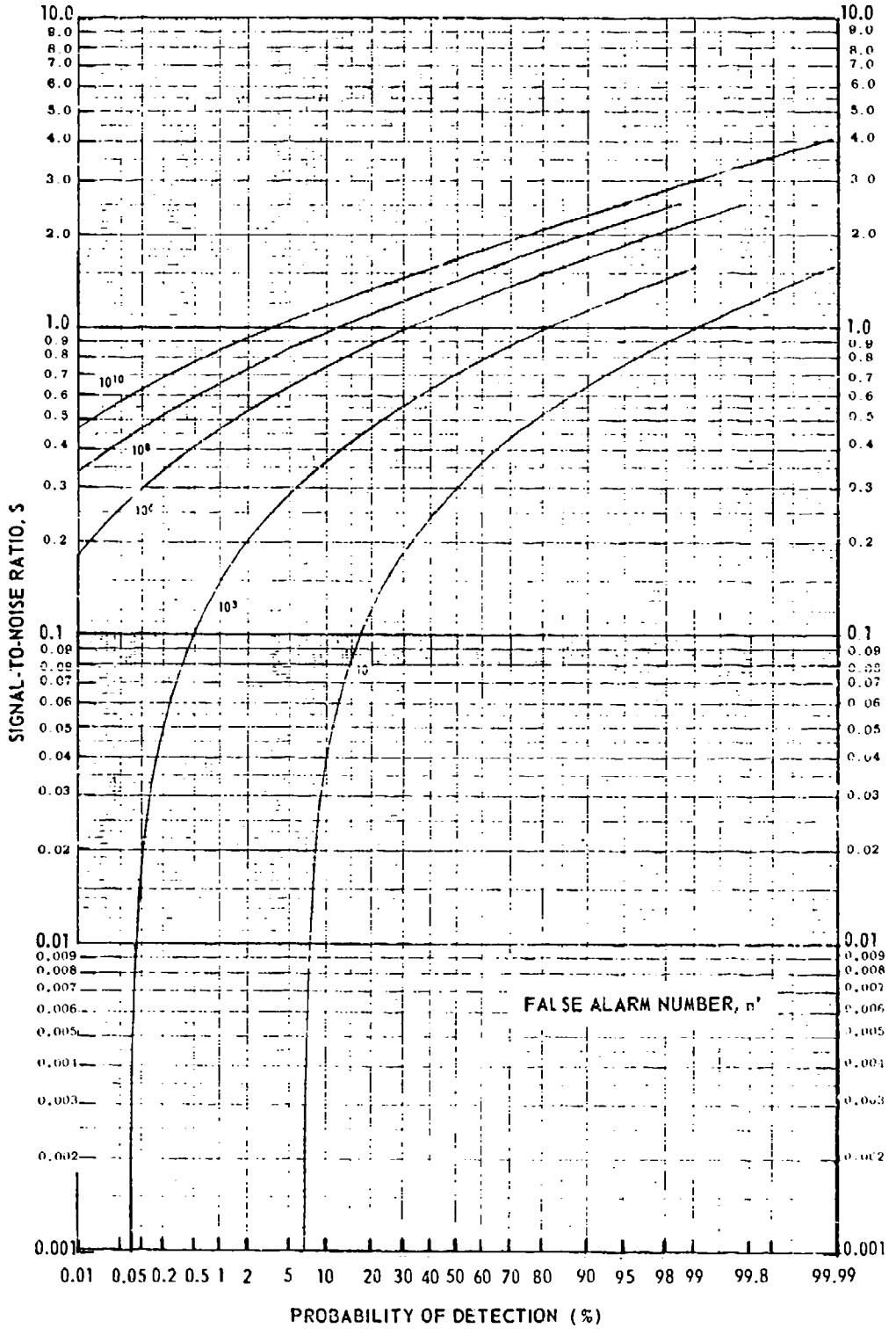

Fig. 45 PROBABILITY OF DETECTING A FLUCTUATING TARGET - CASE 4
Pulses Integrated, N 30

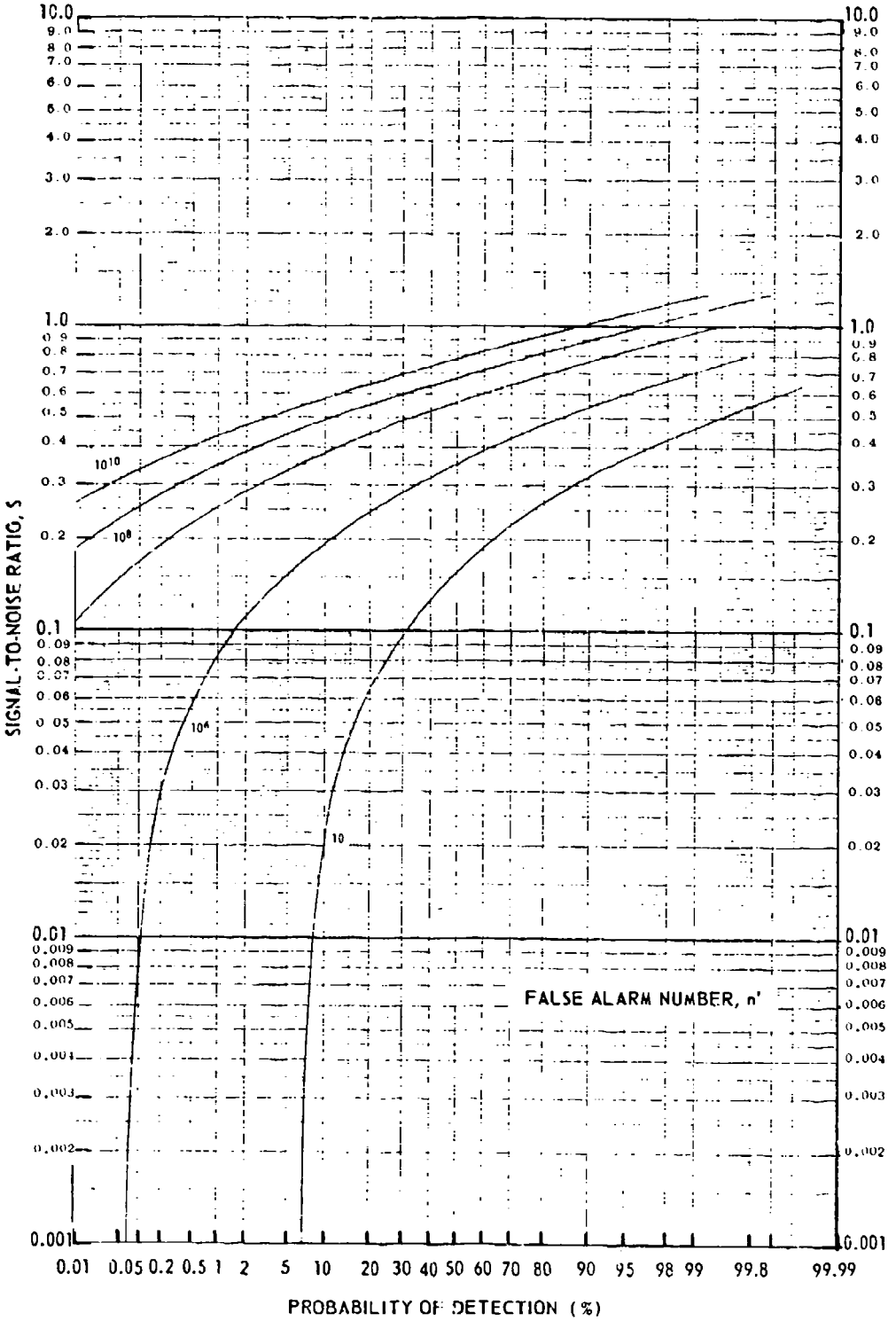

Fig. 46 PROBABILITY OF DETECTING A FLUCTUATING TARGET - CASE 4
Pulses Integrated, N 100

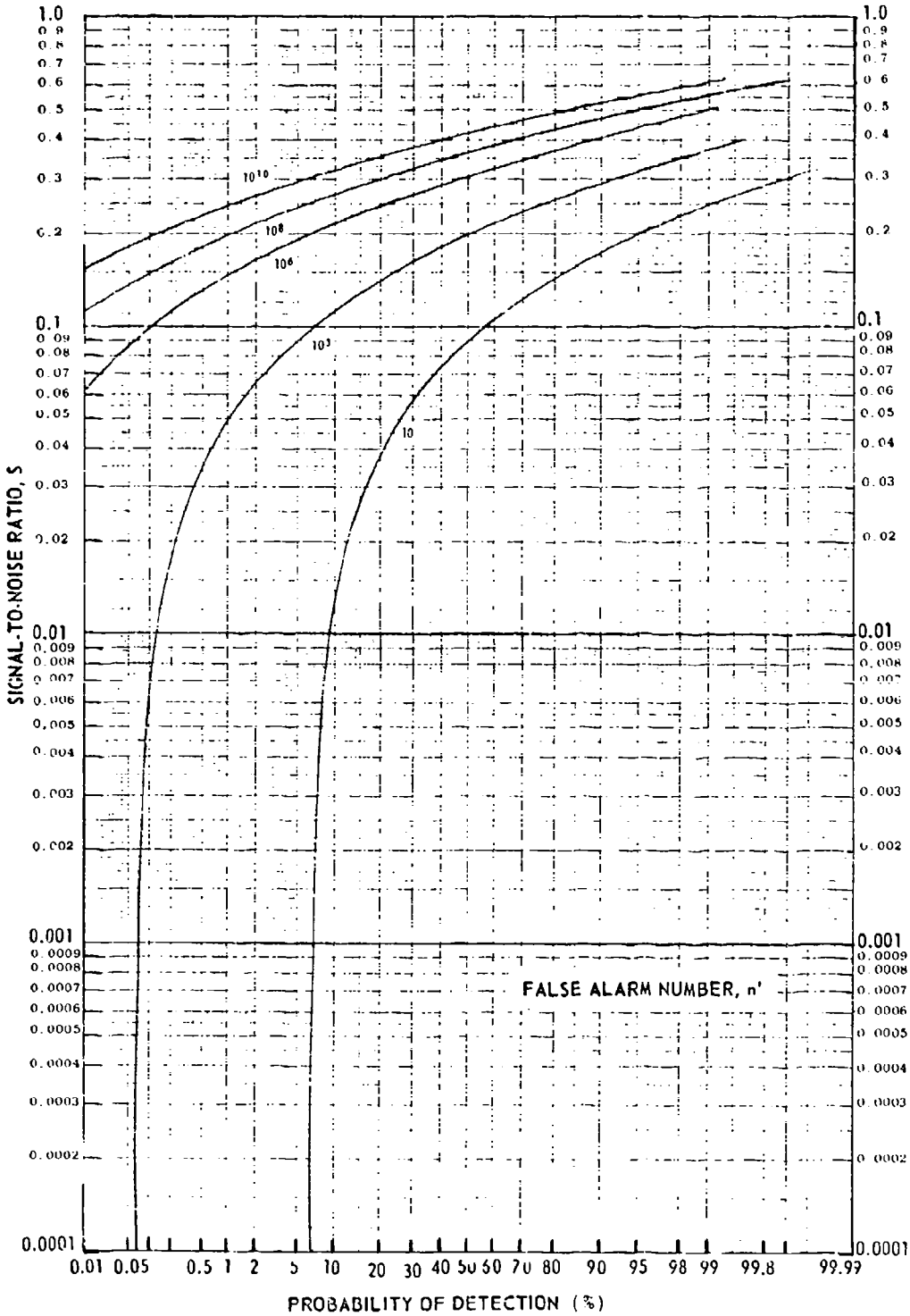

Fig. 47 PROBABILITY OF DETECTING A FLUCTUATING TARGET - CASE 4
Pulses Integrated, N 300

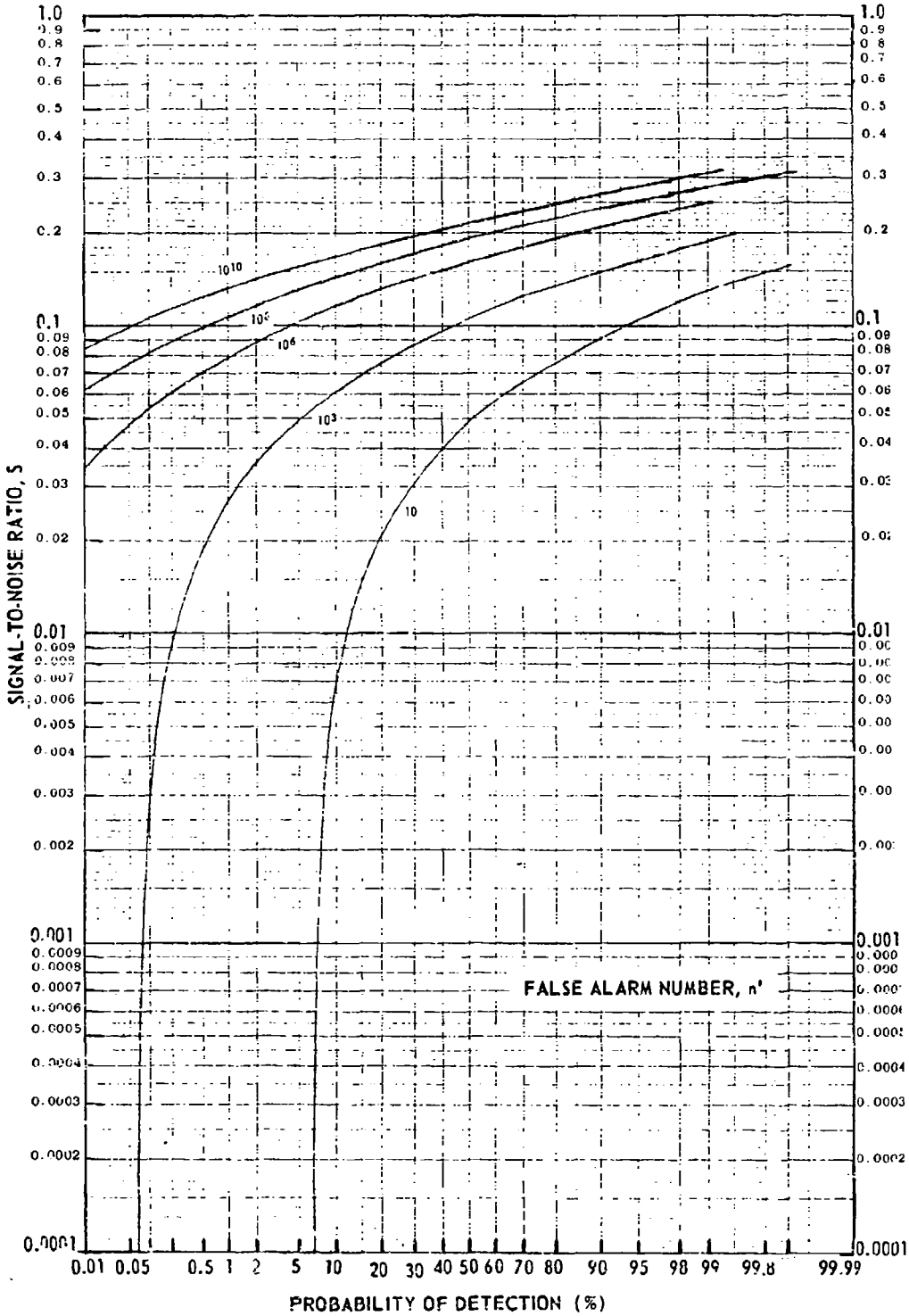

Fig. 48 PROBABILITY OF DETECTING A FLUCTUATING TARGET - CASE 4
Pulses Integrated, N 1000

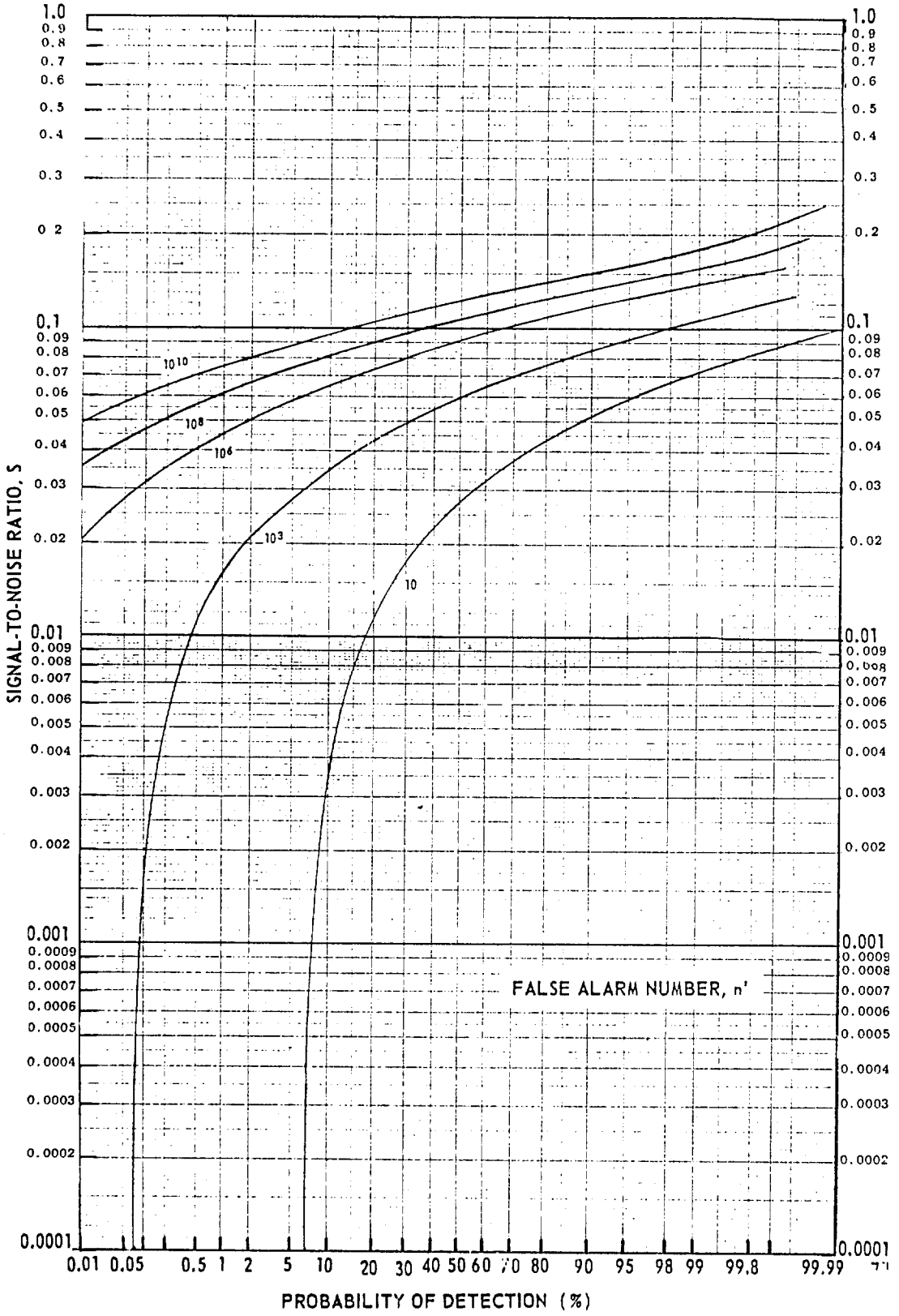

Fig. 49 PROBABILITY OF DETECTING A FLUCTUATING TARGET - CASE 4
Pulses Integrated, N 3000